Techno-Economic Impact Analysis of Renewable Hydrogen Supply Pathways in the Port of Rotterdam

With a Focus on Local Electrolysis and Ammonia Import

Roel Breure

Delft University of Technology

Techno-Economic Impact Analysis of Renewable Hydrogen Supply Pathways in the Port of Rotterdam

With a Focus on Local Electrolysis and Ammonia Import

by

Roel Breure

to obtain the degree of Master of Science in Sustainable Energy Technology
at Delft University of Technology

Dr.ir. M. B. Zaaijer	TU Delft
Prof.dr. D. A. von Terzi	TU Delft
Em.prof.dr. A. J. M. van Wijk	TU Delft
Ir. H. T. C. van der Heijden	Port of Rotterdam

Student Number: 4674383
Wednesday 26th February, 2025

Wind Energy Group, Faculty of Aerospace Engineering
Faculty of Electrical Engineering, Mathematics and Computer Science
Delft University of Technology

Abstract

The transition to a decarbonised energy system requires a cost-effective, reliable and sustainable supply of renewable hydrogen, particularly for industrial hubs like the Port of Rotterdam. Multiple supply pathways could potentially contribute to such an energy system, with each pathway characterised by different advantages and disadvantages. Therefore, it is crucial to consider the system-wide implications of various supply pathways in order to make balanced trade-offs. This study functions as an exploratory investigation into the relations between various system designs and their characteristics. It examines techno-economic trade-offs between local hydrogen production using offshore wind-powered electrolysis and cracking of imported ammonia. Key performance indicators for system affordability, security of supply and sustainability are defined in order to facilitate a comparison of the two supply pathways. Employing a quantitative system model, these indicators are evaluated across different system configurations and demand scenarios for the Port of Rotterdam.

The findings of this research emphasise the complexity of the energy transition and highlight the absence of a universally optimal supply pathway, with each pathway entailing distinct trade-offs that must be carefully balanced. Achieving an effective hydrogen strategy requires consideration of the interplay between affordability, security of supply, and sustainability, while also accounting for the diverse priorities of different stakeholders. Local electrolysis and ammonia import perform distinctly differently on various key performance indicators. The local production pathway offers lower operational costs and independence of import. However, it requires substantial capital investment and competes with power demand in the region. In contrast, ammonia import ensures a stable hydrogen supply with lower capital expenditure in the region of import, yet it is contingent on a resilient long-term supply chain and is highly sensitive to ammonia cost fluctuations. Local hydrogen production is more spatially demanding while having a lower carbon footprint, whereas ammonia imports require less space at the import site but result in higher equivalent emissions.

From the observations from this research it can be concluded that local hydrogen production presents trade-offs in the power distribution, as electrolysis potentially competes with the power demand of the Rotterdam harbour-industrial complex and the hinterland. Crucially, high electrolysis capacities impose an additional strain on the decarbonisation efforts of other electricity consumers, particularly in view of the anticipated increase in power demand. Furthermore, the necessity for multiple salt caverns for hydrogen storage in local production configurations is emphasised, as their constrained extraction limits require several units to satisfy momentary hydrogen demand even in low demand scenarios. In addition, substantial production overcapacity in electrolysis and wind power is necessary to facilitate adequate storage contribution and ensure supply continuity, increasing their techno-economic impact. Conversely, import-dependent systems require substantial quantities of ammonia, with hundreds of necessary annual shipments in scenarios of higher hydrogen demand. As demand for hydrogen increases, the study highlights clear supply limits for local hydrogen production, resulting in an increased reliance on ammonia imports.

Future research should expand model applicability to different locations and supply chains, enhance key performance indicator scope, and incorporate stakeholder-driven decision-making frameworks. Ultimately, an effective hydrogen strategy must balance affordability, security of supply and sustainability, navigating the trade-offs between supply pathways and their broader implications for the energy transition.

Acknowledgements

This graduation project has been a stimulating and educational journey. During the course of my studies, extracurricular work and internships, I became increasingly driven to focus on the energy transition. This complicated yet crucial transformation is having a significant impact on society, and it intrigues me how numerous technical, economic and societal aspects are interconnected in its implementation. This research provided the ideal opportunity to dedicate my enthusiasm to such a project, yet it would not have been possible without the continuous support and patience of many people, some of whom I would like to mention specifically.

Firstly, I would like to express my sincere gratitude to my daily supervisors Michiel Zaaijer and Erik van der Heijden for their consistent engagement and for the substantial freedom I was granted in defining the research topic. Michiel, your meticulous analysis, insightful feedback and the fruitful discussions we have had have raised the level of this research significantly. Erik, your enthusiasm on this project, extensive knowledge of the industrial landscape and readiness to connect your network in favour of this research have been elemental. Dominic and Ad, thank you for being part of my thesis committee, taking the time to evaluate my work and holding it to academic standards.

I would like to extend my appreciation to my colleagues at the Port of Rotterdam for taking me along in the company and for our repeated sparring sessions about the challenges I encountered. Your spirit is contagious and the day-to-day collegiality have significantly elevated the enjoyment in conducting this research. I am also indebted to the long list of industry experts who have been kind enough to provide their valuable insights and enrich this thesis, ensuring it is grounded in the real world.

Finally, my sincerest gratitude goes out to my friends and family, whom I have bothered endlessly with my anecdotes about hydrogen development. You have consequently encouraged me to be articulate about the essence of this research and explain it clearly and comprehensibly. In addition, you have been able to put my challenges considering this research into perspective, for which I am deeply grateful.

Roel Breure
Rotterdam, February 2025

Nomenclature

Abbreviations

Abbreviation	Definition
AC	Alternating Current
AEL	Alkaline Electrolysis
AEM	Anion Exchange Membrane
BoS	Balance of System
CAPEX	Capital Expenditure
CCS	Carbon Capture and Sequestration
CES	Cluster Energie Strategie
COP21	Conference of the Parties 2021
DC	Direct Current
DRI	Direct-Reduced Iron
ETS	Emission Trading Scheme
FID	Final Investment Decision
FLH	Full-Load Hours
HHV	Higher Heating Value
HIC	Harbour-Industrial Complex
HVAC	High-Voltage Alternating Current
HVDC	High-Voltage Direct Current
IEA	International Energy Agency
II3050	Integrale Infrastructuurverkenning 2030 - 2050
KPI	Key Performance Indicator
LCA	Life Cycle Analysis
LHV	Lower Heating Value
LOHC	Liquid Organic Hydrogen Carrier
OPEX	Operational Expenditure
PBL	Planbureau voor de Leefomgeving
PEM	Polymer Electrolyte Membrane
PoR	Port of Rotterdam
RED	Renewable Energy Directive
RFNBO	Renewable Fuel of Non-Biological Origin
SAF	Sustainable Aviation Fuel
SDE	Stimulering Duurzame Energieproductie
SMR	Steam Methane Reforming
SOEC	Solid Oxide Electrolyser Cell
TRL	Technology Readiness Level
TSO	Transmission System Operator
VAWOZ	Verbindingen Aanlanding Wind Op Zee

Symbols

Subscript	Definition
e	Electric Installed Capacity
$H2$	Hydrogen Installed Capacity
LHV	based on Lower Heating Value (*LHV*)
HHV	based on Higher Heating Value (*HHV*)

Contents

1 Introduction

The transition to a sustainable energy system is a defining global challenge of the present age. As global ambitions to reduce greenhouse gas emissions intensify, the way energy is produced, transported and consumed is undergoing a fundamental shift. This chapter provides a background to the key motivations for this research, with a focus on the combined challenge of power and hydrogen decarbonisation. It goes on to highlight the particular considerations for a large harbour-industrial complex, such as the Port of Rotterdam, where the local and import-based building blocks can have a profound impact on the energy system they comprise.

Section 1.1 focuses on a number of general challenges in the energy system transition, while section 1.2 specifies several key challenges for the Port of Rotterdam. Section 1.3 provides a discussion of the current state of development, whereas the subsequent section 1.4 identifies the specific challenge that is the focus of this research. This problem analysis result in the formulation of the research objective in section 1.5, the scope of which is further delineated in section 1.6. Lastly, the methodology employed to reach the research objective is elaborated upon in section 1.7.

1.1. Energy System Transition

The energy transition requires a comprehensive transformation of the energy system. This section explores several major pillars of this transition, starting with the origin of the transformative ambitions. The section then examines the decarbonisation of power generation and hydrogen, before delving into the discussion of hydrogen production origin: locally produced or imported. Finally, the European Commission's definition of renewable hydrogen is elaborated upon.

1.1.1. Emission Reduction Ambitions

The twenty-first Conference of the Parties (*COP21*) in 2015 was a milestone in the campaign against climate change. Informally called 'The Paris Agreement', 196 countries signed a legally binding international treaty to pursue efforts to limit global warming to 1.5 degrees Celsius compared to pre-industrial levels [1]. In accordance, the Dutch government launched the Klimaatakkoord in 2019. This agreement aimed to reduce the Dutch CO_2 emissions by 49% in 2030 [2]. In July of 2021 the European Commission established an additional European objective of a 55% reduction in greenhouse gas emissions by 2030 in comparison to 1990 levels [3]. A number of greenhouse gases are emitted as a result of human activity, but CO_2 emissions are the most significant contributor to global warming [4]. These objectives aim to incentivise decarbonisation and lead the global society to a future powered by renewable energy.

A visual representation of the industrial contribution to CO_2 emissions in the Netherlands is shown in Figure 1.1. Industry and electricity production are responsible for over half of the total 132 Mt Dutch CO_2 emissions in 2022 [5] [6]. Industry accounts for 33% directly, however, it represents the second largest consumer of electricity. Thereby it indirectly contributes to an even more significant footprint, as half of Dutch power production in 2022 was fossil-based [7]. The process of decarbonising the power sector represents a parallel challenge, which is intertwined with the energy transition for industry. The largest proportion of Dutch industrial energy consumption can be attributed to the chemical and petroleum refining industries [8] , whose corresponding CO_2-equivalent emissions added up to 10% of the national total in 2022 [9] [10].

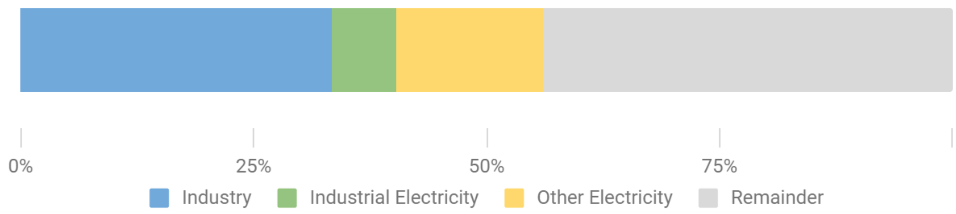

Figure 1.1: Industry contribution of Dutch CO_2-eq emissions in 2022, both directly and based on share in power consumption [5] [7].

1.1.2. Power: Core of Decarbonisation

The decarbonisation of power systems is a cornerstone of the energy transition, requiring both the replacement of existing fossil-based generation and the expansion of capacity to meet growing demand. This provides a massive infrastructural challenge in power networks, both in terms of their enlargement and the inclusion of renewable sources with intermittent production profiles.

Figure 1.2 shows the power profile in the Netherlands. Electricity demand in the Netherlands exhibits a distinctive annual pattern, with an average increase of up to 40% during the winter months [11]. Besides, daily variations significantly impact the shape of the demand profile. Two noticeable peaks occur around 9 in the morning and 6 in the evening, while night-time demand is relatively low.

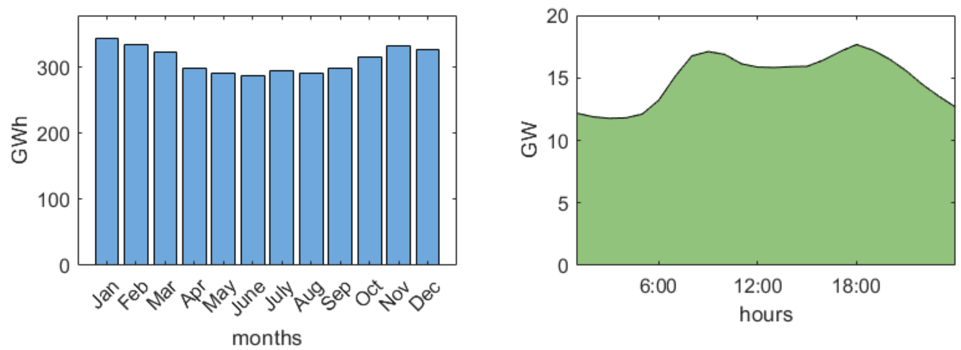

Figure 1.2: Left: Average daily grid load, shown per month for the Netherlands in 2019 [11]. **Right**: Daily grid load profile for February 7th, 2019 [11].

The electricity mix in the Dutch grid leans heavily on natural gas at 39% of the total production in 2022 [7]. Despite the ongoing dependency on natural gas, the increase of low-carbon sources is significant, from a 17% share in 2015 to nearly 50% in 2022. Especially offshore wind power from the North Sea is being considered by the Dutch government [2], partially due to the favourable wind climate and shallow waters. Offshore wind power features relatively high capacity factors for a renewable energy source at 40-50% [12] [13] , indicating they produce this percentage of the total maximum they could yield annually.

1.1.3. Hydrogen: Tiny Molecule, Massive Emissions

A significant contributor to the industrial emissions is the production of hydrogen (H_2), which is a common process feedstock in this sector [14]. Around 95 Mt/y of hydrogen is consumed globally [15]. This leads to an estimated 900 Mt of CO_2 emissions, or 2.5% of the global total [15]. It is consumed primarily in petroleum refining, where it is used to remove sulphur impurities through hydrodesulpurisation. Hydrogen is also used to upgrade heavy oil fractions into lighter oil products source using hydrocracking. Besides, the important primary chemicals ammonia (NH_3) and methanol (CH_3OH) are synthesised using hydrogen feedstock. These are key ingredients for nitrogen fertilisers, plastics, pharmaceuticals, construction materials and numerous other chemicals [14] [16]. Both ammonia and methanol have the potential to be used as a fuel themselves, in addition to a role as a hydrogen carrier for transport and storage [15].

The reason that hydrogen contributes so significantly to global CO_2-emissions is due to its prevalent fossil-based production methods. Figure 1.3 shows the global production sources of hydrogen in 2021. Natural gas is the source of 62% of global hydrogen production in 2021 [15]. Through a process called steam methane reforming (*SMR*), methane (CH_4) in natural gas reacts with hot steam $H_2O(g)$ to create a carbon monoxide (CO) and hydrogen (H_2) gas mixture which is known as synthesis gas [17]. This mixture subsequently reacts with steam again in a water-gas shift reaction to form carbon dioxide (CO_2) and more hydrogen. Besides partially being the source of hydrogen, natural gas also fuels the reforming reaction. The reaction yields a significant amount of CO_2, averaging 9.35 $kgCO_2$ per kgH_2 directly from the plant [18]. Other production sources include coal gasification and hydrogen derived as by-product during naphtha processing, while a minute amount is produced through electricity.

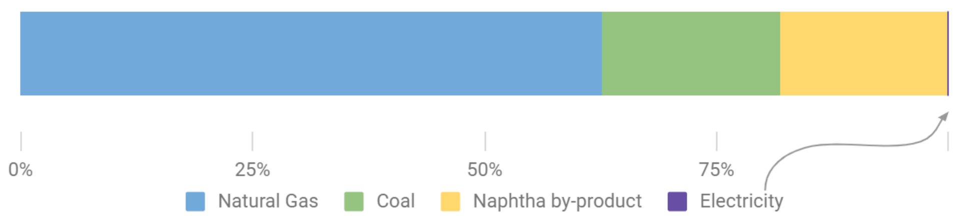

Figure 1.3: Source of hydrogen production, as share of global production in 2021 [15]

Determining the precise amount of hydrogen that is produced and its corresponding footprint is challenging. A multiplicity of production methods with different sources and efficiencies is employed, and it is frequently created as a by-product or intermediary process gas [19]. The production levels in the Netherlands were estimated by TNO for the year 2019 [19]. According to this report, the natural-gas-based production of pure hydrogen and dedicated synthesis gas was 867 $kton/y$, approximately 60% of the total Dutch annual production. Considering the associated footprint of 9.35 $kgCO_2$ per kgH_2 from Hyunah Cho et al [18], over 8 $MtCO_2$ directly resulted from Dutch hydrogen production in 2019. This is equivalent to over 5% of national emissions, even when production methods other than *SMR* and upstream emissions are disregarded.

1.1.4. Decarbonisation of Hydrogen Production

The decarbonisation strategy of the industry relies heavily on electrification and the subsequent use of renewable electricity as a driver [20]. However, in addition to their role as fuels, fossil sources also provide essential chemical building blocks: hydrogen and carbon atoms. These atoms have to be obtained by other processes in order to move away from fossil fuels completely. Renewable hydrogen production is possible through a process called water electrolysis, where renewable electricity separates water (H_2O) into its hydrogen (H_2) and oxygen (O_2) constituents [21]. This is often referred to as 'green' hydrogen, contrasting natural gas-derived grey hydrogen. Electrification and renewable feedstock production are two key pillars of the industrial decarbonisation path. It is crucial to acknowledge that both pillars hinge on a substantial increase in renewable power production and the development of supporting infrastructure [22].

Alternatively, a proportion of the emissions of conventional natural-gas-based production can be captured and sequestrated to create 'low-emission' or 'blue' hydrogen. This reduces the footprint of the resulting hydrogen product compared to conventional steam methane reforming [23]. A number of process flows in the reformer have the potential to facilitate CO_2 capture, notably the synthesis gas, tail gas and flue gas streams [24]. Different combinations lead to different capture rates for the CO_2 gas, although the majority of the capture potential lies in the flue gas stream [24]. Dual capturing constellations have the potential to achieve capture rates between 90% and 95% in the plant [23]. The resulting footprint could approach 3 $kgCO_2$ per kgH_2 [24] [25], although a significant variation exists due to venting, upstream methane leakage and energy consumption of the CO_2 sequestration.

Figure 1.4: Definitions of common hydrogen colours as means of describing their source.

1.1.5. Making or Moving Hydrogen?

In addition to local production, hydrogen demand can be met through import. Once the hydrogen molecule is obtained, its transportation methods are similar regardless of its production method and origin. Figure 1.4 shows the production pathways to blue and green hydrogen. Both of these pathways could be implemented in local production or import chains, but they require a different set of factors to be present. Especially the potential for low-cost renewable, green hydrogen production through electrolysis is not evenly distributed across the globe [26]. Countries that have access to plentiful and affordable renewable electricity could potentially transform their natural resources into export products, similar to the trade of current energy carriers [27]. The transportation of hydrogen across considerable distances can be accomplished through a variety of methods such as gaseous transport in high-pressure pipelines, shipping as a low-temperature liquid or in the form of carrier molecules such as ammonia (NH_3), methanol (CH_3OH) and liquid organic hydrogen carriers (*LOHCs*) [28].

1.1.6. Definition of Renewable Hydrogen

The Renewable Energy Directive (*RED*) legislation of the European Union considers renewable hydrogen a 'renewable fuel of non-biological origin' or *RFNBO* in short [29]. This rationale excludes low-emission hydrogen from conventional production with carbon capture and sequestration (*CCS*) due to its fossil origin, so it does not count as renewable hydrogen. The definition of renewable is contingent upon the source of the incoming electricity in the electrolysis process, which needs to meet an additionality, geographical and temporal correlation. Additionality means that the electrolyser does not merely create new demand, but comes with its own new power production from renewable sources. This must be done within the same bidding zone in the power market to prevent excessive strain on transmission infrastructure, satisfying the second criterion of geographical correlation. The third requirement of temporal correlation specifies that hydrogen must be produced within the same one-hour period as the renewable power production as per 2030.

The main objective of the *RFNBO*-label is to reduce the lifecycle emissions footprint of hydrogen production by 70% to an equivalent of 3.38 $kgCO_2$ per kgH_2 at maximum [29]. The legislation prescribes that 42% of the industrial hydrogen use must meet the *RFNBO* guidelines in 2030, increasing to 60% in 2035 [30].

1.2. Rotterdam: Port in Transition

Rotterdam has the largest European seaport [31] , although it is often referred to as a 'harbour-industrial complex' (*HIC*) due to the tight interwovenness of the industrial activity with the role of the harbour. Multiple facets of the energy transition coincide in this area, given the considerable amount of energy-related shipping traffic, its large energy-intensive industries and its role in the Dutch electricity grid. The Port of Rotterdam is owned by the Dutch State and the Rotterdam Municipality. Its role is to manage the land area, while generating revenue through port dues, land lease and contract revenue [32]. As a result, the interest of the company is to be a highly suitable location for shipping and industrial activities both in current and future times. As the energy transition heavily influences the composition of such activities, it important to the port to be a driver and connecting element to ensure that future-proof development is supported.

In 2021 over 1900 TWh of energy carriers arrived in the port, which is around 12% of Europe's energy supply and more than double the Dutch annual consumption [33]. Fossil fuels comprise practically all of these imports, particularly as crude oil and its products carry 82% of incoming energy content. A different distribution of energy transport is anticipated in the future, leaning more heavily on fuels of biological origin and hydrogen derivatives for both *HIC* and hinterland area demand [34] [35]. In this case, the hinterland is defined as the regions beyond the Port, which could be in other parts of the Netherlands, but also in Germany or Belgium.

Figure 1.5 shows the CO_2 emissions produced in Rotterdam *HIC*. The industrial signature in the *HIC* is mainly focused on petroleum refining and chemicals [33] [36], rendering the Netherlands the third-largest oil refiner in Europe [7]. Resulting from these activities, the *HIC* accounted for 18% of the total Dutch CO_2 emissions in 2021 [33] [37]. The emissions are distributed almost evenly across refining, chemical industries and electricity production [33]. The latter is mostly due to the considerable coal and gas-fired power plants in the *HIC*. Future industrial activities anticipated by the Port of Rotterdam involve production of various biofuels, recycling, carbon capture and sequestration and electrolysis [34].

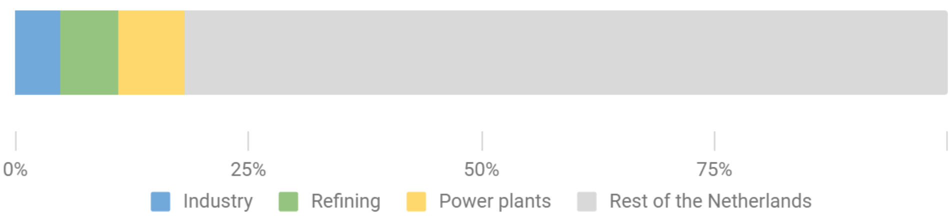

Figure 1.5: Emission sources from Rotterdam *HIC* as share of Dutch CO_2 emissions in 2021 [38] [5]

1.3. State of Hydrogen Development

This section examines the current insights and known challenges associated with the development of renewable hydrogen, with a focus on the industry in the Port of Rotterdam. Renewable hydrogen is an emerging, complex, and challenging sector that is still in early development stages but critical for the energy transition. The aim of this section is to consider the situation as it is known, which allows for a subsequent problem analysis and positions hydrogen within the broader context of energy systems in transition.

First, the current knowledge on the demand development of hydrogen in the Port of Rotterdam is investigated, after which the status of the supply pathways is considered. Next, the influence of stakeholder positions as a driving factor for hydrogen development is studied, followed up by a brief insight in the development challenges with respect to renewable hydrogen.

1.3.1. Demand Development

The Rotterdam Harbour-Industrial Complex is among the largest hydrogen consumption areas in the Netherlands. In 2021, the consumption in this cluster amounted to 400 $kton$ [33], 80% of which was used by refineries. Projections for 2025 estimate a similar consumption [38]. Hydrogen is mostly fed into process plants as a continuous baseload [39] [40] [41].

The Cluster Energie Strategie (*CES* - Cluster Energy Strategy, in Dutch) set up by the Port of Rotterdam provides projections for the hydrogen demand in the industrial cluster Rotterdam-Moerdijk, which are shown in Figure 1.6.

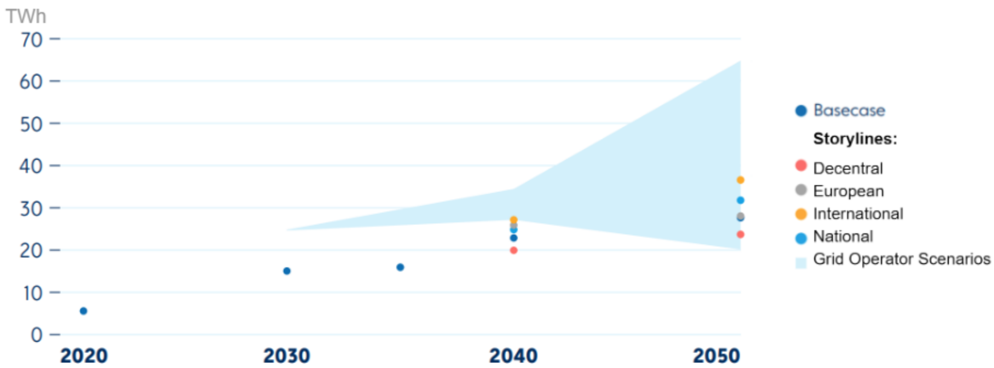

Figure 1.6: Hydrogen demand projections in the industrial cluster of Rotterdam-Moerdijk in TWh. Figure from *CES* 2024 [38], text translated by author.

In the *CES*, a 25 TWh demand is identified for 2030 [38]. The projections for 2040 and 2050 are based on the scenarios used in the Integrale Infrastructuurverkenning (*II3050* - Integral Infrastructural Exploration between 2030 and 2050, in Dutch), which was created by Netbeheer Nederland [22]. For the year 2040, a demand between 20 and 30 TWh is expected, increasing to between 24 and 37 TWh in 2050. It should be noted that the amounts in this figure relate to the hydrogen that will make use of central infrastructure, and production and direct consumption in, for example, a refinery is not included. Besides, any demand beyond the cluster is not considered.

The consumption of hydrogen in the *HIC* is currently mostly dedicated to the refining of oil products and chemical industries [33]. However, future consumption is projected for the production of synthetic fuels for shipping and aviation. Other possible consumption sectors are direct-reduced iron steel production or a certain degree of long-term storage [42] [43].

1.3.2. Supply Pathways

Multiple renewable hydrogen supply pathways are currently undergoing parallel development at a global level, as well as within the Port of Rotterdam. This section provides an overview of their current status as a reference point for future developments. Local electrolysis from offshore wind power, ammonia and alternative pathways such as *LOHCs* and methanol are considered respectively.

Electrolysis

Electrolysis is projected to yield a tiny 0.3% fraction of the global hydrogen production in 2024 [43] at 330 $kton$. However, the installed electrolysis capacity nearly quadrupled in one year to 5.2 GW_e, indicating increasing traction despite its low share of the total production. The Global Hydrogen Review 2024 indicates that the primary challenges facing developers revolve around the considerable amount of uncertainties in regulation and demand, which leads to reluctance among investors [43] [39]. Besides, development is complicated by permitting and practical challenges associated with the scaling of technology [44] [43].

The Port of Rotterdam is home to several new water electrolysis developments, although production has not yet commenced at the time of writing. Several projects have been announced, among which a 1000 MW facility from Zeevonk [45] and a 200 MW electrolyser plant by AirLiquide [46]. However, the only electrolyser that has reached its Final Investment Decision (*FID*) and is under construction is the 200 MW Shell Holland Hydrogen I [47]. An electrolysis capacity target of 2.5 GW is set for 2030, which would be more than half of the total national 3 - 4 GW aim in the Klimaatakkoord [48] [2].

Ammonia Import

Ammonia import is expected to be the largest contributor to hydrogen import globally [49] [26]. It is currently mostly used as a building block for fertilisers and chemicals [14]. Approximately 20 Mt or 10% of global production is shipped annually [49]. Due to its heavily corrosive and toxic nature, elaborate environmental and safety standards are in place [50]. Ammonia is mostly traded as a primary chemical in present times, and not to re-obtain hydrogen molecules [16]. Disintegrating ammonia molecules into its nitrogen and hydrogen constituents is possible through a process called dehydrogenation, which is often referred to as ammonia cracking [51]. This pathway facilitates the overseas production of hydrogen molecules subsequent to the arrival of ammonia at the Port of Rotterdam.

Ammonia projects dominate the plans for low-emission hydrogen trade, at 85% of the total [43]. However, it should be noted that this includes 'blue' ammonia, which is made from blue hydrogen and thus does not categorise as a carrier of renewable hydrogen. Besides, most of the 16 $Mt/y\ H_2$ worth of announced projects worldwide are still in early phases of development. Currently, eight import terminals for hydrogen (carriers) are in development in the Port of Rotterdam, with a total capacity of 1.2 MtH_2 on an annual basis [38]. Four of them are dedicated to ammonia as a carrier molecule.

Alternative Pathways

Hydrogen could be supplied through several other pathways, as discussed in subsection 1.1.5. Although plans exist to import methanol, this is mostly to use the chemical itself instead of re-obtaining the hydrogen from it [44]. An example of this is a 250 $kton/y$ electric sustainable aviation fuel (*e-SAF*) facility that has been announced in the Port of Rotterdam [52]. *LOHCs* are expected to account for some of the hydrogen imports, but the corresponding supply chains are in early stages of development [38] [44]. The same is true for liquid hydrogen, which is not expected to take a large share in hydrogen transport compared to the other technologies [26]. Pipeline transport of hydrogen is considered an important piece of the infrastructural puzzle in the hydrogen system [44]. However, pipelines such as the Delta Rhine Corridor are primarily oriented towards the export of hydrogen to hinterland areas, rather than functioning as a supply pathway.

Despite the Port of Rotterdam's generally neutral stance on the technological approach and its openness to developers of alternative supply pathways, it continues to regard ammonia and local electrolysis as primary pathways for the supply of renewable hydrogen.

1.3.3. Generic System Outlook

A schematic overview of a system that delivers power and hydrogen based on offshore wind and ammonia import is shown in Figure 1.7.

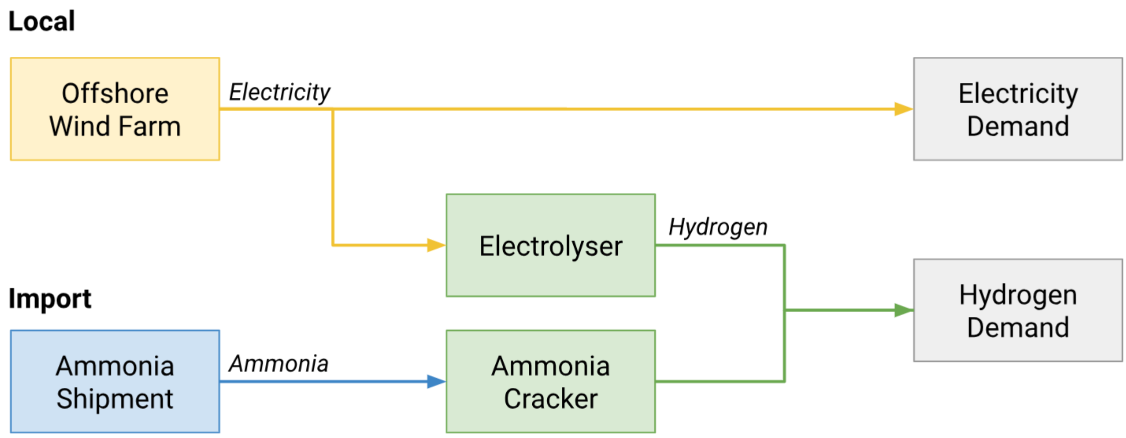

Figure 1.7: Schematic overview of the system considered in this research.

The two input flows in the system are wind energy and ammonia imports, while the outgoing flows are electricity and hydrogen. The basic system components involved are an offshore wind farm, electrolyser and ammonia cracker, which are the means of providing electricity and hydrogen outputs of the system.

1.3.4. Development Challenges

Renewable hydrogen supply pathways face several critical developmental challenges that complicate scaling and deployment. These challenges influence the feasibility and attractiveness of different pathways. This section considers challenges in the realms of Technology & Infrastructure, Economy & Market and Environmental & Social, respectively.

Technology & Infrastructure

Electrolysis in the Netherlands is close-knit with offshore wind capacity on the North Sea, as this source complies with the present subsidy regulations described in the Stimulering Duurzame Energieproductie (*SDE*) [53]. Besides, it provides high capacity factors and large potential installed capacity [54]. The targeted landfall locations for offshore wind are near industrial clusters, according to the Offshore Wind Landfall Program 2031-2040 (*VAWOZ - Exploration of Landfalls for Offshore Wind, in Dutch*) of the Dutch government [55]. It also states that ideally, new demand is situated near these locations to prevent grid congestion as a result of the large offshore wind capacity connecting to the grid. Furthermore, technological limitations exist, as the required scale of ammonia cracking has yet to be achieved [56], and electrolysis remains only known on smaller production scales. Both face considerable challenges in terms of scaling up technology and reducing the cost of components, which is the subject of the next subsection. Furthermore, any hydrogen supply pathway competes for scarce spatial resources in the port area and pressures local infrastructure [44].

Economy & Market

The financial viability of many electrolysis projects is constrained by large investment cost [43] [41]. In addition, the cost associated with power grid connection in the Netherlands are significantly higher than in neighbouring countries [40] [44], and the power from offshore wind is relatively expensive [41]. Besides, uncertain market demand development makes investors reluctant [39], which is partially due to the uncertainty of the consumption that will exist due to current policy measures. Ammonia faces a similar problem, where an additional complicating element is that it already has its own existing consumption sector in the chemical industry, which is currently dominated by fossil fuels. This demand needs to decarbonise in parallel to any role it could fulfil as a hydrogen carrier [16]. Both the market for renewable hydrogen and renewable ammonia are immature, with limited risk-hedging options and a closed market structure focused on long-term agreements as a result [57].

Environmental & Social

The spatial footprint of hydrogen production is considerable, in part due to the large areas covered by its supporting renewable energy sources such as wind farms [58] [39]. Besides, it requires a strong expansion of the power grid, which features a significant amount of land area in addition, often in close proximity to the built environment. Ammonia is a toxic gas and hydrogen is highly flammable and volatile. Although extensive industry experience exists for both, these characteristics render both gases hazardous to handle [56]. The development potential for renewable hydrogen (carriers) is unevenly distributed globally, at times concentrated in regions with limited social equity and economic advancement. As a result, its development involves moral considerations on the distribution of costs and benefits [59].

1.3.5. Influence of Stakeholders

The degree to which a certain pathway of hydrogen supply is developed is shaped by multiple interwoven driving factors and stakeholders, reflecting a range of economic, technological and policy factors. Figure 1.8 reflects potential scales in which stakeholders could have different views. The perspectives of each stakeholder are essentially their world views, which are the way in which they perceive the energy transition landscape and evaluate its future. This world view can be built up from a variety of facets, such as projections for the cost of specific components, regulation or the market [60]. Interpretations for future developments may tend towards optimistic or conservative. In addition to these world views, stakeholders may have different reactions to these perspectives, depending on their character traits and position. For instance, some could have an opportunistic approach, embracing more ambitious projects and focusing on the potential. Others could have a more risk-averse stance, prioritising reliable returns and stable conditions [60] [39]. Besides, the values of stakeholders are how they perceive the impact of hydrogen and power supply chains. Essentially, it describes what their priorities are and what they deem important.

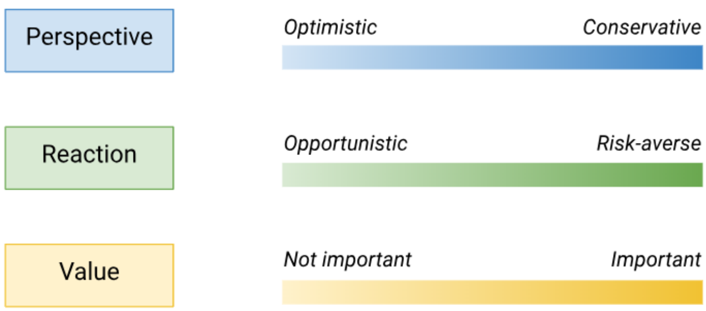

Figure 1.8: Graphical overview of the potential scales in which various stakeholders could have different views

Stakeholders could behave differently when considering development of an electrolysis project, based on their perspectives, reactions and values. An optimistic and opportunistic stakeholder with values rooted in sustainability could perceive a similar project more appealing than a conservative, risk-averse one, who focuses more on predictability and cost-effectiveness. Differences in these perceptions could be even larger between stakeholders in other areas of the hydrogen sector.

Understanding that each stakeholder at least has a unique perspective, reacts in different ways to developments and values distinct impacts in other ways than other stakeholders, is crucial to an evaluation of hydrogen supply pathways. It is an indication that there is not necessarily a hydrogen supply pathway that is the optimal case for each stakeholder simultaneously. Various consequences of developments are not always observed, interpretated and valued equally, which entails that discussion on the envisioned pathway requires stakeholders to understand the influence of differences in their stances.

1.4. Problem Analysis

Renewable hydrogen is a crucial ingredient of the decarbonisation of industry in the Port of Rotterdam and its hinterland area. Major industrial hubs with historically fossil-based hydrogen consumption encounter significant challenges in the energy transition, partially due to the realisation of *renewable* hydrogen supply. This is not merely to substitute existing fossil-fuel-based demand, but also to facilitate the anticipated new demand from other applications. However, renewable hydrogen supply is still in its developmental infancy, with two primary pathways emerging for the Port of Rotterdam: local electrolysis powered by renewable electricity from offshore wind power and hydrogen import through ammonia. Each pathway presents unique opportunities and challenges, particularly in relation to the intertwining of the decarbonisation of power production.

The potential impact of hydrogen supply pathways on the Port of Rotterdam is large, although significant complexity and uncertainty exists, as section 1.3 shows. Multiple interdependent factors -ranging from environmental and practical implications to economic and technical factors- create an interplay that complicates decision-making and strategic planning. Stakeholders such as industry, the Port Authority and the government hold different perspectives on hydrogen development, react in varied ways to new advancements and ascribe different values to the potential impacts of these pathways. The variation in perspectives amplifies the complexity, as no singular solution for hydrogen supply is necessarily optimal for all stakeholders. As a result, the development direction is based on many trade-offs on various impact factors, which could all be valued differently.

To assess the impacts of hydrogen supply pathways in a substantiated manner, a system overview would be able to provide insight on a range of scenarios. It should illustrate what is necessary to realise supply capacities, and quantify technical, but also economic impacts in concrete metrics for comparison. The research would provide a tangible foundation for discussing and comparing the impacts of potential supply pathways, thus offering stakeholders a basis to assess the options and allow a value-based approach to decision-making on these developments.

1.5. Research Objective

The objective of this research report is to provide an understanding of the techno-economic impact of renewable hydrogen supply, through ammonia import and local electrolysis, on the interests of various stakeholders in the Port of Rotterdam.

This evaluation may serve as a foundation for discussion on the development pathway of renewable hydrogen supply, in light of its complexity, uncertainty and relation to the available resources for electricity decarbonisation.

1.6. Scope

The description of the research objective inherently disregards certain facets that are not considered in this research. 'Techno-economic impact analysis' entails that only impact factors in this domain are considered, while the addition of 'renewable hydrogen' neglects classifications of hydrogen supply that do not meet the *RFNBO* requirements discussed in subsection 1.1.6. The objective is to understand the impact on various stakeholders, which means it is not meant to optimise but to explore. Lastly, the supply pathways are investigated in the context of their connection to the Port of Rotterdam.

A variety of other options have the potential to fulfil a role within the supply chains of renewable hydrogen. Although these options have not been selected in the scoping of this research, they could be substituted in follow-up analysis. This section presents an evaluation of the options that have not been considered in this research. As a source of power, only offshore wind power based in the North Sea has been considered. The Dutch *Klimaatakkoord* labels this a 'key contributor' to its future power supply [2], and the Port of Rotterdam area has been marked as a suitable landfall location for significant capacities of offshore wind [48]. Solar power, onshore wind and other forms of renewable electricity are not considered in this research. Ammonia import is the only flow of hydrogen (carrier) into the system, as it is regarded as the most prominent carrier for importation [38] [16].

Methanol, liquid organic hydrogen carriers (*LOHCs*) and liquid hydrogen are thus not accounted for. The production process and journey of the ammonia are not considered in-depth in this research, although the flow can be assigned characteristics that describe its origin, such as its cost to the point of entering the system. The ammonia is introduced to the system through shipping, and not by pipelines or other transportation modes. Besides, it is merely used to re-obtain hydrogen, and any potential alternative use cases or demand for the ammonia are disregarded. Any residual heat created in the electrolyser or cracker is not considered, nor is the option to increase process efficiency by importing heat from elsewhere. Additional system flexibility through inclusion of batteries or electricity imports outside of offshore wind is not considered, to maintain focus on the hydrogen supply chain as key research topic.

1.7. Methodology

To reach the research objective, a structured approach is developed. Figure 1.9 shows a graphic overview of the general steps in this approach.

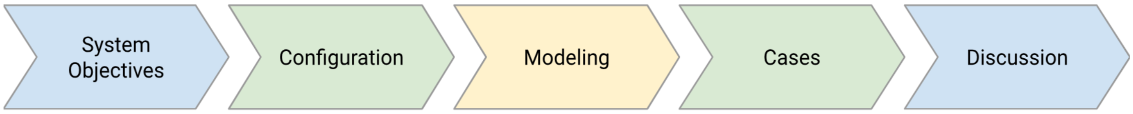

Figure 1.9: Schematic overview of the research approach.

There are five major steps to the methodology of this impact analysis for renewable hydrogen supply pathways. Each step contributes to the research objective, by integrating different building blocks to create the impact analysis.

The initial step is to define the primary objectives of the hydrogen supply system. The key question is what it should ultimately achieve. This step considers which criteria contribute to an ideal hydrogen pathway. Articulating these objectives provides a top-down approach to the high-level system aspirations that are the foundation of measurable impact. Next, concrete, measurable key performance indicators (*KPIs*) are identified that translate the system objectives into metrics. Each *KPI* functions as a quantifiable definition of an objective. As a result, the study can systematically assess each pathway's alignment with the main system targets. The reason for this numerical assessment is that not all objectives are shared among all stakeholders, nor valued equally by them. As a result, the *KPIs* provide information for decision-making, instead of striving for a single optimum. In this way, they aim to create an understanding of system dynamics and form a numerical basis for trade-offs. In order to achieve this identification of objectives and define factors of importance, a series of interviews and conversations is conducted with over 30 industry experts. These experts work in organisations such as Vattenfall, TNO, Shell, Gasunie, Ørsted and the Port of Rotterdam, although the conversations are held on personal account.

The next step is to determine the core system components and relevant technologies to realise hydrogen supply pathways. This step builds on the literature review and interviews with experts from the industry, which create insight into the current state of the research area. The essence of this section is to determine what is necessary to obtain hydrogen through this system outlook. Understanding these elements provides a basis for identifying relevant system processes and technical constraints. Moreover, as the fundamental components of this energy system, they constitute the basis of its potential impact.

The third step involves constructing a system model that maps the flows and processes within the combined hydrogen pathways. This model serves as a bridge between theoretical background and real-world data, enabling the simulation of the production, distribution and consumption dynamics of various system configurations. Using Matlab, the model captures relationships between multiple variables and parameters, ensuring that changes in one component influence outcomes across the system. By structuring the system in a numerical framework, the model allows for systematic analysis of different configurations by identifying their values on the key performance indicators. This approach ensures that the impact of design choices can be evaluated consistently across a range of scenarios. Through this, the model provides valuable insight into the trade-offs and interdependencies that define the feasibility of different hydrogen supply strategies.

In the fourth step of the process, the system model is populated with case-specific information. Relevant cases and parameters that describe the unique characteristics for the Port of Rotterdam are integrated. Consequently, the generic structure of the model is employed in a tailored context for the Port of Rotterdam. Within a comprehensive array of component sizes and operational strategies, specific configurations of interest are defined in scenarios. These scenarios are based on projections for demand of hydrogen and power. Each demand scenario can be achieved in a number of different system configurations, with greater emphasis on locally produced or imported hydrogen. The objective of this approach is to gain an understanding of how different *KPIs* change depending on the system configuration, as well as in different demand scenarios.

The final step of the methodology involves analysing and interpreting the results generated by the case study in the previous step. This discussion focuses on identifying key relations, trade-offs and sensitivities within the configurations. By comparing different system configurations, the impact of various parameters on the *KPIs* is assessed. These insights are contextualised within the broader energy transition landscape. Furthermore, an evaluation is conducted to ascertain the alignment of the results with the expectations established through background research, whilst also considering the limitations and uncertainties inherent to the approach. Ultimately, the discussion synthesises these key insights to draw meaningful conclusions about the impact of renewable hydrogen supply pathways.

1.8. Guide to Reader

In Chapter 2, the system objectives of a hydrogen supply pathway are defined, which are quantified into measurable key performance indicators. Chapter 3 is focused on the detailed system configuration and technological basis that supports it. Subsequently, Chapter 4 describes the system model logic, after which Chapter 5 considers a number of scenarios dedicated to the Port of Rotterdam case. Next, the results are discussed, conclusions are drawn, and a future recommendations section is included.

2
Main System Objectives

In this chapter, several considerations of development complexity are discussed before defining the system objectives. The high-level system objectives are determined subsequently, in combination with their measurable representations in the form of key performance indicators (*KPIs*). This results in a unified framework for evaluating hydrogen supply pathways. The system objectives define the overarching goals of the system and serve as guiding principles for development. These objectives are inherently broad and abstract, requiring translation into specific, quantifiable metrics to enable practical assessment and comparison of scenarios. *KPIs* bridge the gap between conceptual objectives and actionable analysis, offering measurable definitions that together constitute the abstract target. The provision of concrete descriptions of system objectives facilitates discussion on trade-offs, given that stakeholders ascribe different values to different objectives.

Section 2.1 discusses several considerations of development complexity. Next, the foundation of impact assessment is considered in section 2.2 and the ideal supply system is described in section 2.3, after which the high-level system objectives are defined in section 2.4. Subsequently, measurable key performance indicators are established to quantify the high-level objectives in section 2.5. Finally, these *KPIs* are selected in section 2.6.

2.1. Considerations of Development Complexity

Development of renewable hydrogen pathways is influenced by a multitude of systemic factors that underscore the multifaceted nature of the energy transition. A number of key considerations stand out, which are discussed in this section. Its purpose is to illustrate the complex nature of hydrogen development in the Port of Rotterdam, thus reflecting on the research starting principles prior to the definition of the system objectives.

2.1.1. Electrolysis & Offshore Wind Intertwined

The development of offshore wind and electrolysis is deeply intertwined, driven by the increasing need for renewable energy to decarbonise both the electricity grid and hydrogen production. By locating electrolysers near offshore wind landfalls, system benefits such as congestion management could be achieved. In this case, congestion management would be defined as the alleviation of the power grid by preventing large quantities of offshore wind from inundating the power system from the coastal areas. However, from the perspective of decarbonisation of inland electricity consumption through offshore wind power, this is only useful in case of lacking demand from these areas. If electrolysers consume a significant proportion of the wind power generated while the hinterland areas do not see their power demand satisfied, it cannot be said that the electrolysers are aiding the system as a whole. Of course, this only holds when the transportation capacity exists to meet the required hinterland demand in the first place.

Electrolysers are often highlighted for their potential role in grid balancing by absorbing surplus renewable energy during periods of low electricity demand [2]. However, this perspective reveals underlying complexities. As flexible, large-scale power consumers, electrolysers could theoretically stabilise the grid in this manner, yet their high capital costs make frequent operation far below rated capacity economically unfeasible without significant financial incentives. Developers predominantly view electrolysers as industrial decarbonisation tools rather than grid services [61] [41] [60], which introduces tension between their operational goals and potential system-wide benefits. The recent RVO tender scoring schemes for IJmuiden Ver plots reveals their notion of urgence on system integration of new offshore wind capacity: up to 40% of the points is awarded based on efforts to develop power demand in suitable locations or cooperate in uncompensated decrease in transport capacity [62] [63].

A further challenge arises from the allocation of costs and benefits across the system. While curtailment of excess renewable energy is likely to play a role in the future energy landscape, determining the optimal level of curtailment and whether investing in flexible infrastructure, such as electrolysers, is justified requires careful systemic evaluation. The question of cost distribution among stakeholders remains unresolved, emphasising the need for a system-based approach to assess where flexibility is most efficient and how responsibilities and benefits can be equitably shared among stakeholders.

2.1.2. The Future of Dutch Industry

Certainty of demand for renewable hydrogen hinges on strategic decisions regarding the industrial future of Europe and the Netherlands. A lack of clear policy direction or a passive approach risks a gradual departure of energy-intensive industries [64] [65]. Reductions in such industries carries significant side effects, including job losses, diminished economic activity, and reduced strategic autonomy over critical materials and products—a concern highlighted in reports such as Draghi's [66]. Although disappearing industry may yield progress with certain sustainability goals on a *national* scale, as long as it is not coupled with reduction of the consumption of the associated industrial products, it provides no actual improvement on a *global* scale. There is a possibility that the production of the products in other locations may even result in adverse environmental consequences due to increased pollution. Besides, it increases dependence on other countries to provide the resource.

A focused vision is essential to determine which industries the Netherlands and Europe aim to retain or attract and the measures required to support them. As emphasised by the CEO of the Port of Rotterdam, sustaining desired industries demands deliberate effort [67]. This requires a clear assessment of existing industrial assets, identifying those worth maintaining or expanding, understanding their needs, and ensuring affordable, renewable electricity and supply of green feedstocks like hydrogen to meet their electrification and decarbonisation requirements. The energy transition will alter the landscape of optimal locations for industrial activity. Those with access to inexpensive and plentiful renewable electricity may gain a competitive advantage. Consequently, locations with historical significance to industrial activity may experience a decline in their appeal, a phenomenon that some expect in the Dutch clusters [65], in part due to the high grid fees and cost of electricity [68] [69].

The overarching question remains: which industries are most valuable to retain or attract, what do they need, and what is necessary to deliver these essentials? Therefore, the subsequent question of which hydrogen demand will need to be satisfied and which trade-offs in the supply system design reflect proper balance of stakeholder interests is highly relevant, but also complicated.

2.1.3. Demand Dynamics

Demand plays a crucial role in shaping the renewable hydrogen market. The systemic challenge of an immature market is the chicken-and-egg problem between demand and supply. Commodity markets in this phase hinge on long-term agreements between a limited amount of producers and offtakers due to the absence of extensive infrastructure, information systems and regulations [57]. Once more diversity in supplies and offtakers exists, a mature market grows. However, the challenges in this first phase are significant, because of the large capital expenditures associated with the infrastructural and industrial development of renewable energy systems. Especially in the early phases of scaling up and rolling out technology, realising a feasible business case can be difficult [39].

This holds for both hydrogen producers and consumers. Industrial offtakers are hesitant to invest in costly plant adjustments or long-term hydrogen contracts if it remains uncertain whether the added cost can be recuperated in their product, which often competes on the global market [69]. Likewise, these guarantees are a requirement for the production-side to reach their investment decisions [39].

An additional complicating factor is the fact that ammonia consumption is a major target sector for decarbonisation itself. It is among the most important primary chemicals, which are key ingredients for nitrogen fertilisers, plastics, pharmaceuticals, construction materials and numerous other chemicals [14] [16]. The emissions attributed to solely these two commodity chemicals represent approximately 1-2% of global CO_2 emissions, the majority of which are the result of hydrogen feedstock production [14] [70]. In other words, a significant quantity of fossil-based ammonia needs substitution with renewable or low-carbon ammonia. As a result, this process of decarbonisation competes with the potential role for ammonia as a hydrogen carrier.

Besides the chicken-and-egg challenges related to the emergence of new renewable hydrogen industry, other uncertainties with respect to demand exist. Hydrogen is consumed in a range of applications, which do not face equal decarbonisation targets globally [29]. Consequently, for a subset of consumers, blue hydrogen usage may be adequate. In such a scenario, the demand for the gas would not need to be met entirely by renewable hydrogen. Besides, some energy analysts expect that too expensive or otherwise troublesome pathways for renewable hydrogen would lead to the development of alternatives for the desired end product [71]. For example, the use of nitrogen fertilisers could decrease if alternatives prove more interesting in a decarbonised future.

2.2. Foundation for Impact Assessment

The considerations in the preceding section illustrate the multifaceted and interwoven nature of hydrogen development in the Port of Rotterdam. It reflects on the guiding principles of this research. Establishing high-level targets is a crucial step in evaluating the performance and impact of hydrogen supply pathways. These targets represent the fundamental goals that a supply system should aim to achieve, and thus serve as benchmarks for its success. These principles may be regarded as a framework for the general design of energy systems, in particular for the dual supply of hydrogen and power. In theory, an ideal hydrogen supply would perfectly balance all relevant objectives, delivering all of the benefits without any disadvantages. However, in practice, these goals are often in tension, requiring trade-offs between competing interests to address real-world constraints.

To understand and evaluate these trade-offs, it is first necessary to determine what the main system objectives of this hydrogen supply system are. As section 1.3 showed, impacts of hydrogen supply pathways are perceived and valued differently across various stakeholders. As a result, no optimum solution is likely to exist that balances all interests equally. The definition of system objectives serves to provide stakeholders with a framework within which they can identify and prioritise the factors of interest, which may vary in importance.

A schematic overview of the framework is shown in Figure 2.1. The framework constitutes a breakdown tree that starts with abstract ideals and objectives, which are linked to definable key performance indicators. As seen in Figure 2.1, the impact analysis framework has three layers. The ideal situation represents the pinnacle of achievement, wherein all objectives are met without compromise. As this is frequently not the case, reality demands trade-offs between the different objectives. These objectives are high-level ambitions that describe the separate desired outcomes of the ideal situation. As such, these objectives are not directly measurable. Key performance indicators break down the main objectives into specific, measurable targets. They translate the abstract objectives into concrete items or indexes. Often, they are comprised of multiple components, which create a comprehensive overview of factors of influence. The key performance indicators are quantified using metrics, which provide an actual numerical value that can be assessed. Therefore, metrics allow for the comparison of impacts across different pathways.

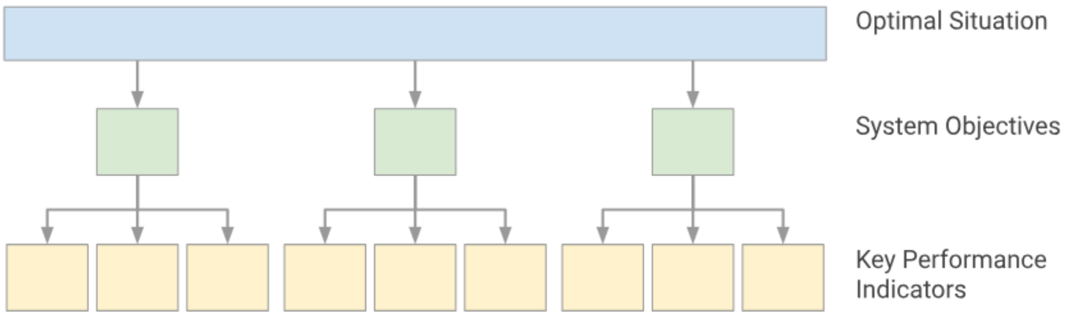

Figure 2.1: Schematic overview of the system objectives of a hydrogen supply.

2.3. The Ideal Hydrogen Supply

The ideal situation with regards to renewable hydrogen supply is one where the supply targets are met without causing side effects. In an ideal case, hydrogen is always delivered in an economically viable, environmentally and socially sustainable way, while a secure and resilient supply is constituted. The selected method would integrate into the current system seamlessly, have a feasible timeline, provide socio-economic benefit to every associated community and have no adverse consequences on ecosystems. Besides, in the case of a well-connected harbour-industrial complex with a large hinterland area, such as the Port of Rotterdam, the pathway should also facilitate the energy transition in hinterland areas.

2.4. Defining System Objectives

The main system objectives of a renewable hydrogen supply serve as the fundamental pillars of ideality. Once all objectives have been met, the result will be an ideal situation as described in section 2.3. To define these objectives, a background study was conducted that consisted of literature review and various interviews with stakeholders. Other conceptions and objectives may exist regardless, however, the three objectives shown in Figure 2.2 form the basis of the impact analysis in this research.

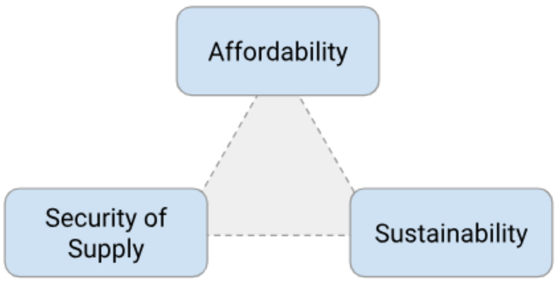

Figure 2.2: The main system objectives that are defined for a renewable hydrogen supply.

A decent affordability, high security of supply and proper sustainability are all valuable objectives for a renewable hydrogen supply. All three combined, they constitute the ideal situation. However, given that reality often precludes the possibility of achieving the ideal situation, the three main objectives cannot simultaneously be fully ideal as a consequence. They form an interconnected trilemma, in which prioritising one objective can often come at the expense of another [72]. The balancing act that results from this relation creates a dynamic in which trade-offs must be done between the main system objectives.

For instance, a pathway that is highly affordable might lack the necessary security of supply. Conversely, pathways with good sustainability and decent security of supply might require costly investments, decreasing their affordability. The interaction between the objectives is not exclusively negative for any pathway, as some combinations where all three benefit from a certain system design could exist. Besides, factors of interest could interact with different objectives. For example: if a slightly more CO_2 intensive pathway is developed within a fraction of the time of another, it could prevent more emissions in its lifetime due to its earlier substitution of fossil-based hydrogen.

2.4.1. Affordability

Affordability is the objective that aims for economic feasibility of a pathway. A high affordability allows for lower risk investment and a more attractive adoption of the hydrogen product, although it is also related to the system cost borne by society, for example through infrastructure expansion. The affordability of hydrogen is an important pillar to stakeholders, and can be a limiting factor in the development of supply pathways [39] [41]. Within projects, affordability often represents a primary objective [60] [72]. As discussed in section 1.3, many projects are paused or canceled prematurely because of issues considering their financial situation. Affordability could also relate to the end product of a process where hydrogen is used as an intermediary or feedstock. The degree to which the cost of a final product increases due to substitution of fossil-based with renewable hydrogen can also be considered in the realm of affordability. Cost can be distributed across various stakeholders, which can each have a different perspective on affordability.

2.4.2. Security of Supply

The security of supply is defined as the reliability of the hydrogen flow originating from a supply pathway. Essentially it means that the hydrogen supply functions orderly at the time of demand, which relies on the development of the supply chains and their resilience. As such, it features both a long-term and short-term definition. Security of supply is highly important to stakeholders [39] [73] [74], and was also identified as a key point of improvement for Europe in the report Mario Draghi wrote for the European Commission [66]. The long-term risk of not achieving legislative renewable hydrogen targets can lead to high emission-related fines or partial shutdown of facilities [41]. Short-term supply interruption is also undesirable, as the product hydrogen often feeds into chemical facilities that can not easily adjust production levels on a momentary basis [40] [41]. Geopolitical fluctuations also influence the supply resilience on the longer term [72], while inclusion of storage facilities provides a potential increase in supply certainty.

2.4.3. Sustainability

This trilemma used to be a dilemma for a long time in the energy sector, often in disregard of the sustainability pillar that became more important in recent years, according to Spencer Dale, Chief Economist at bp [72]. A key driver of the transition to renewable hydrogen is the matured importance of the sustainability pillar. It is described in two main facets in this research: environmental and social sustainability. The concept of environmental sustainability can be defined as the degree in which impact is made on the surrounding environment, nature and resources. Such effects can be either beneficial or detrimental. Social sustainability is defined as its impact on societies, again both in terms of benefits and negative consequences.

2.5. Defining Key Performance Indicators

In this section, the key performance indicators *KPIs* are introduced as measurable definitions of the high-level system objectives established for renewable hydrogen supply pathways. While objectives set the overarching vision, *KPIs* translate these goals into quantifiable metrics, allowing for system configuration comparison. In this way, the *KPIs* are a concrete description of factors of interest that determine the attractiveness of hydrogen supply pathways based on the high-level objectives.

The process of key performance indicator identification takes each system objective as a starting point. Each *KPI* presented in this section is identified through literature research and interviews with stakeholders and industry experts. These sources help to pinpoint the concrete factors of interest that reflect the system objectives. The initial stage of the process is to establish a comprehensive list of potential *KPIs* from the research phase. This list is condensed into a short selection that is considered in this study. The selection process prioritises *KPIs* that do not only reflect the objectives, but are also adaptable to system modeling based on the overview in chapter 3.

Each main system objective is the foundation of concrete metrics to compare pathways, and the *key performance indicators* are considered as descriptions of them. As such, they are used as the starting point to determine them. While the resulting longlist is not claimed to be exhaustive and many other *KPIs* could be considered, it is designed to be sufficiently comprehensive to capture the key dimensions relevant to this study. Overlap and interdependency between *KPIs* is also avoided when possible.

2.5.1. Affordability

The first objective that is quantified into *KPIs* is affordability. The corresponding list of indicators is shown in Table 2.1.

Cost & Benefit	**Uncertainty**
Capital Expenditure	Cost Uncertainty
Operational Expenditure	Exposure to Market Volatility
Economic Value Created	Global Competitiveness
Subsidy Dependence	

Table 2.1: The key performance indicators associated with affordability

Many stakeholders mention that the return on investment of a project is the main driver or hurdle for its development [39] [60] [40] [41]. As this metric encompasses the anticipated revenue generated by the project, which is beyond the scope of this research, the emphasis will be on the key drivers of the cost aspect of the return on investment. One of them is capital expenditure (*CAPEX*), which is an important measure of affordability. It is described as the monetary funds required before revenue can be generated, for example to build facilities, infrastructure or to train employees. Besides this amount, a measure of affordability is the operational expenditure (*OPEX*), which can contain the cost of process feedstock, wages and maintenance. The *OPEX* and annual deprecation of the *CAPEX* could be spread across production volumes of hydrogen and power to provide an indication of their unit cost. These are common means of describing the affordability of these end products, which means they allow comparison with other power and hydrogen-yielding systems. However, it should be noted that this process implies a distinct distribution of these costs across different stakeholders, which goes beyond the objective of this research.

The economic value created through a system configuration essentially defines the significance of its role in the economic ecosystem in the regional or national economy. A part of the value of industrial activity facilitated by this system is created indirectly, through the stimulation of economic activity in supporting sectors such as finance, logistics and services. Currently, ancillary sectors of the industry contribute to a significant added value within the Port of Rotterdam ecosystem [75].

Cost uncertainty is a major factor of interest in the development and financing of system components [39] [60]. Although it could be considered a characteristic of the corresponding cost itself, its effect on the total cost uncertainty in the system is also a system trait of a certain configuration. One of the means of cost-benefit distribution discussed above with respect to hydrogen and power cost is public subsidy schemes. The degree to which the system development leans on such supporting constructs could be a means of describing its affordability with respect to the public cost burden.

Many developers indicate that exposure to market volatility is a major decision factor in their development processes [39] [60]. Essentially, this relates to both revenue and cost sides of the project return rate. Exposure to the ammonia, hydrogen and power markets and resulting cost-benefit fluctuations are mentioned to be challenging to predict and estimate risks for. The degree to which a hydrogen supply system is exposed to market volatility is therefore considered a potential *KPI*. In addition, the uncertain competitiveness of locally produced products on a global scale is a broader indicator of uncertainty

2.5.2. Security of Supply

The second objective that is quantified into *KPIs* is security of supply. The resulting list of indicators is shown in Table 2.2.

Supply Profile	**Supply Chain Resilience**	**Practical Factors**
HIC Hydrogen Loss of Load	Infrastructural Vulnerability	Development Feasibility
HIC Power Loss of Load	Domestic Hydrogen Production	System Adaptability
Hinterland Hydrogen Loss of Load	Diversity of Supply Sources	
Hinterland Power Supply Volume	Geopolitical Robustness	
Hinterland Residual Demand Variability	Strategic Storage	
	System Redundancy	

Table 2.2: The key performance indicators associated with security of supply

The loss of load is defined as the amount of hydrogen or power that is in demand, but not delivered [76]. This metric holds important short-term security of supply information, as it can indicate how much and how often the system is unable to provide. It is both a measure of total supply shortage and supply stability, as high losses of load are undesirable in general. Besides, as a large harbour-industrial complex with extensive connections to its hinterland, the Port of Rotterdam could play a pivotal role in the energy and materials transition of these areas. This holds for both hinterland contributions in terms of electricity and hydrogen supply. The total delivered amount of electricity and hydrogen is a factor of interest, but for power in particular the profile variability of the residual power is important too. In case a strongly varying power demand profile remains after the contribution of this power system, this presents challenges for its alternative supply. Therefore, low variability of the remaining power demand is a valuable supply quality [77].

’Supply chain resilience’ is a wider category that encapsulates multiple *KPIs* that describes the degree to which the system can withstand destabilisation, for example through temporary loss of components. Infrastructural vulnerability as a result of dependency on remote submersed power cables is an example of this [78]. Susceptibility to disruption of import flows is another indicator of this, which relates to import dependency [79]. This is captured in the *KPI* ’domestic hydrogen production’. Besides the distinction between local production and import, general diversity of supply sources is another means of describing supply chain resilience. The retrieval of system imports from a wide range of sources can enhance the resilience of the system in the event of the loss of a source. This is often mentioned by experts as a characteristic for the demand-side to strive for [60] [74] [73] [57]. It is considered a way of spreading risk across a variety of supply sources or pathways. Geopolitical robustness of a supply chain indicates its resilience to shifting relations between nations and modified political situations. Major dependency on specific nations in particular is a potential risk for the supply, as indicated by several experts [60] [80] [66].

The amount of strategic storage available in the system is another indicator of the supply resilience to disruptions. For example, dunkelflautes or unnatural causes could result in the requirement for longer storage than would be necessary in normal operating conditions. System redundancy expresses the degree to which the system is vulnerable to disruptions from single components being out of order. Designing systems with redundancy is common practice in engineering to increase availability and reliability of a system [81].

The next *KPI* is whether the development of system components is feasible on a specified timeline. This indicator considers the feasibility of the construction of infrastructure, production and storage facilities. These are heavily influenced by permitting and regulatory developments, as well as component sourcing constraints and logistical challenges. The development feasibility reflects the probability that the supply chain is developed to satisfy demand, which is a means of supply security.

Lastly, system adaptability indicates the degree to which the system design can be adjusted based on progressive insight through the years. It is possible that as the energy transition unfolds, an updated design philosophy leads to the desire to change the initial system configuration to realise a more successful design. A large degree of inflexibility to this could be a downside of a supply chain development [78].

2.5.3. Sustainability

The third objective that is quantified into *KPIs* is sustainability. The resulting list of objectives is shown in Table 2.3.

Emissions	**Resource Impact**	**Safety**
Carbon Footprint	Resource Intensity	Annual Ammonia Shipments
Emissions Prevented	Circularity of Components	Average Ammonia Storage Volume
NO_x Footprint		Average Hydrogen Storage Volume

Quality of Living Environment	**Societal**
Spatial Footprint	Job Creation
Noise Pollution	Social Justice
Ecological Impact	

Table 2.3: The key performance indicators associated with sustainability

The carbon footprint serves as a primary catalyst for the transition from fossil-based to renewable hydrogen [82], as discussed in chapter 1. As a result, the equivalent carbon intensity of the replacement supply pathway is an important measure of sustainability. In addition, the displaced greenhouse gas emissions are a valuable insight into the averted climate impact. It is not by definition the same as the difference in footprint between fossil and renewable pathways, as a pathway with a much more condensed development timeline and earlier operational date could potentially displace more emissions across its lifetime. Nitrous oxides emissions are a major bottleneck in construction in the Netherlands, especially in Natura2000-labeled areas, which also border with the port area [44]. Ammonia cracking has a tendency to produce these gases during operation [80], which is an impact in the realm of environmental sustainability.

Energy systems based on renewable sources tend to be demanding on the living environment, especially when they must be developed in an already strongly occupied area such as the Netherlands [78]. The impact of the development on the quality of the living environment can be considered a mid-level target encompassing multiple *KPIs*. The Port of Rotterdam is particularly confronted with significant challenges in terms of spatial organisation [44], which make the spatial footprint of each pathway a highly important *KPI*. Limited -suitable- space is available, and renewable power production and infrastructure involve considerable surface area requirements [73] [80] [44]. In an already heavily industrialised area, noise pollution and the corresponding permitting considerations are factors of interest for the comparison of pathways and the necessary components [44]. Besides, again partially due to the proximity to natural areas, ecosystem impact reflects concerns about the effects on the surroundings.

Another important category of *KPIs* is the use of resources. Resource intensity covers the use of rare earth elements, which has become more important in Europe following the Critical Raw Materials Act [83] and report of Mario Draghi [66]. Besides, it could reflect the use of fresh water as a process feedstock or cooling medium. In accordance with this *KPI*, the circularity of components is indicative of the extent to which the recycling of key or scarce materials is feasible from the system components [82].

As a result of industrial activity and economic development in the *HIC* area, job creation across various sectors and skill levels underlines the socio-economic role of the port, influencing its social sustainability. Besides, elaborate development could involve new cost and benefit distributions of its yields and burdens. Social equity considers the fairness of these distributions. Many interpretations of social equity for energy systems are possible, focusing on different parts of the distribution of yields and burdens [78]. For example, distributional justice describes the extent to which these are not spread unfairly across specific parts of society or stakeholders. Historical justice acknowledges the damages of previous energy system configurations, such as historical carbon emissions or mining legacy in specific regions. Intergenerational justice involves realising the righteous shares of system cost and benefits between current and future generations, as international justice does between nations.

The last *KPI* considers the handling and storage of hazardous substances. For example, ammonia is highly toxic and corrosive [84], rendering its use and transportation potentially dangerous and therefore highly regulated [56]. Both hydrogen and ammonia are often stored as compressed gases, which imposes handling risks [50] [85]. In addition, hydrogen has a wide flammability range in air and extremely low ignition energy compared to other fuel gases [86], which counts to its handling challenges. The annual ammonia shipments and average ammonia and hydrogen storage volumes can be considered measurable *KPIs*.

2.6. Key Performance Indicator Selection

The selection of key performance indicators in this study was guided by two primary considerations: suitability for system modelling and relevance to an exploratory assessment of hydrogen supply pathways. In light of the intricacy of the hydrogen supply chain, the selected *KPIs* were chosen to provide a comprehensive yet manageable depiction of system behaviour, thereby ensuring that crucial trade-offs could be analysed effectively. Metrics that are quantifiable within a techno-economic modeling framework were emphasised, allowing for consistent numerical evaluation across different system configurations. The selection of *KPIs* is shown in Table 2.4.

Affordability	**Security of Supply**	**Sustainability**
Capital Expenditure	Hydrogen Loss of Load to *HIC*	Annual-equivalent CO_2 Footprint
Operational Expenditure	Power Loss of Load to *HIC*	Spatial Footprint in North Sea
	Hydrogen Loss of Load to Hinterland	Spatial Footprint on Land
	Hinterland Power Supply Volume	Annual Ammonia Shipments
	Hinterland Residual Demand Variability	
	Domestic Hydrogen Production	

Table 2.4: The selection of key performance indicators considered.

The selected *KPIs* include capital and operational expenditures, which provide insight into the economic feasibility of various supply pathways. These can be defined system-wide, thus avoiding the implication of cost and benefit distributions across different stakeholders for the purpose of this research. The objective of each indicator is to be as low as possible.

The loss of load for hydrogen and power in Rotterdam, as well as the loss of load for hydrogen in the hinterland, were incorporated as indicators of security of supply. The rationale behind this selection is that unmet demand constitutes a fundamental metric in the evaluation of supply systems, which should ideally be as low as possible. A contrasting approach is adopted for hinterland power supply volume, wherein any supply volume is considered beneficial. In order to capture the dynamics of power distribution, hinterland residual demand variability was included, in recognition of the fact that increased variability may pose challenges for grid stability and energy planning. It is essential to emphasise the distinction between these concepts, as the supply volume is representative of the power that is delivered, while the variability of the residual demand offers insight into the characteristics of the remaining demand load. Furthermore, domestic hydrogen production was analysed in order to evaluate the system's reliance on local versus imported supply sources. Several other *KPIs* in the realm of security of supply are not considered on account of their more subjective or ambiguous measurability.

In the context of sustainability, the carbon footprint and the spatial footprint were identified as the primary indicators. The spatial footprint was further categorised into offshore (North Sea) and onshore land use, acknowledging the distinct spatial constraints and order of magnitude of both. The objective is to minimise each of the footprints. Finally, annual ammonia shipments were incorporated into the study to reflect the logistical and infrastructural demands of an import-dependent hydrogen supply chain. It can be argued that a large number of shipments presents a potential downside.

While other *KPIs* could potentially offer further insights, the selection was constrained by the scope and expertise of this particular study. Factors such as the broader socio-economic impact and policy feasibility were not included due to the difficulty of integrating them into a numerical modelling framework. Nevertheless, these factors remain relevant for future research and can provide valuable supplementary insights to the quantitative analyses conducted using the selected *KPIs*.

3
System Configuration

This chapter covers the second step in the methodology, which is to identify the system components required to create a hydrogen supply pathway. The essence is to determine what is necessary to obtain both power and hydrogen from a system. First, a more detailed schematic system outlook is drawn up, which consists of three sections, based on power, ammonia and hydrogen-related components. Each of the components and their respective underlying technologies are subsequently investigated and considerations with regards to the complexity of their development are discussed.

3.1. Schematic Overview

The complete schematic overview of the complete system is shown in Figure 3.1. This is a more specific system outline compared to Figure 1.7 and involves the actual components and process flows considered in the system configuration of this research. The 'Production & Shipping' component in the bottom left is drawn in dashed lines, as it is not considered in this research, but indicates the origin of the ingoing ammonia.

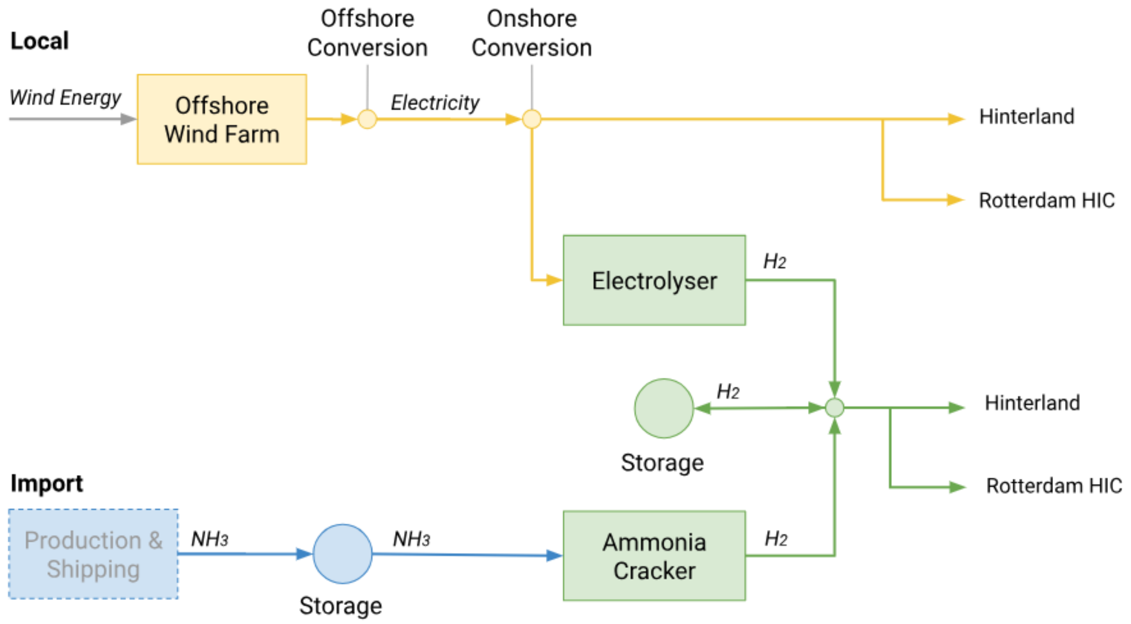

Figure 3.1: Schematic system overview of the considered components and flows in this research.

Three main segments are identified, which are related to power (**yellow**, on top), ammonia (**blue**, bottom left) and hydrogen (**green**, middle and bottom right). In the next sections, each of these segments is considered.

3.2. Power Components

The first segment of the total system outlook is related to the power components, as distilled in Figure 3.2. Wind energy is converted into electricity in the offshore wind farm, discussed in subsection 3.2.1, after which it is converted and transported. This process is described in subsection 3.2.2. Lastly, the power demand is considered in subsection 3.2.3.

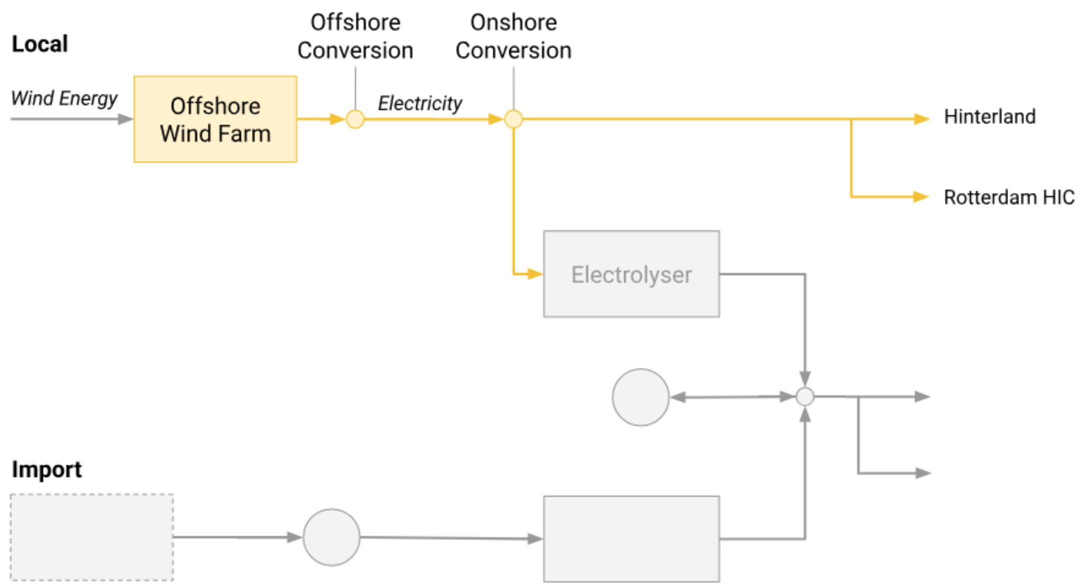

Figure 3.2: Power components highlighted in total system schematic

3.2.1. Offshore Wind Power

Wind can be defined as a flow of air relative to the surface of the Earth. This flow contains kinetic energy, a proportion of which can be extracted and converted into electricity through the use of wind turbines. The specific design of the turbine blades results in a pressure differential across the upper and lower surfaces, which generates a lift force that induces the rotation of the rotor [87]. The rotor is connected to a power generator, either directly or via a series of gearboxes. This enables the extraction of a proportion of the wind energy present in the airflow, and its respective conversion to electricity [88].

The velocity of the airflow is dependent on its height with respect to the surface [87]. Due to friction effects, the wind speed is lower near the surface and recovers with increasing height. In order to predict the energy yield of a wind turbine, it is necessary to determine the wind speed at a reference height. This is typically the height of the hub of the turbine, which depends on the specific model type and construction configuration. The potential power output of a turbine depends on the wind speed [87].

In order to determine the power production of a turbine, the wind speed is required, corrected to the hub height of the turbine. The turbine-specific power curve leads to the corresponding power production, based on the wind speed at hub height. In this research, the power curve of the Vestas V164 10 MW with a hub height of 104 m was selected in renewables.ninja to obtain the annual power production curve. Besides, the meteorological information for the year 2019 was used at the location of the IJmuiden Ver wind farm.

3.2.2. Offshore Power Conversion & Transmission

Between the offshore wind farm and the power consumers onshore the produced power is converted and transmitted through the grid, which is operated by the Transmission System Operator (*TSO*), which is TenneT in this area of the North Sea [89]. TenneT has a standardised layout for the grid connections of offshore wind farms further away from the coast, which would be applicable to new farms that connect to Rotterdam *HIC*. As shown in figure Figure 3.3, this involves a high-voltage direct current (*HVDC*) transmission.

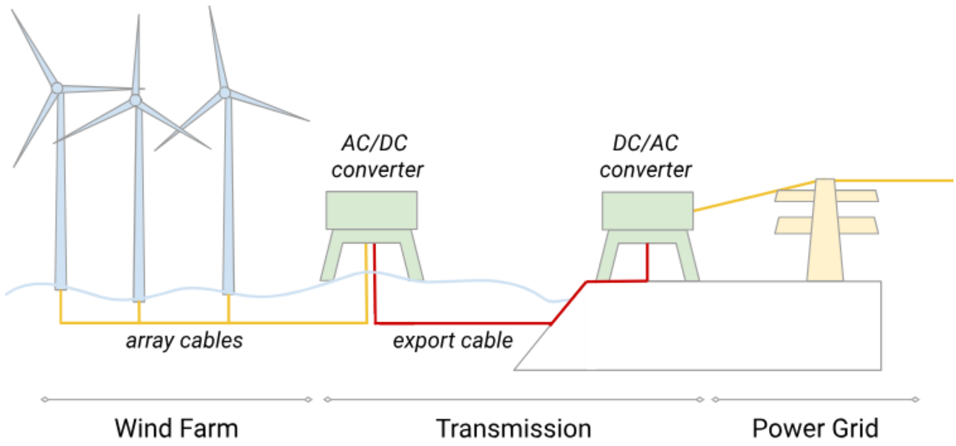

Figure 3.3: Schematic of power conversion and transmission Net op Zee, freely adapted from TenneT [90]

The 66 kV *AC* array cables from the wind farm connect to the *AC/DC* converter station of the grid operator, where their loads are combined into a single 2 GW export cable of 525 kV *HVDC* that covers the distance to the landfall onshore. A *DC/AC* converter station and subsequent substation connect the wind power to the 380 kV *AC* grid [89]. The transmission of power beyond the onshore converter station is conducted exclusively via the power grid, where this research assumes no onshore transmission within this system. The electrolyser location is assumed to coincide with the onshore converter, and both other power consumers attach to the power grid without additional boundary conditions.

3.2.3. Demand

Demand is essentially the basis of the system operation. Power demand within the Rotterdam *HIC* and the hinterland represent two distinct profiles. The *HIC* power demand is defined as the industrial processes and facilities in Rotterdam, generally characterised by a flat, baseload demand. This consistent energy requirement reflects the steady operations of industrial users. The hinterland has a more dynamic power demand profile, which might request more power at some instances than others, as seen in subsection 1.1.2. The hinterland power demand may vary based on patterns influenced by seasonal and daily energy needs. The demand profile height can be scaled depending on the targeted fraction of power delivery for the system design. The final power demand in the system is internal, from the electrolyser that requires a significant amount of power to operate. Electrolyser hydrogen output is related to its power consumption, which is allowed to vary upon availability of wind power.

3.3. Ammonia Components

The second segment of the total system outlook is related to the ammonia components, as distilled in Figure 3.4. Ammonia is produced and shipped, which will be briefly touched upon in subsection 3.3.1. Next, its storage is considered in subsection 3.3.2, followed up by the cracking process in subsection 3.4.2.

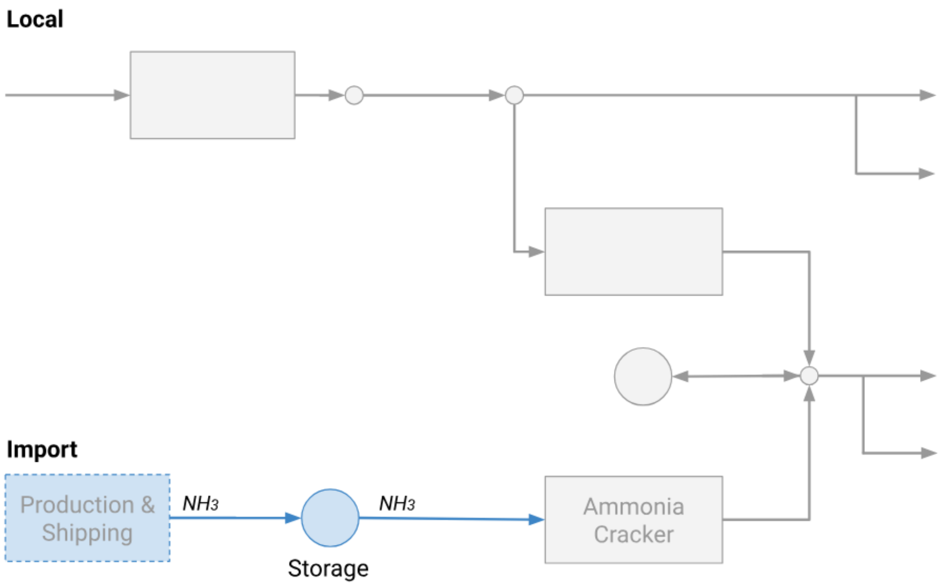

Figure 3.4: Ammonia components highlighted in total system schematic

3.3.1. Prior to System Entry

Although no in-depth evaluation of the ammonia production and shipping process is done in this research, a brief high-level overview is given in this section to provide context for the characteristics of the ammonia flow and its impact.

Production

Ammonia (NH_3) is commonly synthesised through the Haber-Bosch process, where nitrogen (N_2) from the outside air reacts with hydrogen (H_2) [16]. Production of ammonia on a large scale is common, as it is an important primary chemical for nitrogen fertiliser production, among other applications [14]. However, it should be noted that the production process is almost exclusively based on fossil fuels. The majority of these fuels is used in the extraction of the hydrogen building block [16], as discussed further in subsection 3.4.1. Due to the renewable hydrogen requirement set forth in the scope of this research, only ammonia produced with renewable electricity is considered as a hydrogen carrier.

Shipping

Approximately 20 Mt or 10% of global production is shipped annually [49], mostly in liquefied state through refrigeration to -33 $°C$ or pressurised to 20 bar at ambient temperature [50] [16]. Upon system entry, the ammonia is considered to be inside a shipping vessel in refrigerated condition at ambient pressure in this research. This is in line with the design choice made by Fluor in their ammonia cracking study for the Port of Rotterdam [56].

3.3.2. Ammonia Storage

Liquid ammonia is typically stored in refrigerated insulated tanks with capacities in proximity to 60 $kton$ each. Elaborate safety standards are in place for ammonia storage and transportation, due to its toxic and corrosive nature [50]. Despite the insulation, heat ingress in the tank results in premature ammonia vapourisation, leading to pressure increase in the vessel [56]. The vapour is routed to a compressor and condensed, to ensure that the maximum vessel pressure is respected.

3.4. Hydrogen Components

The third segment of the system is related to the hydrogen components, as distilled from the total system outlook in Figure 3.5. First, hydrogen is produced from electricity through electrolysis, which is elaborated upon in subsection 3.4.1. After production in either the electrolyser or the ammonia cracker previously considered in subsection 3.4.2, the hydrogen is transported, which is discussed in subsection 3.4.3. Storage of hydrogen is elaborated upon in subsection 3.4.4, after which subsection 3.4.5 focuses on the demand and how energy and mass are related when considering hydrogen.

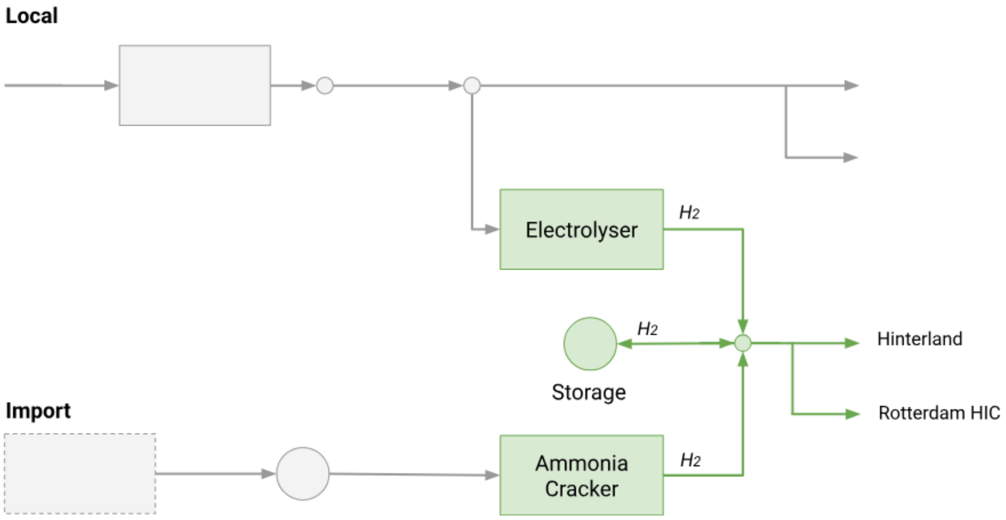

Figure 3.5: Hydrogen components highlighted in total system schematic

3.4.1. Electrolysis

This section considers the overall chemical reaction, after which the two primary electrolysis technologies are discussed: alkaline and polymer electrolyte membrane electrolysis. Lastly, the additional system components that comprise an electrolyser plant are discussed under 'Balance of System'.

Overall Reaction

Water electrolysis is the process of water (H_2O) decomposition into its fundamental atomic constituents: one oxygen atom and two hydrogen atoms. The presence of a direct electric current (*DC*) forces redox reactions at the anodes and cathodes of the electrolyser cell, which result in the net production of oxygen (O_2) and hydrogen (H_2) gas in the cell [91]. The overall chemical reaction is shown in Equation 3.1 [92].

$$2 \quad H_2O \quad + \quad 237.2 \quad [kJ.mol^{-1}]_{electric} \quad + \quad 48.6 \quad [kJ.mol^{-1}]_{heat} \quad \longrightarrow \quad 2 \quad H_2 \quad + \quad O_2 \tag{3.1}$$

The current industry standard technologies are Alkaline Electrolysis (*AEL*) and Polymer Electrolyte Membrane (*PEM*), although prospective electrolysis methods such as Solid Oxide Electrolysis Cells (*SOEC*) and Anion Exchange Membranes (*AEM*) are being investigated [25]. *AEL* and *PEM* are discussed in the subsequent sections.

Alkaline Electrolysis

Alkaline electrolysis has been in existence for nearly two centuries and was previously the primary method for hydrogen production. However, the advent of natural gas-based *SMR* made electrolysis a less prevalent technology [91]. An alkaline water solution of $NaOH$ or KOH transports OH^- ions through a porous zirconia diaphragm separating the electrodes. A nickel anode and nickel-alloy cathode allow the two product gases to be formed.

Alkaline electrolysis is well-established and features large stack sizes, relatively low capital cost, stability and non-noble catalysts. However, it also has a relatively low current density, slow dynamics due to the thermal inertia of the electrolyte liquid and safety boundaries resulting from undesirable gas permeation through the separator [91]. Although advanced stack control based on predictions of the variable power input provides enough flexibility for normal operation [41] [93], its lack of ramping capability can still be considered a potential downside of this technology. Besides, its operating conditions are at relatively low pressures, which means the produced hydrogen gas must go through energy-intensive compression before transportation or consumption in various industrial processes [85]. Its total system efficiency, including compression to 30 $barg$ is between 50 and 56 kWh/kgH_2, according to TNO [94], which corresponds to efficiencies estimated by the ISPT [58].

Polymer Electrolyte Membrane

Polymer Electrolyte Membrane electrolysers have a solid polymer electrolyte that transports protons (H^+ *ions*) between electrodes made from noble metals from the so-called platina-group, notably platina, iridium and ruthenium. Operation of *PEM* electrolyser cells has a rapid dynamic response, high current density and compact system size. However, their capital intensity is higher due to the membrane and electrode costs and the lifetime is relatively short [91]. It is capable of operating at elevated pressures, which diminishes or decreases the need for hydrogen product gas to be compressed after electrolysis. Efficiencies similar to alkaline electrolysis are projected for systems from 2030 onwards [95].

Balance of System

Merely a stack of electrolyser cells is insufficient in order to produce hydrogen from electricity; rather, a larger system of components, known as the balance of system (*BoS*), is required. The stack is the primary constituent, but a range of other elements are necessary. The present study will consider alkaline electrolysis, on the basis of the more substantial data relating to cost and efficiency at a larger scale, and in accordance with the design choice of the current electrolyser plant built in Rotterdam *HIC*.

Within the balance of plant, grid power at 380 kV is first converted to a lower voltage and rectified from AC to DC. Then it is fed to the stack, in combination with deionised or ultrapure water [58]. The electrolysis process gives rise to two distinct exit streams, those being a hydrogen-rich and an oxygen-rich electrolyte flow. Through gas/liquid separators, both gases are isolated from the exit streams. Hydrogen is purified and dried until it matches the required specifications. Lastly, it is compressed before injection into a transmission system or consuming facility. The electric components constituting the *BoS* all contribute to the parasitic power consumption of the electrolyser beyond merely the stack. Especially hydrogen compression and circulation of cooling liquids can require notable power input [58] [41]. The hydrogen purity of alkaline electrolysis is 99.99% according to the ISPT [58].

3.4.2. Ammonia Cracking

Disintegrating ammonia molecules into its nitrogen and hydrogen constituents is possible through a process called dehydrogenation, which is often referred to as ammonia cracking [51]. The process is described by the following reaction [96]:

$$2 \quad NH_3 \quad \rightleftharpoons \quad N_2 \quad + \quad 3 \quad H_2 \tag{3.2}$$

The required process steps are shown in Figure 3.6, from ammonia storage to hydrogen product gas.

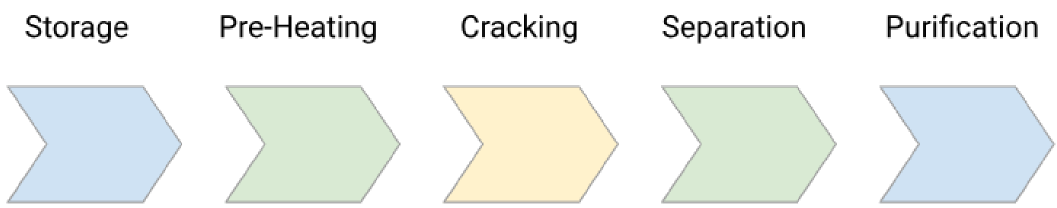

Figure 3.6: Steps of ammonia cracking, freely adapted from Fluor research [56]

The liquid ammonia feedstock is pumped from the storage area to the vapourisation and preheating section, where it undergoes a phase change to become gaseous feedstock [56]. The cracking process itself is a catalytic, endothermic process, which means it requires energy input to ensure the breaking of the $N-H$ bonds and to reach the temperature necessary to ensure favourable reaction kinetics in presence of a catalyst. After cooling and separation from other reaction gases, the hydrogen product gas is purified using pressure-swing adsorption and generally compressed before insertion in a hydrogen network or consumer facility. The purity that is achieved varies on the process steps included to treat the outgoing hydrogen. Approximately 99.9 $_{mol}$% product gas purity is deemed possible, in correspondence with Delta Rhine Corridor specifications [56].

To pre-heat the ammonia inflow and provide process heat, fuel is commonly fired to provide the energy input. In a licensor investigation for a potential cracking facility in the Port of Rotterdam, Fluor requested to employ no carbon-containing fuel sources as to prevent direct CO_2 emissions from the cracker [56]. A number of alternative fueling options were identified, after which the parasitation of ammonia feed was determined to be the most efficient additional fuel source, in combination with the combustion of tail gas from the purification process. However, it is noted that ammonia is notoriously difficult to combust efficiently and has a tendency of major NO_x formation. Some licensors indicated that development of electric crackers is in progress, which use electricity as a source of heating [97]. However, as their Technology Readiness Level (*TRL*) is deemed low [80], this research does not consider this technology.

3.4.3. Hydrogen Transportation

Hydrogen is often transported through at elevated pressures of around 50 to 80 $barg$ in pipelines, due to its low volumetric energy density [98]. Although plans for a large-scale (inter)national hydrogen network have been announced [99] [100], transportation across such distances is not common in current times [101]. Besides constructing new pipelines dedicated for hydrogen transport, the Dutch gas network operator Gasunie aims to repurpose existing natural gas pipelines to transport hydrogen instead [102]. Their overall estimate is that 85% of the hydrogen network can be based on former natural gas infrastructure [100].

3.4.4. Hydrogen Storage

The large-scale storage of hydrogen is a relatively novel field of research and development [103], given that its necessity was previously negated by the continuous production from fossil sources [15]. However, with the introduction of hydrogen production from intermittent renewable power sources, the availability of storage to ensure security of supply has become more important. Research by TNO indicates that the Netherlands has potential for underground hydrogen storage in salt caverns and depleted gas fields [103].

Salt caverns are created artificially by drilling into an underground salt layer and dissolving the salt into a water or brine solution. This creates a cavity in a geological layer made of low permeability rock salt [103]. The cavern is filled with a 'cushion gas', to increase the pressure and thus ensure the stability of the rock formation [100]. Next, the 'working gas' is injected, which is the hydrogen that is stored. Among the challenges related to subterranean hydrogen storage are leakage due to its small molecular size, undesirable reaction with (biological) substances in the geological formation and pollution of the hydrogen product gas, reducing its purity [104]. According to specification by HyStock -a salt cavern storage operator- hydrogen purities of 99.5 $_{mol}$% can be guaranteed.

Onshore salt cavern locations are potentially suitable to store the volatile hydrogen gas at pressures between 80 and 180 $barg$, allowing for average storage capacities around 3500 $tonH_2$ each, according to Gasunie [100]. HyStock is developing multiple 6000 $tonH_2$ storage caverns in Zuidwending (NL) [105], of which the first is planned to be in operation in 2029. Each cavern corresponds to around 236 GWh of hydrogen storage each, using the Higher Heating Value (*HHV*) by HyStock standards. Maximum injection and extraction rates are fixed at 20 ton/h, to maintain a maximum pressure differential of 10 $barg/day$ in the reservoir [105]. This is a relatively conservative requirement in practice, as temporal fluctuations above this limit are impossible, even if the actual reservoir pressure differential never exceeds the limit.

Salt cavern technology readiness level is deemed higher than for offshore caverns or depleted gas fields, although the latter has a significantly higher potential storage capacity [103] [100]. Due to the unique geological conditions required to facilitate this type of storage, the suitable locations are heavily location-dependent. The vast majority of potential sites are located in the northern and eastern regions of the Netherlands, necessitating a connection to the national network and subsequent operationalisation to fulfil the projected storage function [100].

3.4.5. Demand

Hydrogen is commonly used in chemical facilities, in processes that are continuous. The resulting demand profile is therefore characterised as a flat baseload. This consistent energy requirement reflects the steady operations of industrial users. Among the challenges for renewable hydrogen development is to allow continuous consumption, especially with regards to potentially intermittent power sources such as offshore wind. In this research, both the hydrogen demand in the *HIC* and hinterland are considered baseloads.

3.5. Key Performance Indicators

In the preceding chapter, the key performance indicators of a hydrogen supply pathway were defined. The system configuration is discussed in this chapter, and an overview is given in this section of which components are considered in the determination of which *KPI*.

3.5.1. Affordability

The components that are included in the calculation of capital and operational expenditure are shown in Table 3.1.

Components	**CAPEX**	**OPEX**
Offshore Wind Farm	✓	✓
Offshore Power Conversion & Transmission	✓	✓
Electrolyser	✓	✓
Ammonia Cracker & Storage	✓	✓
Ammonia Cost	×	✓
Hydrogen Transportation	✓	✓
Hydrogen Storage	✓	✓
Onshore Power Grid	×	×

Table 3.1: Table of included components in *CAPEX* and *OPEX*.

3.5.2. Security of Supply

As indicated in Table 3.2, the consumers for which loss of load is determined of hydrogen and power, and in which cases the focus lies on delivered power, are specified.

KPI	**HIC**	**Hinterland**	**Electrolyser**
Hydrogen Loss of Load	✓	✓	–
Power Loss of Load	✓	×	×
Power Supply	×	✓	✓

Table 3.2: Table of included consumers in security of supply indicators.

3.5.3. Sustainability

Table 3.3 outlines the components under consideration in the determination of both carbon and spatial footprint.

Component	Carbon Footprint	Spatial Footprint
Offshore Wind Farm	✓	✓
Electrolyser	✓	✓
Ammonia Production & Transport	✓	×
Ammonia Cracking & Storage	✓	✓

Table 3.3: Table of included components in annual equivalent carbon footprint and spatial footprint.

The lifecycle analysis (*LCA*) includes the carbon emissions from materials sourcing, production, installation, operation and decommissioning. For components where lifetime CO_2 emissions are available in literature regardless of operating time or output, annual equivalent emissions are calculated using this value directly. However, it is also possible to include emission intensity factors in $kgCO_2/kgH_2$ or $kgCO_2/kWh$, another common means of denoting *LCA* for production facilities [106] [107]. The annual equivalent CO_2 emission thus corresponds to a theoretical value, based on an equivalent annual share of the lifetime emissions of the considered components. For power transmission and hydrogen transmission and storage, resulting life cycle analysis (*LCA*) values were negligible in comparison to those of the considered components. The corresponding emission values are listed in section 4.5.

With regard to spatial requirements, the production and transportation of ammonia, as well as hydrogen storage, have not been taken into consideration. The underlying rationale for this exclusion is that detailed ammonia production is not considered in this study. Furthermore, hydrogen storage demands comparatively negligible area above ground, despite its substantial volume deep within the Earth.

4 Model

With the system objectives and associated key performance indicators (*KPIs*) established, the aspects of the hydrogen supply system that are important to evaluate have been defined. As the system configuration has been determined in chapter 3, this chapter transitions to constructing a Matlab system model that enables quantitative analysis of the supply pathways. The model is designed to capture the interactions and relations between components, providing a structured framework to evaluate their impact on the defined *KPIs*. Through this modeling approach, the aim is to simulate various configurations, identify trade-offs and assess the influence of design choices on the *KPI* outcomes.

First, a schematic overview of the model logic is shown in section 4.1. Next, the model components and flows are discussed in section 4.2, after which section 4.3 describes the energy management logic. Subsequently, the determination of the *KPIs* in the model is considered in section 4.4, followed by a list of standard model parameters in section 4.5. The last section verifies the model through a demonstration case, in section 4.6.

4.1. Model Overview

The global schematic overview of the model is shown in Figure 4.1. It consists of two sections: the system model and the key performance indicator calculation. Firstly, the system model employs the parameters and its internal logic to determine the dynamics of the hydrogen supply pathway, thus identifying the flows and their respective sizes. This provides a comprehensive overview of the system outputs, which can be considered the indicators of its internal dynamics. These outputs are then incorporated into the *KPI* calculation, which translates them into values for the specified *KPIs*. Consequently, the *KPIs* can be utilised to compare performance across different system configurations.

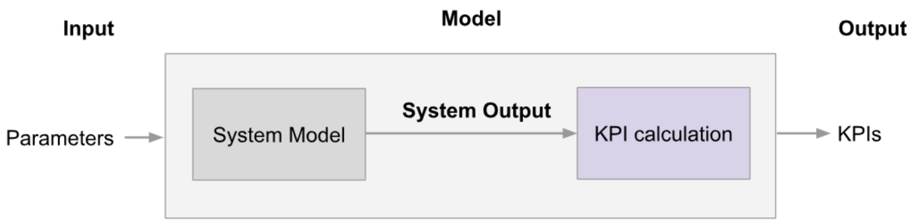

Figure 4.1: Schematic overview of the model functionality, with a system model and subsequent *KPI* calculation.

Figure 4.2 shows the system model overview in more detail. It consists of four modules, which are ammonia, power, hydrogen and an energy management system (*EMS*). Each module contains functions specific to its role in the model. The global interactions are indicated in the figure, which is merely to show which modules interact. The KPI calculation module uses the outputs of this system in combination with other input parameters to determine the KPI output values, as mentioned earlier in this section.

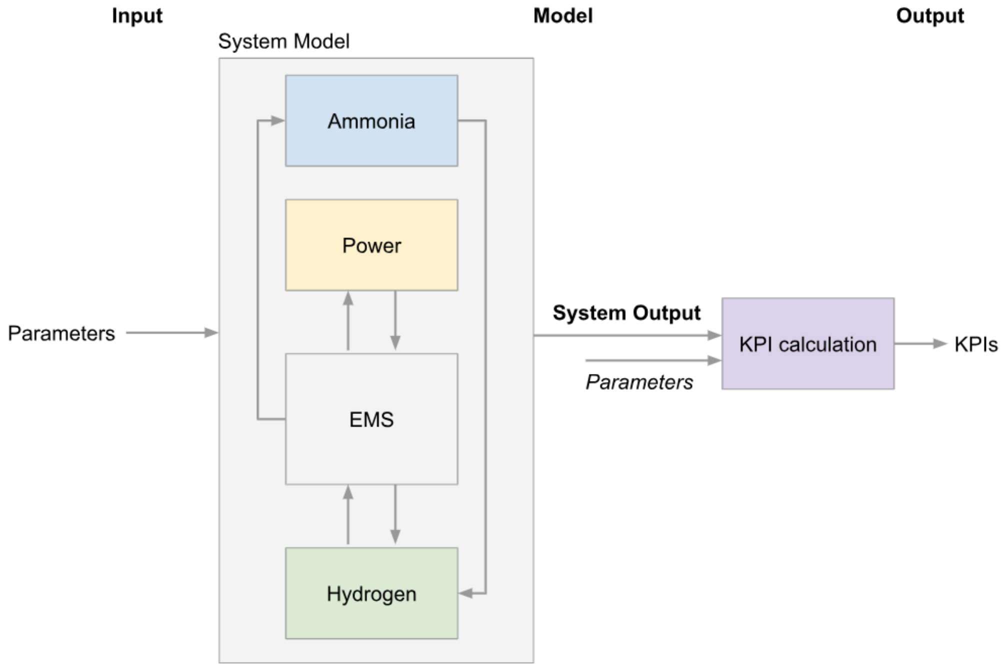

Figure 4.2: Schematic overview of the system model, including its power, ammonia, hydrogen and Energy Management System (*EMS*) modules.

4.2. Components & Flows

The process flows within the system and the components that perform actions on these flows are discussed in this section. Besides the *EMS*, the same three modules are identified as in chapter 3. First, the components associated to power are described in the model, followed by the ammonia and hydrogen-related components.

4.2.1. Power

Figure 4.3 shows the internal functions and interactions of the power module. It contains two functions, one describing the offshore wind farm and one that discusses the offshore power conversion and transmission.

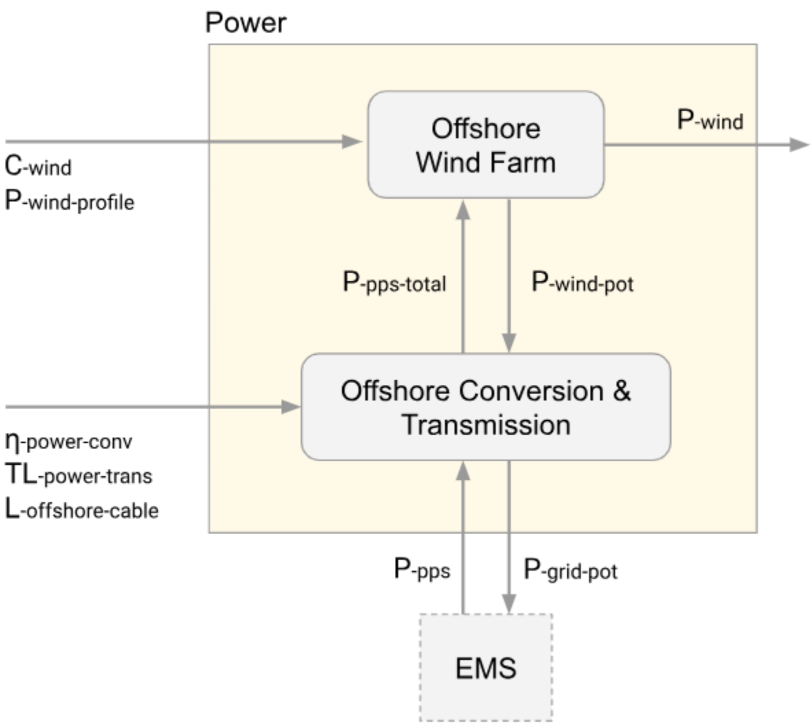

Figure 4.3: Schematic overview of the power module.

Offshore Wind Farm

A dataset with power production based on hourly wind speeds in a reference year ($P_{wind-profile}$) is loaded into the model from renewables.ninja. The corresponding output power is dependent upon the turbine type and geographic location. The turbine type was determined in subsection 3.2.1, while the location of the wind farm is a predefined input parameter specified in section 4.5. The power production data is scaled in accordance with the installed capacity of the wind farm (C_{wind}), which is a modeling input parameter. The total potential wind power production ($P_{wind-pot}$) is then defined by:

$$P_{wind-pot} = C_{wind} * P_{wind-profile} \tag{4.1}$$

Not all wind power can be consumed, which leads to a total potential power surplus ($P_{pps-total}$). This is wind power that could be produced, but has no consumer in this system design. It is determined by the *EMS*, creating an actual power production (P_{wind}) that is related to the potential power production through:

$$P_{wind} = P_{wind-pot} - P_{pps-total} \tag{4.2}$$

Offshore Power Conversion & Transmission

The offshore power conversion and transmission function is the connection between the wind power that is (potentially) produced and the power that is delivered to the grid, thus available to the *EMS*. It accounts for systemic losses by considering conversion efficiency ($\eta_{power-conv}$) and transmission loss ($TL_{power-trans}$), the latter of which depends on the transmission length ($L_{offshore-cable}$). The resulting potential grid power ($P_{grid-pot}$) has a reduced magnitude compared to the potentially produced wind power ($P_{wind-pot}$) as shown in:

$$P_{grid-pot} = P_{wind-pot} * \eta_{power-conv} * (1 - TL_{power-trans}(L_{offshore-cable})) * \eta_{power-conv} \tag{4.3}$$

In addition, this function receives the net potential power surplus (P_{pps}) from the *EMS*. This is converted to the actual wind power production that is a potential surplus ($P_{pps-total}$), which uses the same efficiencies as Equation 4.3 to indicate this surplus:

$$P_{pps-total} = \frac{P_{pps}}{\eta_{power-conv} * (1 - TL_{power-trans}(L_{offshore-cable})) * \eta_{power-conv}} \tag{4.4}$$

Consequently, the total conversion loss (P_{loss}) can be determined based on the difference between actual production and consumption. The actual production is the difference between $P_{wind-pot}$ and $P_{pps-total}$, while actual consumption is the difference between $P_{grid-pot}$ and P_{pps}. Put together, the power loss is found through:

$$P_{loss} = (P_{wind-pot} - P_{pps-total}) - (P_{grid-pot} - P_{pps}) \tag{4.5}$$

4.2.2. Ammonia

The module of ammonia is shown in Figure 4.4 and contains a single function, which is the ammonia storage.

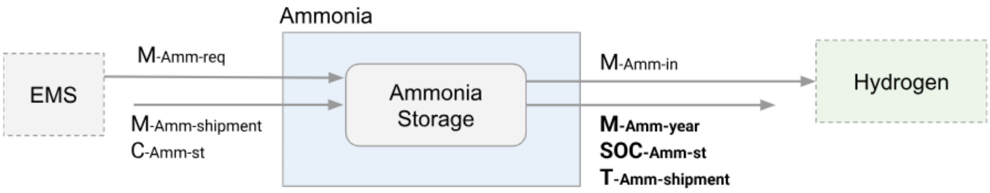

Figure 4.4: Schematic overview of the ammnonia module.

Ammonia Storage

The *EMS* inputs a requested ammonia mass ($M_{Amm-req}$) to the ammonia storage function, which is the necessary amount to produce the hydrogen the *EMS* demands from the ammonia cracker. The storage function subsequently supplies M_{Amm-in} to the cracker, which is in the 'hydrogen' module. The ammonia storage function governs the delivery interval of ammonia shipments ($T_{Amm-shipment}$) based on the ammonia shipment size ($M_{Amm-shipment}$):

$$T_{Amm-shipment} = \frac{M_{Amm-shipment}}{M_{Amm-in}} \tag{4.6}$$

The delivery interval ($T_{Amm-shipment}$) is then used to define timesteps in which ammonia shipment is required to prevent an empty storage. Based on the design choice of continuous ammonia cracking upheld in this research, the model logic deliberately prevents a loss of load for ammonia by setting the delivery interval using the ammonia cracker input. Consequently, the ammonia influx (M_{Amm-in}) equals the requested mass ($M_{Amm-req}$) at any instant:

$$M_{Amm-in} = M_{Amm-req} \tag{4.7}$$

M_{Amm-st} represents the mass stored within the ammonia tank. Its value changes depending the cracker influx ($M_{Amm-in}(t)$) and the potential arrival of shipments of size $M_{Amm-shipment}$, with the relation:

$$M_{Amm-st}(t+1) = M_{Amm-st}(t) - M_{Amm-in}(t) + M_{Amm-shipment}(t) \tag{4.8}$$

$M_{Amm-shipment}(t)$ equals zero in all cases where no delivery occurs and has the value $M_{Amm-shipment}$ when the delivery interval ($T_{Amm-shipment}$) indicates that delivery is necessary. The ammonia storage level (M_{Amm-st}) and the ammonia storage capacity (C_{Amm-st}) are used to determine the storage state of charge (SOC_{Amm-st}) through:

$$SOC_{Amm-st} = \frac{M_{Amm-st}}{C_{Amm-st}} \tag{4.9}$$

The annual ammonia mass ($M_{Amm-year}$) required for system operation is the sum of the ammonia influx to the cracker for each timestep ($M_{Amm-in-t}$), which is given by:

$$M_{Amm-year} \quad = \quad \sum_{t=1}^{8760} M_{Amm-in-t} \tag{4.10}$$

4.2.3. Hydrogen

The schematic overview of the hydrogen module is shown in Figure 4.5. It has three functions: the electrolyser, ammonia cracker and hydrogen storage.

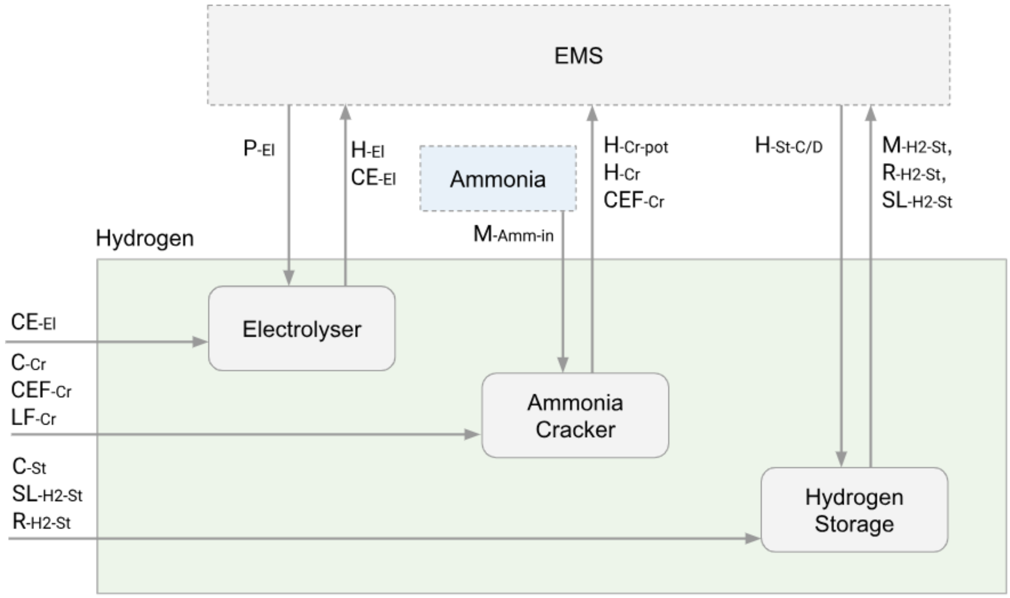

Figure 4.5: Schematic overview of the hydrogen module.

Electrolyser

The electrolyser receives power (P_{El}) from the *EMS*, which it converts to an amount of hydrogen (H_{El}) based on the conversion energy (CE_{El}):

$$H_{El} \quad = \quad \frac{P_{El}}{CE_{El}} \tag{4.11}$$

Ammonia Cracker

The ammonia cracker function uses the cracker capacity (C_{Cr}), ammonia conversion efficiency (CEF_{Cr}) and load factor (LF_{Cr}) to determine the potential hydrogen production of the cracker (H_{Cr-pot}) using:

$$H_{Cr-pot} \quad = \quad \frac{C_{Cr}}{CEF_{Cr}} \quad * \quad LF_{Cr} \tag{4.12}$$

The load factor (LF_{Cr}) indicates a predefined maximum operational capacity, which can be lower than the actual cracker capacity (C_{Cr}) during specific time periods. For example, a load factor of 0.9 indicates operation at 90% of the maximum capacity. It should be noted that the model has the option to use load factors other than 1, although this is explicitly mentioned in the case configuration.

The *EMS* uses the potential hydrogen output to determine how much it should actually produce. Based on this, the ammonia influx to the cracker (M_{Amm-in}) is determined through the 'ammonia' module, as seen in subsection 4.2.2. Using this influx, the actual hydrogen output of the cracker (H_{Cr}) is calculated with the ammonia conversion efficiency (CEF_{Cr}):

$$H_{Cr} = \frac{M_{Amm-in}}{CEF_{Cr}} \tag{4.13}$$

Hydrogen Storage
The hydrogen storage function provides its stored hydrogen mass (M_{H2-St}), injection and extraction limit (R_{H2-St}) and storage loss (SL_{H2-St}) to the *EMS*, so it can determine hydrogen availability.

The stored mass (H_{St}) is iterated using the hydrogen storage charging and discharging activity ($H_{St-C/D}$), which is obtained from the *EMS* as it governs the storage behaviour. The updated stored mass is found through:

$$H_{St}(t+1) = H_{St}(t) + H_{St-C/D}(t) \tag{4.14}$$

The state of charge has the following relation to the storage capacity (C_{St}) and stored mass (H_{St}):

$$SOC_{H2-St} = \frac{H_{St}}{C_{St}} \tag{4.15}$$

4.3. Energy Management System

This section discusses the energy management system that governs the distribution of power, ammonia and hydrogen flows between model components. The schematic overview of its internal functions and interactions with the other modules is given in Figure 4.6. Arrows on the left side of a function indicate inputs, while arrows on the right side are outputs.

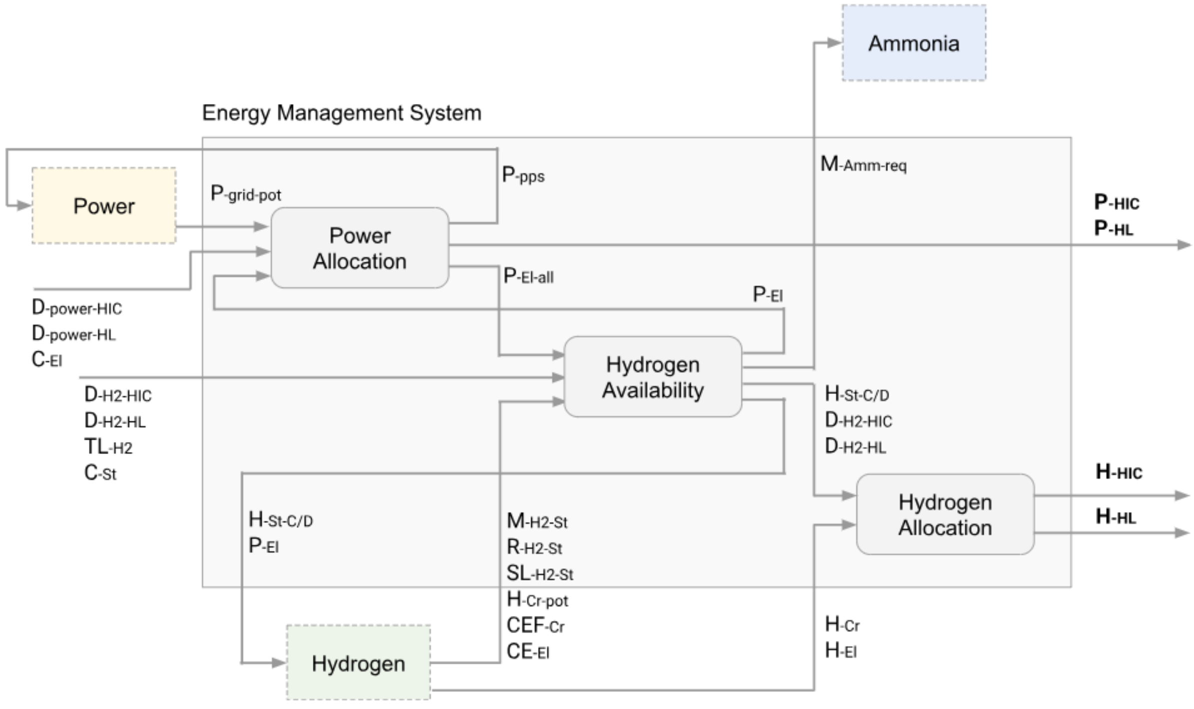

Figure 4.6: Schematic overview of the Energy Management System.

4.3.1. Power Allocation

The power allocation function has potential grid power ($P_{grid-pot}$) from the 'power' module as an input, and is aimed to distribute this power between *HIC*, hinterland and electrolysis. In order to achieve this, the annual power demand for *HIC* ($D_{power-HIC}$) is inputted in the function and converted to a hourly baseload power demand ($D_{power-HIC-h}$) using:

$$D_{power-HIC-h} = \frac{D_{power-HIC}}{8760} \tag{4.16}$$

Hinterland power demand ($D_{power-HL}$) is determined by scaling a total grid load profile ($D_{power-grid}$) with a predefined scaling factor (SF_{grid}):

$$D_{power-HL} = D_{power-grid} * SF_{grid} \tag{4.17}$$

Based on $P_{grid-pot}$ and a power distribution hierarchy, the *EMS* assigns outgoing electrolyser allocated power (P_{El-all}) using the electrolyser capacity (C_{El}) as an upper boundary. The hydrogen availability function subsequently determines the actual electrolyser power it requires (P_{El}), which is an input to the power allocation function. Based on this value, the final power distribution is completed, resulting in a four-way apportionment to *HIC* (P_{HIC}), hinterland (P_{HL}), the electrolyser (P_{El}) and a potential power surplus (P_{pps}). The potential power surplus is returned to the power function as discussed in section 4.2. Which priorities in power distribution are upheld is dependent on the operational strategy that is determined in a specific case configuration. However, in any case $P_{grid-pot}$ is equal to the sum of all four power categories:

$$P_{grid-pot} = P_{HIC} + P_{HL} + P_{El} + P_{pps} \tag{4.18}$$

4.3.2. Hydrogen Availability

The hydrogen availability function aims to balance supply and demand for hydrogen. The annual demand for *HIC* (D_{H2-HIC}) is converted to hourly baseload hydrogen demand ($D_{H2-HIC-h}$) using the following relation:

$$D_{H2-HIC-h} = \frac{D_{H2-HIC}}{8760} \tag{4.19}$$

The same logic is used to convert the annual hydrogen demand for hinterland (D_{H2-HL}) to the hourly baseload hydrogen demand ($D_{H2-HL-h}$):

$$D_{H2-HL-h} = \frac{D_{H2-HL}}{8760} \tag{4.20}$$

From the hydrogen function, the potential hydrogen output of the cracker (H_{Cr-pot}) is given. Besides, the *EMS* determines the potential hydrogen supply from the electrolyser (H_{El-pot}) using the conversion energy (CE_{El}) and the initially allocated power to the electrolyser (P_{El-all}) as follows:

$$H_{El-pot} = \frac{P_{El-all}}{CE_{El}} \tag{4.21}$$

In addition, the stored hydrogen mass (M_{H2-St}) is an input to the *EMS*, as well as the maximum injection and extraction rate of the storage (R_{H2-St}) and the storage losses (SL_{H2-St}). The available hydrogen from storage (H_{St-pot}) is the minimum of the extraction rate and stored hydrogen mass in relation to the storage losses, and is shown in:

$$H_{St-pot} = min(M_{H2-St}, R_{H2-St}) * (1 - SL_{H2-St}) \tag{4.22}$$

The potentially available hydrogen supply is equal to the sum of these three parameters, considering a transport loss (TL_{H2}) independent of pipeline length. The relation is described by:

$$H_{pot} = (H_{Cr-pot} + H_{El-pot} + H_{St-pot}) * (1 - TL_{H2}) \tag{4.23}$$

Both hydrogen demands can be summed into a cumulative hydrogen demand ($D_{H2-total}$), given by:

$$D_{H2-total} = D_{H2-HIC} + D_{H2-HL} \tag{4.24}$$

The value of H_{pot} is compared to the total hydrogen demand ($D_{H2-total}$). The difference between supply and demand is covered by the hydrogen storage activity ($H_{St-C/D}$) when possible. Otherwise, a loss of load for hydrogen (H_{LOL}) is created. The relation is shown in:

$$H_{pot} = (D_{H2-HIC} + D_{H2-HL}) + H_{St-C/D} - H_{LOL} \tag{4.25}$$

It should be noted that $H_{St-C/D}$ can be both positive and negative, and has boundaries of $-R_{H2-St}$ and $+R_{H2-St}$ in order to respect the maximum injection and extraction rates of the hydrogen storage. A positive storage activity indicates charging behaviour, while negative activity is related to discharging. H_{LOL} can only be larger than zero, which occurs exclusively when the combined hydrogen demand exceeds H_{pot}. Besides, the maximum hydrogen storage capacity (C_{St}) is respected in case of charging.

Figure 4.7 shows a visual of three example situations of Equation 4.25. In case H_{pot} exceeds the total demand, $H_{St-C/D}$ is positive, charging the storage, and H_{LOL} does not exist. In a situation of production deficit, $H_{St-C/D}$ is negative, indicating storage discharge to cover the difference between production and demand. Once $H_{St-C/D}$ is limited by either storage level (M_{H2-St}) or extraction rate (R_{H2-St}), it can not cover the complete deficit. Therefore, H_{LOL} is larger than zero in these situations.

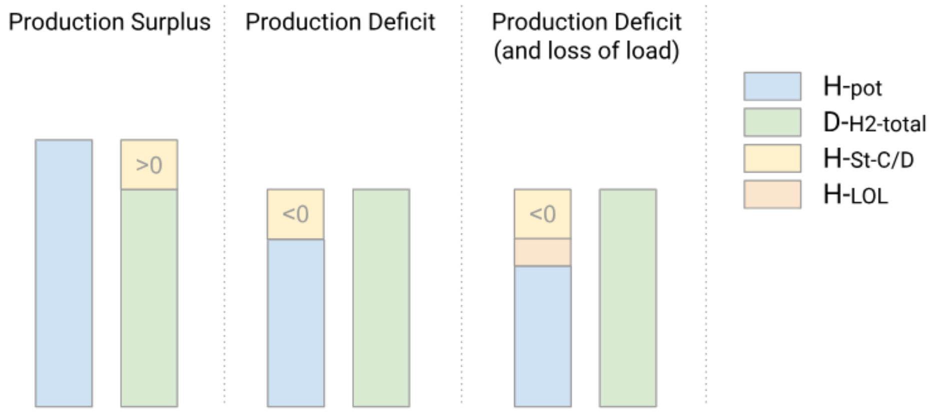

Figure 4.7: Visual example of three situations of mismatch between hydrogen production of the electrolyser and cracker and the corresponding demand for *HIC* and hinterland.

In case of a hydrogen production surplus that can not be stored, the hydrogen availability function must balance this. The two situations in which this occurs are when exceeding the storage injection rate (R_{H2-St}) or when the hydrogen storage is full. The *EMS* will reduce the power initially allocated to the electrolyser (P_{El-all}) to the actually allocated power (P_{El}). This value is returned to the power allocation function, which uses it to rearrange its initial power distribution based on the predefined hierarchy.

P_{El} is also used as an input for the hydrogen module, in addition to $H_{St-C/D}$. The actual hydrogen output from the cracker (H_{Cr}) is equal to the potential hydrogen output (H_{Cr-pot}) in this study. Thus, the required ammonia ($M_{Amm-req}$) to supply the specified H_{Cr} is found by using the ammonia conversion efficiency (CEF_{Cr}):

$$M_{Amm-req} = H_{Cr} * CEF_{Cr} \tag{4.26}$$

The value for $M_{Amm-req}$ is returned to the ammonia module, which provides M_{Amm-in} to the hydrogen module, as seen in subsection 4.2.2.

4.3.3. Hydrogen Allocation

In the hydrogen allocation function, the hydrogen storage activity $H_{St-C/D}$ and respective production from the ammonia cracker (H_{Cr}) and electrolyser (H_{El}) are used as inputs. Together with both *HIC* and hinterland hydrogen demands (D_{H2-HIC} and D_{H2-HL}), it distributes the available hydrogen through a predefined hierarchy. This prioritisation is explicitly part of the operational strategy defined in a specific case configuration.

Independent of the distribution strategy, the supplied hydrogen to *HIC* (H_{HIC}) and hinterland (H_{HL}) must be in balance with cracker production (H_{Cr}) and electrolyser production (H_{El}). The storage activity, which can either be positive or negative, assists in this balance. The relation is shown in:

$$H_{Cr} + H_{El} = H_{HIC} + H_{HL} + H_{St-C/D} \tag{4.27}$$

In case of a positive $H_{St-C/D}$, indicating a charging of the storage, it absorbs the overproduction of the cracker and electrolyser. When $H_{St-C/D}$ is negative, the hydrogen storage discharges, effectively becoming a supplier on top of H_{Cr} and H_{El}.

4.3.4. Systems Dynamics Parameters

This section considers several parameters that provide insight in the system dynamics, without corresponding to particular *KPIs*. The electrolyser full load hours (FLH_{el}) and fraction of reduced production (P_{el-red}) are considered first. Subsequently, the hydrogen storage supply share ($H_{st-share}$) and equivalent charge cycles (ECC_{H2-st}) are discussed.

Electrolyser Full Load Hours

The full load hours of the electrolyser (FLH_{el}) correspond to the equivalent amount of hours in which it operates at rated capacity (C_{el}). Essentially, it is a means of describing the capacity factor in hours per year. Besides the rated capacity, the sum of the consumed power (P_{el}) is used to determine the electrolyser full load hours in the relation:

$$FLH_{el} = \frac{\sum_{n=1}^{8760} P_{el-n}}{8760 * C_{el}} \tag{4.28}$$

Electrolyser Reduced Production

The electrolyser can be operated at a lower setpoint than its rated capacity by the *EMS*, even if sufficient wind power is allocated. These instances occur when the hydrogen it would produce is not in demand and can not be stored, either through injection rate limitations or a full storage. The fraction of reduced electrolyser power (P_{el-red}) compared to the allocated power (P_{el-all}) is indicative of the hydrogen overproduction potential of the system configuration. It is based on the actual electrolysis power (P_{el}) as well, according to the relation:

$$P_{el-red} = 1 - \frac{\sum_{n=1}^{8760} P_{el-n}}{\sum_{n=1}^{8760} P_{el-all-n}} \tag{4.29}$$

Hydrogen Storage Supply

Hydrogen storage can supply different shares of the total hydrogen supply, depending on the system configuration and operation. The total hydrogen supply consists of the *HIC* and hinterland supplies (H_{HIC} and H_{HL}, respectively). In combination with the storage supply (H_{St}), the storage supply share can be determined through:

$$H_{st-share} = \frac{H_{St}}{H_{HIC} + H_{HL}} \tag{4.30}$$

Hydrogen Storage Charging Cycles

The amount of equivalent charging cycles (ECC_{H2-st}) is indicative of storage activity in the year. It is determined using the total charging amount (H_{St-C}) from the storage activity ($H_{St-C/D}$):

$$H_{St-C} \quad = \quad H_{St-C/D} > 0 \tag{4.31}$$

Besides, the storage capacity (C_{St}) is used, creating the following relation:

$$ECC_{H2-st} \quad = \quad \frac{\sum_{n=1}^{8760} H_{St-C-n}}{C_{St}} \tag{4.32}$$

4.4. Key Performance Indicators

Besides the system dynamics with respect to process flows, the model is designed to determine the measurable *KPI* outputs of each system configuration that is used. This section discusses the methodology on how these are calculated for each indicator. Figure 4.8 shows the schematic overview of the parameters and system outputs used in the calculation of each *KPI*. Input parameters indicated in *italics* are based on research or predefined in a case configuration, while **bold** parameters were defined in the system model.

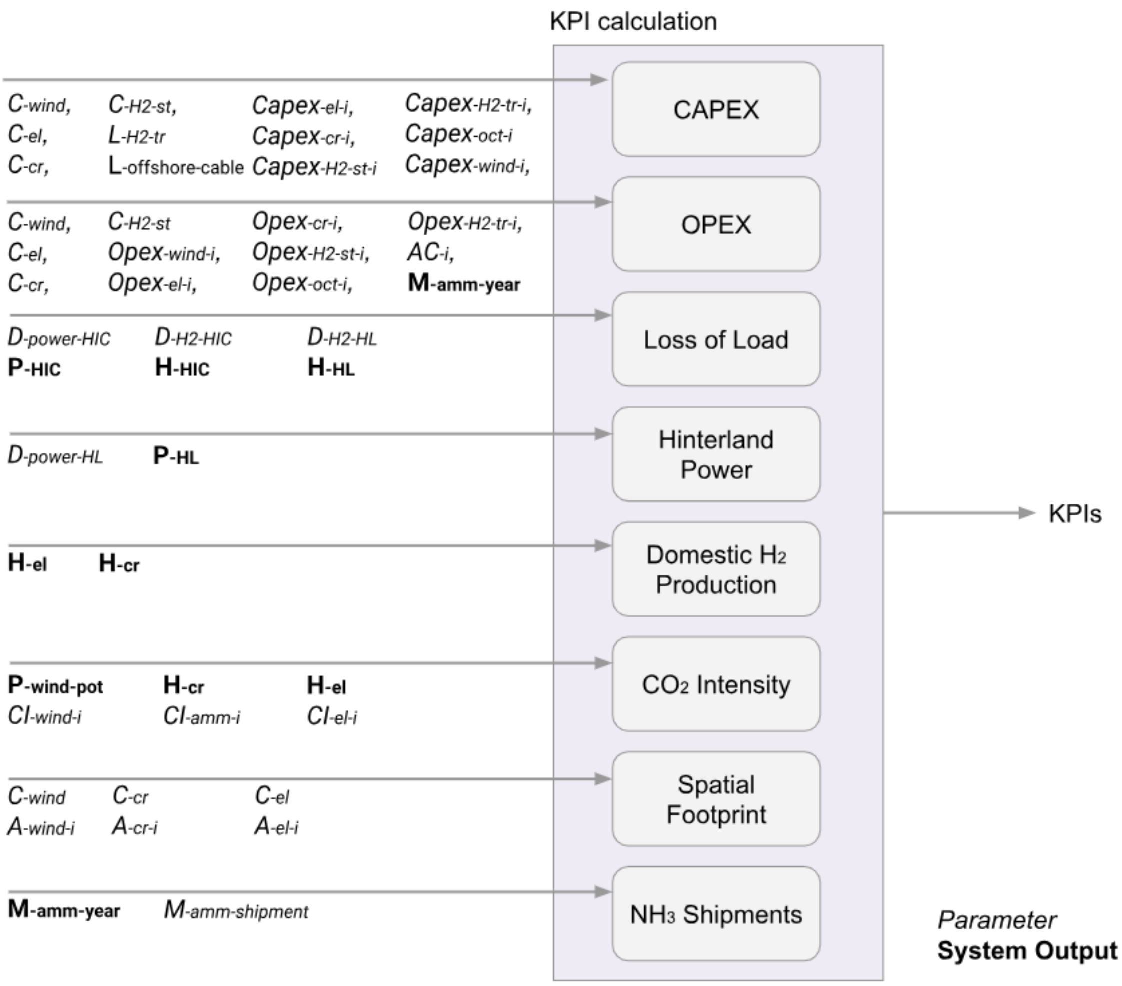

Figure 4.8: Schematic overview of the parameters and system outputs used to calculate each *KPI*.

4.4.1. Affordability

This section delves into the determination of indicators with respect to the objective of affordability, consisting of capital and operational expenditure. The system components considered in either are listed in Table 3.1.

Capital Expenditure

Total system *CAPEX* ($CAPEX_{total}$) is calculated by determining the investment cost of individual system components and summing these values. Individual system component costs are calculated by multiplying capacity-dependent *CAPEX* ($CAPEX_{component-i}$) with their associated capacities ($C_{component}$) as shown in:

$$CAPEX_{comp} \quad [€] \quad = \quad CAPEX_{component-i} \quad * \quad C_{component} \tag{4.33}$$

To determine the component *CAPEX* for offshore power conversion and transmission, C_{wind} and cable length ($L_{offshore-cable}$) are used to scale the cost in relation:

$$CAPEX_{oct} \quad = \quad C_{wind} \quad * \quad L_{offshore-cable} \tag{4.34}$$

Besides, the *CAPEX* calculation includes the total length of hydrogen pipeline (L_{H2-tr}). Several pipelines transport the hydrogen at elevated pressures through the system. The schematic overview and corresponding labels are shown in Figure 4.9.

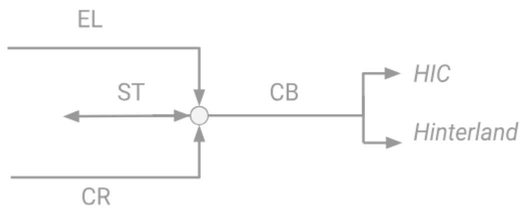

Pipe Label	Start	End
EL	Electrolyser	Central Backbone
CR	Cracker	Central Backbone
ST	Hydrogen Storage	Central Backbone
CB	Central Backbone	HIC & Hinterland

Figure 4.9: Left: schematic of pipelines segments considered
Right: labels and descriptions of pipeline segments.

HIC and hinterland are assumed to be at the end of the central backbone, without a dedicated pipeline segment. The pipelines are assumed to have no storage capacity in them, although this 'line-packing' is technically possible according to [100]. Each pipeline segment has a length, for example L_{H2-ST} in the case of the connection between hydrogen storage and central backbone. The total system pipeline length is therefore:

$$L_{H2-tr} \quad = \quad L_{H2-EL} \quad + \quad L_{H2-CR} \quad + \quad L_{H2-ST} \quad + \quad L_{H2-CB} \tag{4.35}$$

The total *CAPEX* for the hydrogen transmission ($CAPEX_{H2-tr}$) is then given by:

$$CAPEX_{H2-tr} \quad = \quad CAPEX_{H2-tr-i} \quad * \quad L_{H2-tr} \tag{4.36}$$

The respective values of $CAPEX_{comp}$ are summed for each of the six components that are considered in the total *CAPEX*:

$$CAPEX_{total} \quad [€] \quad = \quad \sum_{n=1}^{6} CAPEX_{comp-n} \tag{4.37}$$

The *CAPEX* for each individual component is determined through literature research and in some cases validated in interviews. The unit costs include raw materials, production, installation and in many cases also an advance on the decommissioning. The breakdown and values used in the case study of this research will be given later, in section 4.5.

Operational Expenditure

Operational expenditure is defined as the annual expenses for system operation. The *OPEX* includes the cost of maintenance and normal component operation, but also the cost of ammonia feedstock. Individual component *OPEX* is calculated by multiplying capacity-dependent *OPEX* ($OPEX_{component-i}$) with their associated capacities ($C_{component}$) as shown in:

$$OPEX_{comp} \quad [€] \quad = \quad OPEX_{component-i} \quad * \quad C_{component} \tag{4.38}$$

As the only component that has an *OPEX* that consists of a feedstock, the ammonia cracker has a different calculation, which includes the annual ammonia consumption ($M_{amm-year}$) and ammonia cost (AC_i):

$$OPEX_{cr} \quad [€] \quad = \quad OPEX_{cr-i} \quad * \quad C_{cr} \quad + \quad M_{amm-year} * AC_i \tag{4.39}$$

The respective values of $OPEX_{comp}$ are summed for each of the six components that are considered in the total *OPEX*:

$$OPEX_{total} \quad [€] \quad = \quad \sum_{n=1}^{6} OPEX_{comp-n} \tag{4.40}$$

As with the capital expenditure, the specific values used in the case study of this research will be given later in section 4.5.

4.4.2. Security of Supply

In this section, the calculation method for *KPIs* related to security of supply is elaborated upon. First, the methodology for loss of load calculation is given, after which hinterland power supply volume and variation are discussed. Lastly, the determination of domestic hydrogen production is shown.

Loss of Load

Loss of load is a measure of system reliability relating to the security of supply. The term is defined as the quantity of demand that is not satisfied by the supply. In this system design, three types of loss of load can be defined, related to their pre-defined demand: a loss of load in power supply to Rotterdam *HIC* ($LOL_{power-HIC}$) and hydrogen supplies to Rotterdam *HIC* (LOL_{H2-HIC}) and the hinterland (LOL_{H2-HL}). The relation for $LOL_{power-HIC}$ is:

$$LOL_{power-HIC} \quad = \quad 1 \quad - \quad \frac{P_{HIC}}{D_{power-HIC}} \tag{4.41}$$

Hydrogen loss of load for *HIC* (LOL_{H2-HIC}) compares the demand (D_{H2-HIC}) and supply (H_{HIC}), and is given by:

$$LOL_{H2-HIC} \quad = \quad 1 \quad - \quad \frac{H_{HIC}}{D_{H2-HIC}} \tag{4.42}$$

Lastly, the same logic applies to H_{HL-LOL}, which relates demand (D_{H2-HL}) and supply (H_{HL}), and is defined as:

$$LOL_{H2-HL} \quad = \quad 1 \quad - \quad \frac{H_{HL}}{D_{H2-HL}} \tag{4.43}$$

Hinterland Power Supply Volume

The supply volume of hinterland power ($SV_{power-HL}$) is determined as a share of the total hinterland power demand demand ($D_{power-HL}$) that is delivered by hinterland power (P_{HL}), as seen in:

$$SV_{power-HL} \quad = \quad \frac{P_{HL}}{D_{power-HL}} \tag{4.44}$$

Hinterland Power Supply Variability

The variability of power yield represents a considerable potential challenge for renewable power systems. The definition of variability employed in this research is defined as the standard deviation of the set of hour-to-hour power differences for the residual power demand profile for the hinterland. This will be explained further in this subsection.

To account for the original variability of the hinterland demand profile ($D_{power-HL}$) as well as that of the supplied power (P_{HL}), the variability is determined for their difference: the residual demand (P_{HL-res}), which is calculated as follows:

$$P_{HL-res} \quad = \quad D_{power-HL} \quad - \quad P_{HL} \tag{4.45}$$

This difference in residual power profile (ΔP_{HL-res}) is defined as the residual power demand that must be met within the hinterland itself, as the energy system in this research does not supply this power. Variability is measured as the difference in residual demand level between each timestep. It is evaluated with respect to the mean demand ($\overline{D}_{power-HL}$). This is shown in:

$$\Delta P_{HL-res}(t+1) \quad = \quad \frac{P_{HL-res}(t+1) \quad - \quad P_{HL-res}(t)}{\overline{D}_{power-HL}} \tag{4.46}$$

All instances for P_{HL-res} in which two (or more) subsequent zero values exist are deliberately not discarded, as these reflect situations in which the system ensures no remaining residual. In such cases, the power profile delivered is in fact perfect, so it must be classified as favourable in the variability set as well. In addition, using the average hinterland power demand ($\overline{D}_{power-HL}$) is deemed a usable normalisation method, as it is only dependent on the scaling factor of the grid profile (SF_{grid}), as determined in Equation 4.17. Thus, it has no sensitivity to varying residual profiles across different system configurations.

ΔP_{HL-res} contains the differences in residual profile for each hourly time interval. The variability is defined as the standard deviation of this set of values (VR), which is calculated using the mean difference of the normalised hinterland power residual ($\overline{\Delta P}_{HL-res}$) and the amount of hours in a year (N):

$$VR \quad = \quad \sqrt{\frac{\sum_{n=1}^{N} \quad (\Delta P_{HL-res-n} \quad - \quad \overline{\Delta P}_{HL-res})^2}{N-1}} \tag{4.47}$$

In this research, VR is considered the variability of residual power demand. A high variability indicates an unfavourably fluctuating power demand that must be satisfied, while a low variability holds that the power that must still be supplied in an alternative way for the hinterland has a relatively constant profile.

Domestic Hydrogen Production

Another *KPI* in the category of security of supply is the amount of production from domestic electrolysis (DP_{H2}), compared to the amount of import. This is defined as the percentage of electrolyser hydrogen production (H_{el}) in relation to the total hydrogen production, which also depends on (H_{Cr}):

$$DP_{H2} \quad = \quad \frac{H_{el}}{H_{el} \quad + \quad H_{Cr}} \tag{4.48}$$

4.4.3. Sustainability

This section considers the three *KPIs* under the sustainability system objective, carbon and spatial footprint and annual ammonia shipments.

Carbon Footprint

The carbon footprint of the components listed in Table 3.3 is considered in the model, which are the offshore wind farm, electrolyser and complete ammonia cracking pathway. The sum of the potential wind power production ($P_{wind-pot}$) is used to scale the unit carbon intensity of wind power production (CI_{wind-i}) to the full carbon footprint associated to the wind power (CFP_{wind}):

$$CFP_{wind} = \sum_{n=1}^{8760} P_{wind-pot-n} * CI_{wind-i} \tag{4.49}$$

The carbon footprint of electrolysis (CFP_{el}) is calculated based on the electrolyser hydrogen production (H_{el}) and the unit carbon intensity of electrolysis (CI_{el-i}) as follows:

$$CFP_{el} = \sum_{n=1}^{8760} H_{el-n} * CI_{el-i} \tag{4.50}$$

Lastly, the carbon footprint of the ammonia pathway (CFP_{amm}) is determined using the same logic. It is based on the unit carbon intensity (CI_{amm-i}) and cracker hydrogen output (H_{cr})

$$CFP_{cr} = \sum_{n=1}^{8760} H_{cr-n} * CI_{cr-i} \tag{4.51}$$

The total footprint of the system (CFP_{total}) is the sum of the footprints of the components, using:

$$CFP_{total} = CFP_{wind} + CFP_{el} + CFP_{cr} \tag{4.52}$$

Spatial Footprint

The wind farm is the only component considered to use area at sea, while the ammonia cracker and storage and electrolyser add to the land use. The total spatial use at sea (A_{sea}) is determined using the unit power density (A_{wind-i}) and the installed capacity (C_{wind}):

$$A_{sea} = A_{wind-i} * C_{wind} \tag{4.53}$$

The spatial footprint on land (A_{land}) is found through the unit spatial densities for electrolysis (A_{el-i}) and cracking (A_{cr-i}) and their respective capacities (C_{el} and C_{cr}). The relation is described by:

$$A_{land} = (A_{el-i} * C_{el}) + (A_{cr-i} * C_{cr}) \tag{4.54}$$

Annual Ammonia Shipments

The amount of ammonia shipments required on an annual basis ($N_{amm-shipments}$) is related to the total ammonia consumption ($M_{amm-year}$) and the size of a single shipment ($M_{amm-shipment}$). Their relation is described by:

$$N_{amm-shipments} = \frac{M_{amm-year}}{M_{amm-shipment}} \tag{4.55}$$

4.5. Standard Values for Model Parameters

This section outlines the standard model parameters used in the model, which remain constant across different cases unless specified explicitly. These parameters form the foundational assumptions for the analysis, ensuring consistency and comparability in results for variables of interest. The standard parameters are determined based on literature research and in several cases validated using expert input. Parameters for which elaboration of their value in relation to the original source is necessary are discussed more in-depth in this section.

The parameters have been categorised by their respective components. First, Table 4.1 shows those related to offshore wind power. The location is set at the IJmuiden Ver site, which is used a reference point for the wind power profile mentioned in subsection 3.2.1. The values for cost have been adapted from the cost of recent Dutch wind farms with similar geographical characteristics. Decommissioning cost is included in *CAPEX*, as well as array cable cost, which depends on capacity and not on a set distance to a substation. The total cost is assumed to scale linearly with installed capacity, while the carbon footprint is based on theoretically produced energy directly from the wind power profile.

Parameter	Variable Name	Value	Unit	Source
Capital Expenditure *(excl. transmission)*	$CAPEX_{wind-i}$	1850	€$/kW_e$	[108] [109]
Operational Expenditure	$OPEX_{wind-i}$	3	$\%_{CAPEX}$	[110]
Power Density	A_{wind-i}	4.66	MW_e/km^2	[111]
Carbon Intensity	CI_{wind-i}	15.5	gCO_2/kWh	[107]
Location		53.0 ; 3.8	degree (Lat; Long)	[112] [113]

Table 4.1: Offshore Wind Parameters

Parameters relating to offshore power conversion and transmission are shown in Table 4.2. A proportion of the *CAPEX* is dependent on the cable length, which is determined based on the distance to port for the wind farm. Distance-dependent cost factors are the cable manufacturing cost and its installation and decommissioning. The standard cable length is 110 km, equaling the distance between IJmuiden Ver wind farm and the landfall at the *HIC* [112]. The efficiencies are assumed to be constant, regardless of power throughput or variation. As a sanity check, a comparison is made with the cost of Net op Zee, the new Dutch offshore power transmission. According to the government, its projected cost is 26 billion euros [114], with announced plans to connect around 14 GW_e of wind per 2035. This leads to an investment of 1850 €$/kW_e$, which is in the vicinity of the 1350 €$/kW_e$ total for the standard situation in this research.

Parameter	Variable Name	Value	Unit	Source
Constant *CAPEX*	$CAPEX_{cable}$	314	€$/kW_e$	[110]
Distance-dependent *CAPEX*	$CAPEX_{cable}$	9.4	€$/kW_e/km$	[110]
Operational Expenditure	$OPEX_{cable}$	1	$\%_{CAPEX}$	[90]
Transmission Loss	$TL_{power-trans}$	0.5	$\%.100km^{-1}$	[115]
Conversion Efficiency	$\eta_{power-conv}$	97.5	%	[115]
Length of Offshore Power Transmission	$L_{offshore-cable}$	110	km	[112]

Table 4.2: Offshore Power Conversion & Transmission Parameters

Standard modeling parameters associated to the electrolyser are shown in Table 4.3. Its cost values are based on TNO research, while the power consumption information is retrieved from ISPT data. Hydrogen separation and compression to 50 $bara$ are considered within the power consumption. Hydrogen compression from 50 to 80 bar is not considered, despite it being a possible operational pressure for the transportation network. This compression consumes around 0.66 kWh/kgH_2, or 2% of *LHV* [85]. At 1 $MtH_2.y^{-1}$, this equals 75 MW_e continuously, which is considerable compared to *HIC* power demand. Nevertheless, this study neglects this potential additional power requirement. The total conversion energy of 51.95 kWh/kgH_2 is assumed to be constant regardless of production level. The degradation of the stack is not considered in the efficiency, although a single electrode replacement during the electrolyser lifetime is considered in the carbon footprint. The carbon footprint is the middle value of the range given by the source. Stack lifetime is not adjusted depending on the annual load hours or variable load behaviour, but the reference lifetime of the source is upheld. Again, the component cost is assumed to scale linearly with capacity, so in disregard of economy of scale effects that are known to have strong influence in plants of several hundred MW_e [61] [94].

Parameter	Variable Name	Value	Unit	Source
Capital Expenditure	$CAPEX_{el-i}$	2650	€$/kW_e$	[94]
Operational Expenditure	$OPEX_{el-i}$	4	$\%_{CAPEX}$	[94]
Conversion Energy	CE_{el}	51.95	kWh_e/kgH_2	[58] [94]
Spatial Footprint	A_{el-i}	10	ha/GW_e	[58]
Carbon Intensity (*excl. power*)	CI_{el-i}	112	gCO_2/kgH_2	[116]

Table 4.3: Electrolyser Parameters

Parameters related to the ammonia cracker are displayed in Table 4.4. This research considers a constant conversion efficiency for ammonia to hydrogen, which is unrelated to load factor or external influences such as temperature or humidity. The ammonia cracker is assumed to operate steadily, as mentioned in subsection 3.4.2. In addition, no supply risk for ammonia is assumed and the storage capacity scales with the annual hydrogen production. The required power to compress hydrogen to 50 $barg$ is included in the conversion efficiency. The carbon intensity of the ammonia pathway is mostly due to the footprint of the renewable power that is used to produce the ammonia. The load factor LF_{Cr} is 1, indicating operation at full capacity, unless explicitly specified differently.

Parameter	Variable Name	Value	Unit	Source
Capital Expenditure	$CAPEX_{cr-i}$	*undisclosed*		[56]
Operational Expenditure	$OPEX_{cr-i}$	*undisclosed*		[56]
Ammonia-Hydrogen Conversion Efficiency	CEF_{Cr}	*undisclosed*		[56]
Ammonia Storage Capacity	C_{Amm-st}	340	$ktonNH_3/Mt.H_2.y^{-1}$	[56]
Spatial Footprint	A_{cr-i}	*undisclosed*		[56]
Carbon Intensity of Import Pathway	CI_{amm-i}	2,500	gCO_2/kgH_2	[117]
Ammonia Cost	AC_i	900	USD/tNH_3	[56]
Cracker Load Factor	LF_{cr}	1	$-$	

Table 4.4: Ammonia Storage & Cracking Parameters

Hydrogen pipeline parameters are shown in Table 4.5. The *CAPEX* is based on the HyWay27 report, in which the authors consider a standard 36 inch, 9.1 GW_{H2} pipeline. The report indicates that 85% of the hydrogen network would consist of repurposed gas pipelines at costs of 0.85 million euros per kilometer, while the remainder is dedicated new pipeline at a cost of 3.2 million euros per kilometer. These numbers constitute the cost of hydrogen pipelines in this research, the segments of which were determined in Section 4.4.1. A transport loss of 2% of hydrogen is considered, regardless of the length of the pipeline. The assumption that electrolyser and cracker connect directly to the central backbone is laid out in the same section, as well as the notion that both consumers, *HIC* and hinterland are at the end of the central backbone section. The length of the storage pipeline segment is based on the estimates in HyWay27 [100]. The transport capacity (GW_{H2}) is based on the maximum hydrogen throughput and the Higher Heating Value of hydrogen, at 39.3 kWh/kgH_2, according to the conventions of HyWay27 and HyNetwork [118]. The central backbone capacity is scaled based on the maximum simultaneous hydrogen production of the combined cracker and electrolyser. This logic is also applicable to the capacity of the storage pipeline, but in this case the maximum storage injection and extraction rates must be used.

Parameter	Variable Name	Value	Unit	Source
Capital Expenditure	$CAPEX_{pipe}$	0.13	$M€.km^{-1}.GW_{H2}^{-1}$	[100]
Operational Expenditure	$OPEX_{pipe}$	1	$\%_{CAPEX}$	[100]
Transport Loss	TL_{H2}	2	%	[100]
Length of EL segment	L_{H2-EL}	0	km	
Length of CR segment	L_{H2-CR}	0	km	
Length of ST segment	L_{H2-ST}	300	km	[100]
Length of CB segment	L_{H2-CB}	50	km	[44]

Table 4.5: Hydrogen Pipeline Parameters

Table 4.6 displays the standard modeling parameters with regards to the hydrogen storage. The *CAPEX* is adjusted to a capacity-dependent value, based on the indicated source. Marginal cost associated with the storage of each kgH_2 is accounted for, which was extracted from an example calculation in the report.

Parameter	Variable Name	Value	Unit	Source
Capital Expenditure	$CAPEX_{H2-st-i}$	30.6	$M€.kton_{H2}^{-1}$	[100]
Operational Expenditure (*charge cycle-dependent*)	$OPEX_{H2-st-i}$	0.08	$€/kgH_2$	[100]
Injection & extraction rate limit	R_{H2-St}	0.33	$\%_{capacity}.h^{-1}$	[105]
Storage Loss	SL_{H2-st}	2	$\%_{H2}$	[105]
Standard Cavern Size	C_{H2-St}	6	$ktonH_2$	[105]

Table 4.6: Hydrogen Storage Parameters

Lastly, the standard profile for the hinterland power demand is derived from the European Network of Transmission System Operators for Electricity [11]. The total grid load is used for the Netherlands in 2019, in correspondence to the year of wind power production that is considered in this study. This profile is scaled using a grid scaling factor (SF_{grid}), as mentioned in section 4.3. This scaling factor is an input variable that has no standard value and is determined based on the configuration of the case.

4.6. Model Demonstration

This section is intended to illustrate the functionality and reliability of the developed model by applying it to a demonstration case study. A series of plots is presented to highlight the system's behaviour under various configurations, thereby showcasing the interactions between its components. In addition, the results are analysed to verify that the model operates as intended, ensuring consistency with theoretical expectations and system design principles.

Table 4.7 comprises the parameters that were the subject of consideration in the demonstration case study. The demonstration case modeling parameters were selected to demonstrate a wide range of system dynamics in a clear way. Nevertheless, the values for demand are in close proximity of the current situation and conservative future projections. *HIC* power consumption was 7.3 TWh in 2021 [33], but an increase to 10 TWh near 2030 is deemed conceivable [38]. Approximately 0.5 MtH_2 (both renewable and fossil-based) is used in the cluster annually, while a 0.5 MtH_2 throughput is in line with estimates of the Port of Rotterdam for 2030 [38]. Power plants in the port area supply a sixth share of Dutch national power demand nowadays [33] [7]. Given a doubling in electricity consumption, a similar production share from the *HIC* involves a factor 0.33 scaling of the current hinterland grid profile.

Parameter	Variable Name	Value	Unit
Demand			
Power Demand HIC	$D_{power-HIC}$	10	TWh/y
Hydrogen Demand HIC	D_{H2-HIC}	0.5	MtH_2/y
Hydrogen Demand Hinterland	D_{H2-HL}	0.5	MtH_2/y
Hinterland Grid Load Scaling Factor	SF_{grid}	0.33	$-$
Supply			
Capacity Wind	C_{wind}	12	GW_e
Capacity Electrolyser	C_{el}	4.8	GW_e
Capacity Cracker	C_{cr}	0.44	MtH_2/y
Capacity Hydrogen Storage	C_{H2-st}	6	$ktonH_2$

Table 4.7: Demonstration Case Parameters

The allocation strategy for power has a distinct hierarchy for wind power distribution in the demonstration case. First, the *HIC* power demand is satisfied, after which the electrolyser is turned on to its maximum rated capacity. The remainder is allocated to the hinterland grid or labeled as potential power surplus in case of complete demand satisfaction. Hydrogen priority lies with the *HIC*, which means the first loss of load is taken by the hinterland. The ammonia cracker operates constantly at full capacity in this model demonstration, which means its LF_{cr} equals one. To provide insight into the system operation in context of its annual behaviour, a specific time period with clear dynamics is highlighted in several figures.

4.6.1. Power Distribution

The distribution of wind power is considered in this section, highlighting how the available electricity is allocated among the consumers in the system, or is otherwise curtailed. This distribution is shown in Figure 4.10.

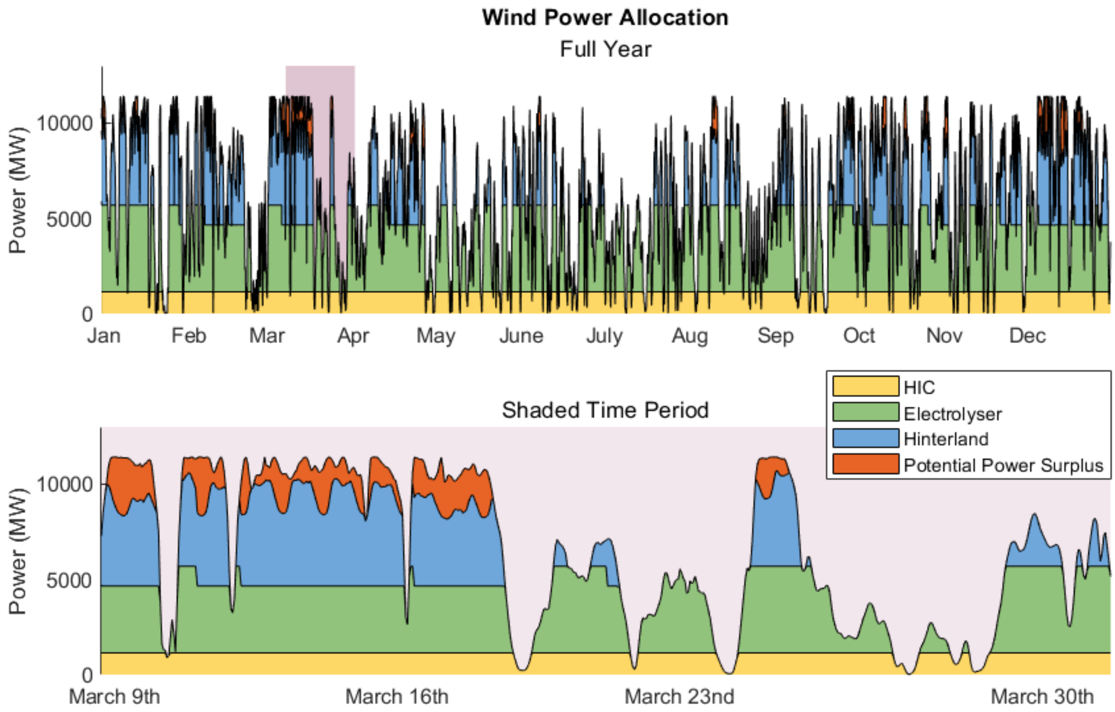

Figure 4.10: Top: Full year wind power distribution
Bottom: System dynamics for a specific time period

The first-in-line to be allocated power is the *HIC*, which is indicated in the yellow area on the bottom of the power profile. The green area on top of it represents the power consumption of the electrolyser. As can be observed more clearly in the bottom subfigure, the electrolyser is sometimes ramped down. In these situations, less power is made available for it than its rated capacity, despite sufficient wind power production. This power is re-allocated to the hinterland, in the blue area above the electrolyser power. In case of production excess, the remaining power is marked potential power surplus at the source, while accounting for losses.

The behaviour of hinterland power demand, supply and potential power surplus is also shown in Figure 4.11. Similarly to Figure 4.10, this figure indicates more hinterland power supply in winter months, when overall power production is considerably higher. Potential power surplus occurs more frequently in these periods as well, in particular when additional power is allocated to the hinterland due to reduced electrolyser production.

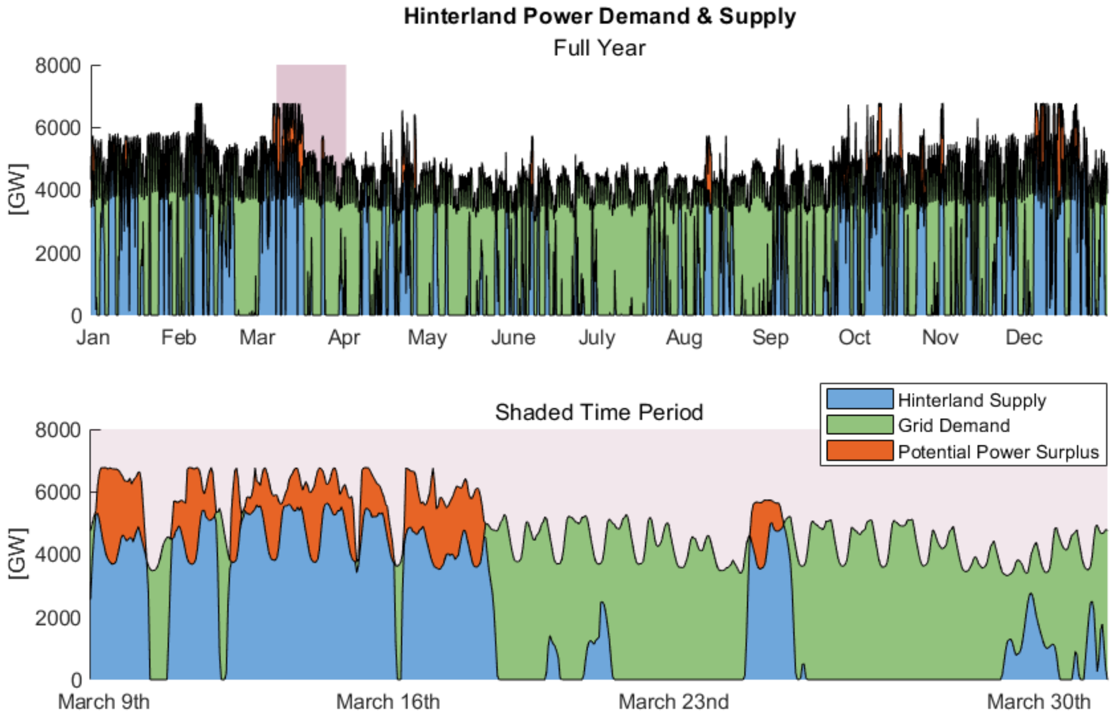

Figure 4.11: Top: Full year hinterland power demand, supply and potential power surplus
Bottom: System dynamics for a specific time period

4.6.2. Hydrogen Production

The electrolyser power profile from Figure 4.10 can also be observed from the hydrogen production and demand in Figure 4.12. The ammonia cracker produces a baseload hydrogen flow, while the electrolyser production is variable. In case of hydrogen shortage, when demand exceeds momentary production, the hydrogen storage can mitigate some of the impact by supporting supply. It is expected that the maximum electrolyser hydrogen output is also governed by the hydrogen storage injection rate. The energy management rationale in the model describes that any hydrogen that can not either be delivered to the demand side or stored should not be made. Any hydrogen excess on top of what can be injected in the storage is capped as a result. The extraction limit of the storage can be observed in the bottom subfigure as well. After March 23rd, the storage is not empty, as it continues supply until the next production excess slightly before Match 30th. However, the amount of hydrogen it can supply at each time is inadequate to satisfy the demand, indicating that the extraction boundary condition is limiting.

Hydrogen production in case of purposeful reduced electrolyser production slightly exceeds demand, as seen in the middle of March in Figure 4.10. This situation depicts a balance of supply and demand, as the electrolyser ramping only occurs in case of a full storage. The slight overshoot can thus be attributed to system hydrogen losses in transportation.

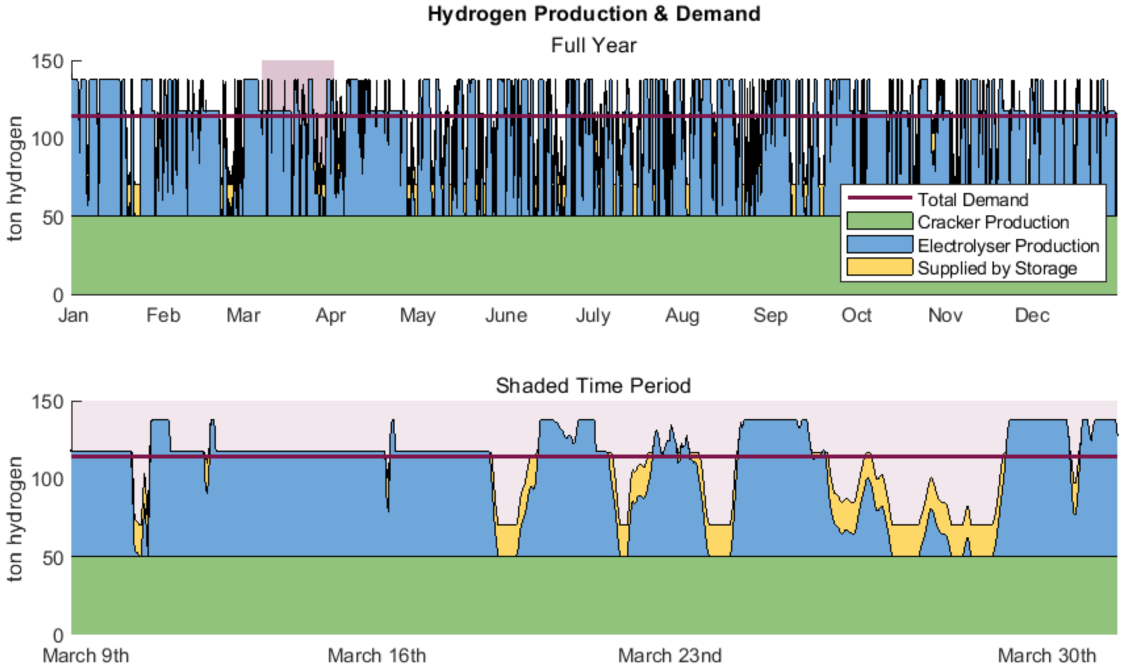

Figure 4.12: **Top**: Full year hydrogen demand and production per source
Bottom: System dynamics for a specific time period

Figure 4.13 shows the hydrogen storage level in the salt cavern for a full year, although the same period is highlighted as in the previous figures.

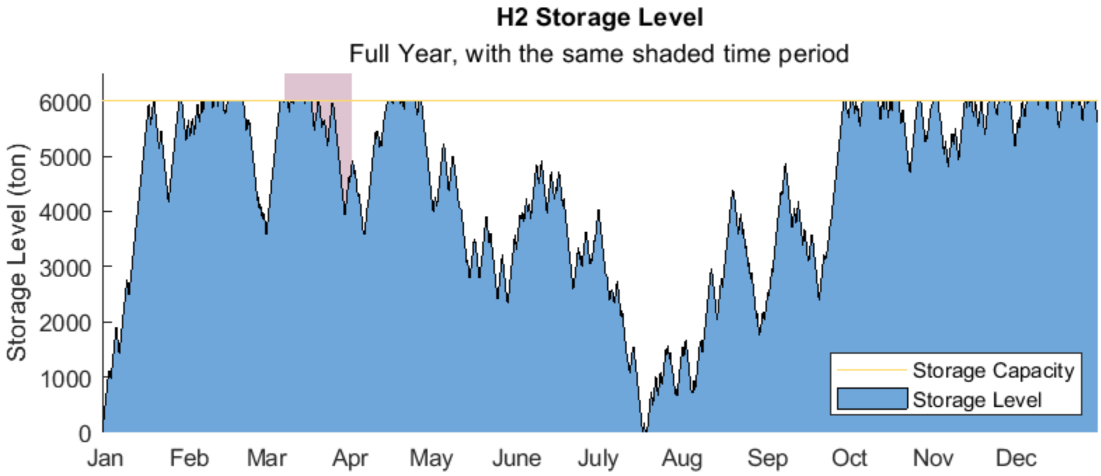

Figure 4.13: Hydrogen storage level in the salt cavern

The storage level confirms that the electrolyser was ramped down correctly in Figure 4.10, as it has reached maximum capacity during the highlighted time period. Besides, the storage appears to provide functionality on multiple timescales. Its levels appear to fluctuate on short timescales, indicating frequent, minor support to the hydrogen supply. Additionally, a strong seasonal profile can be observed, where higher hydrogen production in winter months leads to a storage buffer that is subsequently drained in the summer months with lower hydrogen production. The storage appears to be (nearly) empty only a single instant in the middle of July. This confirms the earlier notion in Figure 4.12 that the unmet demand in March is due to the hydrogen storage extraction limit and not due to an empty storage.

To gain a more in-depth understanding of the hydrogen storage, the charging and discharging behaviour is shown in Figure 4.14.

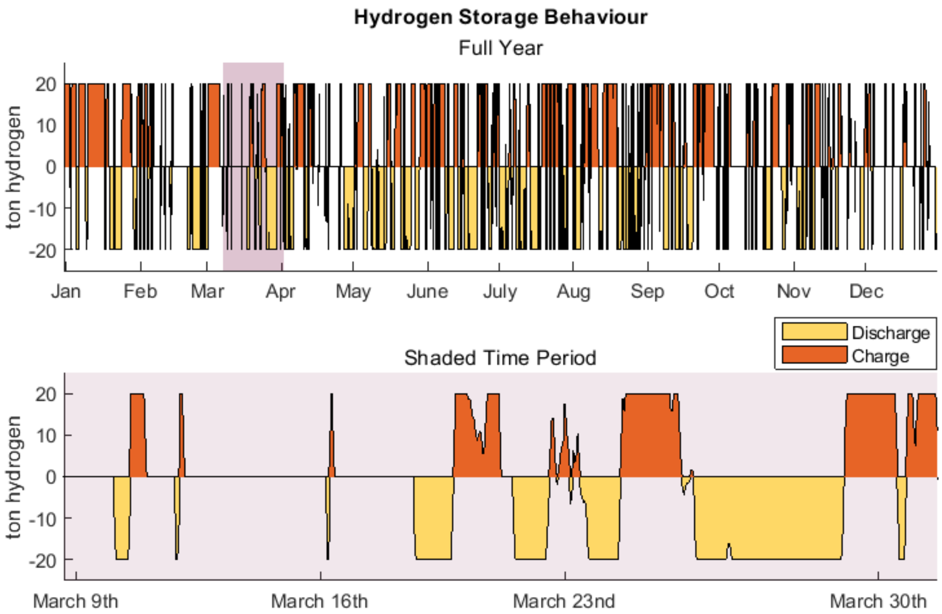

Figure 4.14: Hydrogen storage charging and discharging behaviour

The injection and extraction limits can be clearly noticed, as (dis)charge levels never exceed 20 $tonH_2$ per hour. The behaviour confirms the observations done for the hydrogen storage. Stronger charging is seen in winter, while discharging is dominant in summer periods. Besides the seasonal pattern, the frequent short-term support to hydrogen supply is confirmed, as charging and discharging show a highly alternating arrangement year-round.

In addition, the full storage results in a pauze in storage activity during the middle of March. This can be noticed clearly from the highlighted time period in Figure 4.14. The discharging behaviour, the area below zero shown in yellow, matches the storage supply profile shown in Figure 4.12, also in yellow. Figure 4.14 confirms that the hydrogen output from the storage is indeed insufficient at the end of March, despite the storage still containing plenty of the gas.

The previously illustrated situation is an example of the expected hydrogen loss of load profile from the system configuration. These can be validated through Figure 4.15. Two distinct types of loss of load for hydrogen are indicated in Figure 4.15: due to an empty storage and due to the storage discharging limit. This also holds true for the potential hydrogen surplus, which can originate from both a full storage and the injection limits of the storage. An important note is that the hydrogen surplus is theoretical, as it will result in the subsequently reduced production of the electrolyser. As a result, the *EMS* can re-allocate this power to another consumer. If it can not be consumed by re-allocating it, it becomes what is termed as a potential power surplus. This holds that there can be overlap between potential hydrogen and power surpluses.

The potential surpluses due to a full storage correspond to periods where maximum storage capacity is reached, as seen in Figure 4.13. Potential surpluses due to storage injection limits are much smaller, and indicate efficient component scaling. As mentioned in the analysis of Figure 4.12, the storage injection limit governs the total electrolyser power allocation. High potential surpluses of this type would mean a considerable overcapacity of electrolysis that can never operate, because its hydrogen can neither be delivered nor stored.

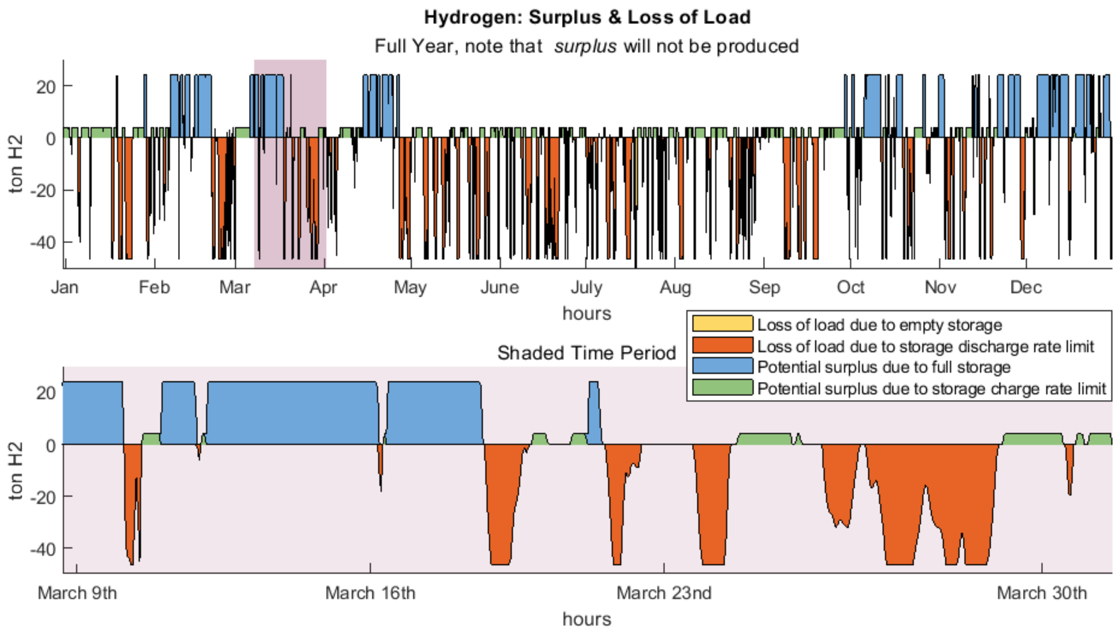

Figure 4.15: Potential surplus and loss of load profiles for hydrogen

Loss of load due to storage extraction limits is the most pronounced type of storage limit in this configuration. Throughout the year, many instances occur where the system is subjected to considerable loss of load for this reason. The maximum size is slightly over 40 $tonH_2/h$, which corresponds to the hydrogen deficit between demand, cracker production and the 20 $tonH_2/h$ storage output seen in Figure 4.12. Essentially, these are instances where no electrolysis is present, and the storage fails to extract enough hydrogen to meet demand. The expected hydrogen loss of load at the end of March is confirmed in the bottom subfigure of Figure 4.15.

Only a single period occurs where an empty storage leads to loss of load, which is a barely visible area mid-July. The loss of load significantly exceeds 40 $tonH2/h$ in this instant, which is only possible if the storage cannot facilitate supply. In this case, the cracker would remain the only hydrogen production source. An empty storage in this particular time period corresponds to the observations from Figure 4.13.

Figure 4.16 shows several system dynamics in case the hydrogen storage is doubled to 2 caverns, which equals 12 $ktonH_2$ capacity. The hydrogen supply attributed to the storage -indicated in yellow in the top subfigure- is significantly larger compared to the original case. This is due to the increased extraction output, which is directly linked to the storage capacity. As a result, the more significant storage supply is not explicitly linked to the higher storage capacity itself, but to the extraction limit. This behaviour is validated in the bottom subfigure, where the storage discharge increases to the new maximum of 40 $tonH_2/h$ in the majority of instances. Coincidently, the loss of load due to storage discharge limit has decreased, as the storage output yields smaller shortages.

In contrast, the charging levels undergo only a marginal increase to a level slightly greater than the original 20 $tonH_2/h$. This is due to the efficient sizing of the hydrogen production sources in the initial system configuration, as mentioned in the analysis of Figure 4.15. The minor potential surplus of hydrogen at any instant, resulting from electrolysis overcapacity, is now always produced. As a result, the total hydrogen production capacity is now limiting in this regard, not the hydrogen storage injection limit. This is confirmed by the limited increase in hydrogen production from electrolysis, as plentiful wind power would be available to support this production increase if only the electrolysis capacity were present.

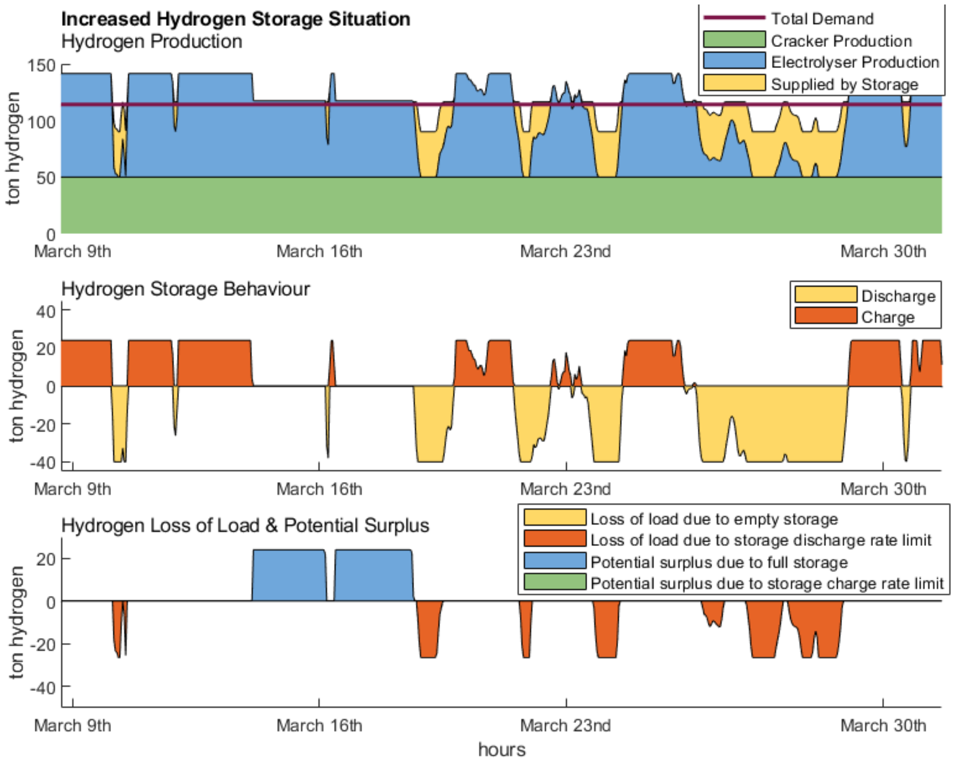

Figure 4.16: Top: Hydrogen production and demand for increased storage capacity from 1 to 2 caverns. **Bottom**: Hydrogen storage charging and discharging behaviour for increased storage capacity from 1 to 2 caverns.

4.6.3. Ammonia Dynamics

The ammonia storage level for a full year is shown in Figure 4.17.

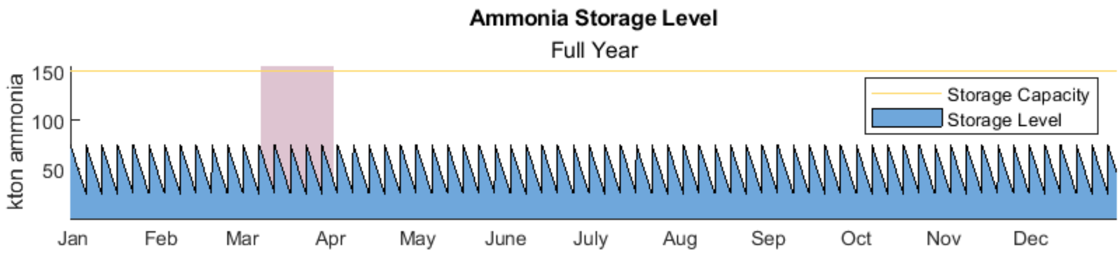

Figure 4.17: The ammonia storage level through the year, including the same shaded time period as in previous plots

Resulting from the constant withdrawal of ammonia from storage to cracker and the periodic ammonia parcel delivery, the ammonia storage level displays a regular sawtooth profile. It should be noted that the ammonia storage is never full or empty, as the model adjusts the delivery frequency to the required cracker input, and does not consider variable delivery times. However, the storage size still scales with the cracker capacity, as discussed in section 4.5.

An alternative operating strategy is to reduce the cracker production level in specific periods by adjusting the load factor (LF_{cr}), an example of which is shown in Figure 4.18. This adjusts the potential cracker production from Equation 4.12. The six months of highest average daily wind power production could be selected to reduce cracker production in. These wind-swept periods directly yield more hydrogen production through electrolysis and thus potentially require less direct support from cracking. For the purpose of this version of the demonstration case, the winter load factor was used of 70% of the total.

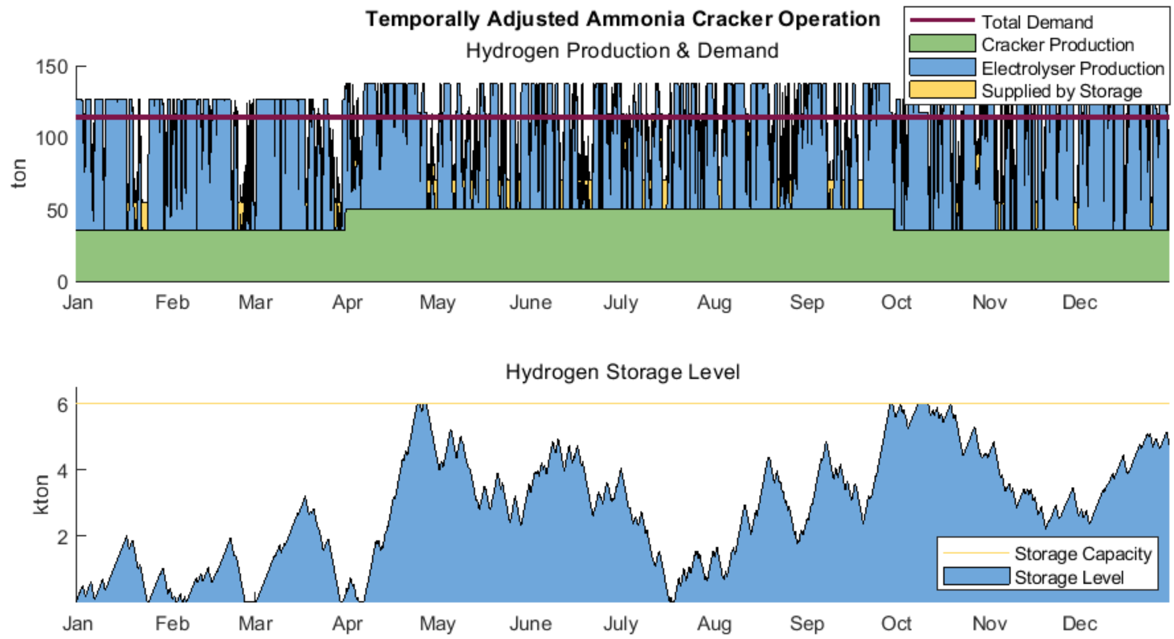

Figure 4.18: TOP: Temporally adjusted ammonia cracker production, with a 70% capacity factor in winter
Bottom: The hydrogen storage level in the adjusted situation

From the storage behaviour it is derived that the decrease in winterly overproduction of hydrogen results in a lack of hydrogen storage buffering. However, this is completely recovered in the month of April, when cracker production increased to 100%. However, it is observed that the decrease in cracker production capacity in the first three months has led to a more significant loss of load. Since the total hydrogen production capacity could apparently increase from its winter level in April, the storage injection limit was not constraining in winter.

The ammonia delivery interval undergoes fluctuations in accordance with the cracker input requirement. A 45% increase in the delivery interval during winter in comparison with full capacity operation during summer has been observed. This increase is consistent with the observed decrease in ammonia requirements resulting from the 70% capacity factor operation.

4.6.4. Key Performance Indicators

Every possible system configuration has a specific output on all *KPIs*. The values for the demonstration case are shown in Table 4.8. Categorised by their corresponding high-level objectives, several *KPIs* are investigated more in-depth in this section.

Indicator	Variable Name	Value	Unit
Affordability			
Capital Expenditure	$CAPEX_{total}$	52.3	$Billion$ €
Operational Expenditure	$OPEX_{total}$	4.8	$Billion$ €
Security of Supply			
Loss of Load *HIC*: Hydrogen	LOL_{H2-HIC}	0	%
Loss of Load *HIC*: Power	$LOL_{power-HIC}$	8.7	%
Loss of Load Hinterland: Hydrogen	LOL_{H2-HL}	16.1	%
Hinterland Power Supply Volume	$SV_{power-HL}$	23.7	%
Hinterland Power Supply Variability	VR	0.0868	–
Domestic Hydrogen Production	DP_{H2}	53.9	%
Sustainability			
Annual Equivalent CO_2 Emissions	CFP_{total}	2.0	Mt
Spatial Footprint: North Sea	A_{sea}	55,920	km^2
Spatial Footprint: Land	A_{land}	70.3	ha
Annual Ammonia Shipments	$N_{amm-shipments}$	67	–

Table 4.8: Demonstration Case Key Performance Indicators

Affordability

The *CAPEX* and *OPEX* associated with the system configuration in this demonstration case are shown in Figure 4.19.

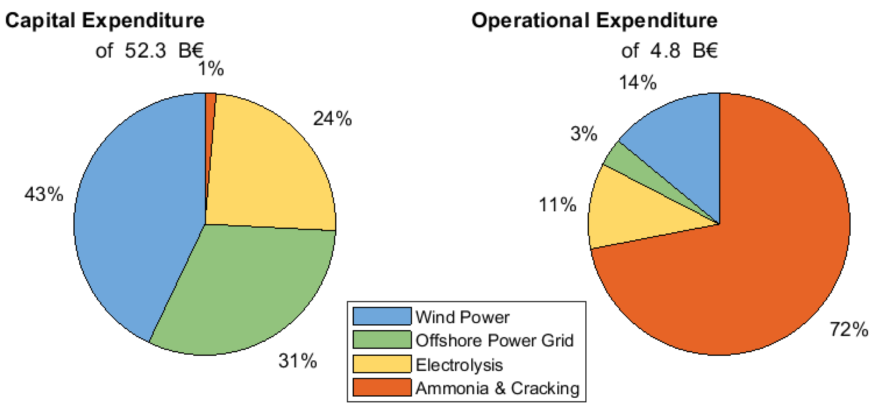

Figure 4.19: Capital and operational expediture in the system configuration of the demonstration case.

The total *CAPEX* is constituted by four main components. The wind farm and offshore power conversion and transmission are the largest contributors, followed by electrolysis. The ammonia cracker adds merely 1% of the system investment, while hydrogen storage and transport are each below a percent and thus neglected in the pie chart.

The operational expenditure is dominated by the cracker-related cost, which consists of the ammonia feedstock cost for over 90%. It should be noted that the annual electrolyser cost merely covers its operational cost and does not feature any cost of power, although this is often a significant proportion of the cost of hydrogen derived from it [94].

Security of Supply

Figure 4.20 shows heatmaps of the loss of load profiles for the baseload demands, notably hydrogen supply to *HIC* and hinterland in addition to the *HIC* power demand.

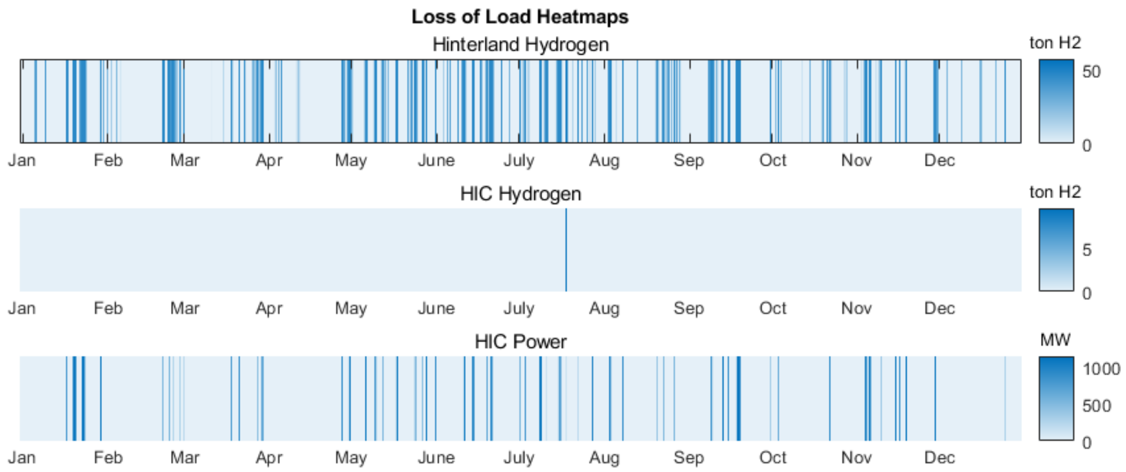

Figure 4.20: Heatmaps for loss of load profiles of hinterland hydrogen demand, *HIC* hydrogen demand and *HIC* power demand, respectively.

The difference in loss of load between both hydrogen demands is due to the hierarchy commanded in the energy management system of the model. This results in a more frequent and higher loss of load for the hinterland compared to the *HIC*. Hinterland must manage loss of loads throughout the year of up to 50 $tonH_2/h$, which is over 80% of its demand. Despite rounding off to 0% loss of load on annual basis, *HIC* experiences a minor loss of load nonetheless. The mid-July time period of this event corresponds to the hydrogen storage depletion observed in Figure 4.13.

Power supply to the *HIC* is more intermittent in the summer period, in accordance to Figure 4.10. The implications of the hierarchy in power distribution can also be observed in its relation with the hydrogen loss of load of the hinterland. Phases with significant loss of load for hydrogen in the hinterland are partially caused by low wind power production. These occurrences also have a visible impact on the *HIC* power supply continuity, albeit to a lesser extent due to the allocation hierarchy.

The variability of the residual power demand profile is shown in Figure 4.21, where it is normalised to observe the relation with the original profile more accurately. It can be seen that strong spikes and fluctuations within the residual profile result in higher variability in the time intervals in early March. More gradual fluctuation at the end of March yields lower variability, but at an increased number of time intervals. It should be noted that the residual profile is merely focused on the grid demand that is not met, not at the variability of the potential power surplus. The latter is wind power that has no current use in the system dynamics, but has the potential to be produced. The alternative is to curtail it, but it could also be stored or consumed in case of demand response. As a result, it would be a 'negative' residual in this figure, of which the variability could be determined as well. However, this is not considered in this research.

All variability values are sorted in a probability density distribution, which is shown in Figure 4.22. The figure demonstrates a substantial prevalence of values around zero, indicative of a flat residual profile without fluctuation between subsequent values of zero. The variability of the residual profile is considerably higher at 0.08678 compared to the variability of merely the grid profile itself at 0.0434. This could be explained by the variability of supply resulting from a variable wind power profile.

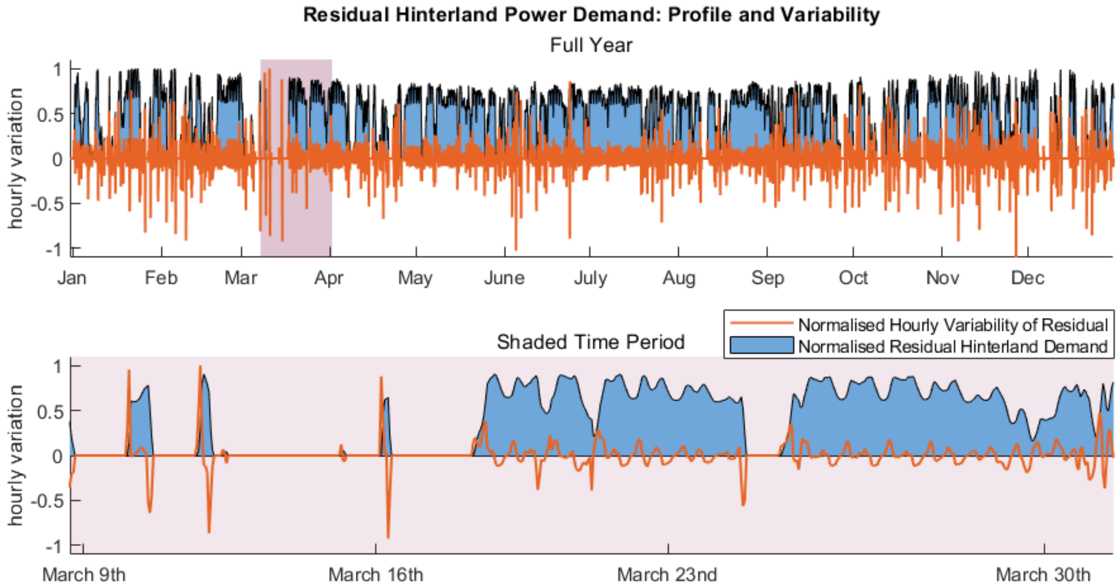

Figure 4.21: The residual power demand profile for hinterland, which is the original hinterland power demand with the supplied power subtracted. The figure includes the hourly variability of the residual profile.

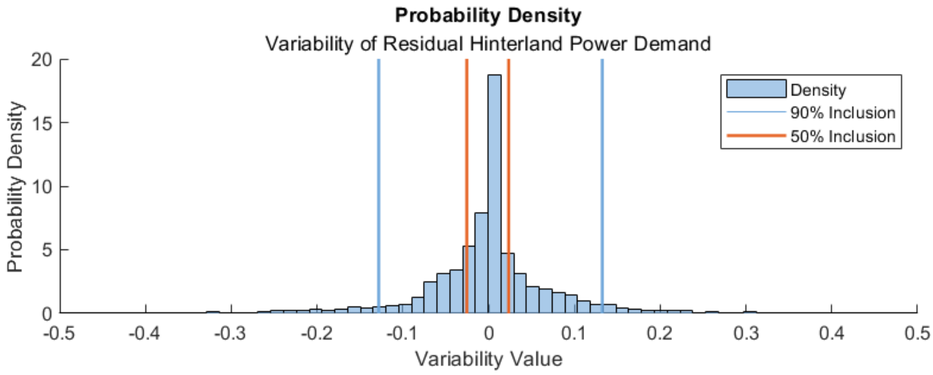

Figure 4.22: Probability density figure of the hourly variability of the residual power profile, including 50% and 90% inclusion boundaries.

Sustainability

Annual equivalent CO_2 emissions are shown in Figure 4.23. The largest contributor to CO_2 emissions is ammonia import. The underlying emissions source for this is the carbon footprint of the power used to produce the hydrogen and subsequently ammonia. The next largest contributor is wind power, which is responsible for 42% of equivalent annual emissions.

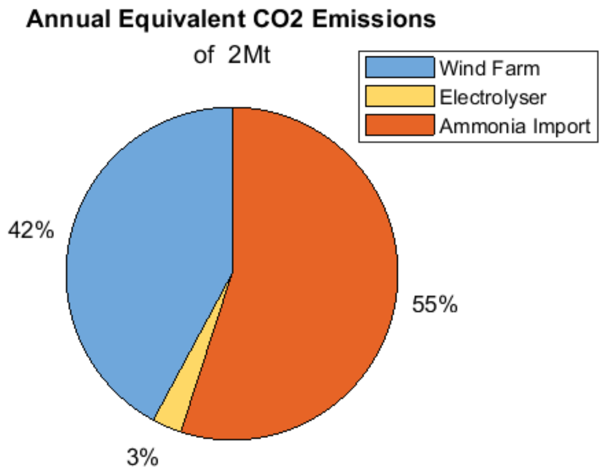

Figure 4.23: Annual equivalent CO_2 of system configuration for demonstration case

4.6.5. System Dynamics Parameters

In order to facilitate a more profound comprehension of the system dynamics, a number of informative parameters are presented in Table 4.9. In addition to the *KPI* outcomes, this table offers supplementary insight into the underlying factors that contribute to the system operation and performance.

Parameter	Variable Name	Value	Unit
Wind Power Potentially Produced	$P_{wind-pot}$	54.1	TWh
Electrolyser Full Load Hours	FLH_{el}	5522	$hours$
Hydrogen Storage Equivalent Charge Cycles	ECC_{H2-St}	10.9	$cycles$
Hydrogen Storage Supply	$H_{st-share}$	6.3	% of total supply
Electrolyser Reduced Production	P_{el-red}	9.2	% of potential production

Table 4.9: Demonstration Case System Dynamics Parameters

Wind Power Distribution

The distribution of wind power is discussed more in-depth in this section, based on the visualisation in Figure 4.24.

In the system configuration of the demonstration case, the electrolyser receives the largest share of wind power at 49%. Hinterland consumes around a quarter, while *HIC* is allocated 17%. However, it should be noted that this figure considers the theoretical wind power that can be generated. Consequently, potential power surplus constitutes a proportion of the total, yet due to its non-production, the actual wind power generation falls short of the indicated theoretical maximum.

Notably, over two-thirds of the produced power does not leave the *HIC* as electrons, although a share of it will leave it as hydrogen.

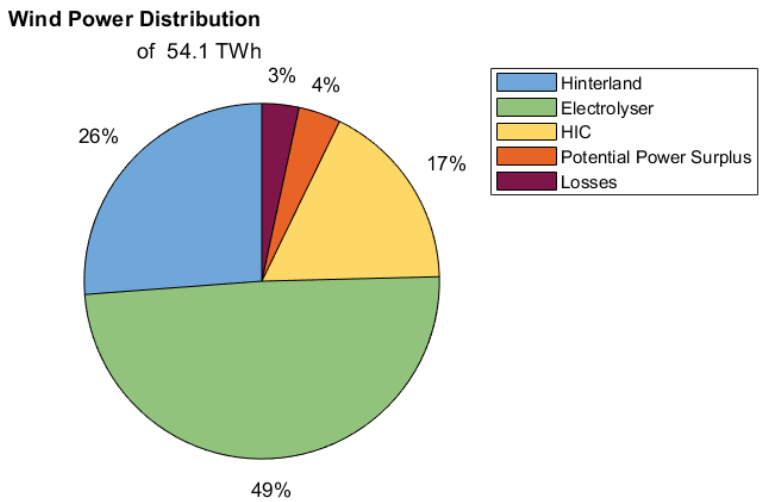

Figure 4.24: Power distribution of maximum wind power production in demonstration case.

4.6.6. Model Verification

This section is focused on the model verification process, which is a crucial aspect of ensuring the model's functionality and alignment with expectations. The model demonstration is evaluated against the theoretical framework, and in certain instances, the validity of the demonstration is substantiated through manual calculations.

The potential power surplus ($P_{pps-total}$) is 2.1 TWh, which equates to 3.9% (rounded to 4%) of the total potential wind power production ($P_{wind-pot}$). The 180.6 TWh total hinterland grid profile is scaled with a factor 0.33, meaning the sum of all $D_{power-HL}$ is 59.6 TWh. Therefore, the model demonstration configuration has supplied approximately 14.1 TWh, which corresponds to the indicated 23.7% of the hinterland power supply volume. This is equivalent to 26% of the allocated potential wind power production, which is in accordance with the power distribution in Figure 4.24. *HIC* power demand is 10 TWh annually, with this system configuration resulting in 8.7% loss of load. Therefore, 9.1 TWh is supplied, which equates 16.9% of total potential wind power production, as specified in the wind power distribution.

When the power distribution is taken into consideration, it is shown that 49% of 54.1 TWh results in 26.5 TWh being allocated to the electrolyser, thereby equating to the calculated 5,522 FLH given the specified electrolyser capacity. Consequently, the power input results in 0.51 MtH_2 production, which corresponds to 53.9% of the total production, aligning with the domestic production share. It can be seen in the figures in section 4.6 that both capacity and injection and extraction rates are adhered to, thus demonstrating compliance with storage limits.

It is demonstrated that the costs associated with hydrogen storage and transportation each constitute well below a percent of *CAPEX* and *OPEX*, and are thus not shown in the charts of Figure 4.19. The storage *CAPEX* from literature 30.6 $M€/ktonH_2$ of capacity, resulting in 183.6 $M€$ total, which is 0.35% of *CAPEX*. Transportation *CAPEX* is less, as 350 km length at 0.13 $M€/km$ yields 45.5 $M€$. The relatively low *OPEX* of storage and transportation compared to other components is noteworthy, with each component accounting for around 0.1% of total *OPEX*.

The loss of load can be verified by comparing the sum of H_{LOL} from the hydrogen availability function in the *EMS* to the sum of LOL_{H2-HIC} and LOL_{H2-HL} from the *KPI* calculation module. Total H_{LOL} equals 80.5 $ktonH_2$, while *HIC* and hinterland have respectively 0% and 16.1% loss of loads for hydrogen on their total 1 MtH_2 demand. As their demands are equal, total loss of load is 8.05% of 1 MtH_2, so this is an accurate representation.

The carbon footprint of ammonia is 2.5 $kgCO_2/kgH_2$, with a H_{Cr} yield of 0.44 MtH_2. The ammonia pathway thus contributes 1.1 $MtCO_2$, which is equivalent to the indicated 55% of the total annual-equivalent carbon footprint of 2 $MtCO_2$. The potential wind power production, denoted by $P_{wind-pot}$, is estimated to be 54.1 TWh, with a corresponding carbon intensity of 15.5 gCO_2/kWh. This contributes to a total of 0.84 $MtCO_2$, which is indeed equivalent to 42% of the total. For electrolysis, the H_{El} of 0.51 MtH_2 and 112 gCO_2/kgH_2 result in 2.9% of the total annual-equivalent carbon footprint, in correspondence with Figure 4.23.

Conclusively, the model adequacy has been shown based on the demonstration case. Multiple output parameters were checked through manual calculation and observations on the magnitude of cost components were verified. The results obtained provide substantiation that the model functions in accordance with its intended design.

5
Port of Rotterdam: A Case Study

Having established the system objectives and a model to describe the dynamics of different configurations, this chapter applies them to a case study of the Port of Rotterdam. The model is populated with specific information based on demand scenarios and possible system configurations that aim to achieve it. In this way, the relation between system design and *KPI* outputs is identified.

In section 5.1, the rationale behind the design of experiment is explained and demand scenarios are introduced. Next, the low demand scenario is investigated in-depth in section 5.2. Alternative cases that test different system operations and configurations in context of the low demand scenario are discussed in section 5.3, after which higher demand scenarios are discussed in section 5.4.

5.1. Design of Experiment

This section outlines the approach for designing the cases used in the study, forming the foundation for exploring system behavior and evaluating performance on selected KPIs. The design of the experiment involves identifying adjustable parameters within the model and strategically defining demand scenarios to extract meaningful insights about the parameter space. The model includes numerous adjustable variables, each influencing the system in unique ways. Collectively, these variables define a vast parameter space, where each combination represents a specific system configuration. The objective of this section is to identify areas of particular interest within this space, with a focus on cases relevant to the Port of Rotterdam. This involves setting practical boundaries for key variables and designing scenarios that facilitate understanding the interplay between local and imported hydrogen pathways under varying demand conditions.

Demand scenarios are created as a basis for the case study. Using the projections for hydrogen and power demand collected in the Cluster Energy Strategy of the Port of Rotterdam [38], three scenarios are drawn up. The low, middle and high demand scenarios and their corresponding values are show in Table 5.1.

Demand Type	**Low Scenario**	**Middle Scenario**	**High Scenario**
HIC Hydrogen	0.5 $Mt.y^{-1}$	0.5 $Mt.y^{-1}$	1.0 $Mt.y^{-1}$
Hinterland Hydrogen	0.5 $Mt.y^{-1}$	2.0 $Mt.y^{-1}$	4.0 $Mt.y^{-1}$
HIC Power	10 $TWh.y^{-1}$	15 $TWh.y^{-1}$	25 $TWh.y^{-1}$
Hinterland Power Scaling Factor	0.25	0.29	0.33

Table 5.1: Demand scenarios with low, middle and high projections.

For the hinterland power demand, the scaling factors for the load profile are set using estimates of consumption increase and the desired share of power originating from *HIC*, using the logic set forth in subsection 3.2.3. A power distribution hierarchy is used that favours the *HIC*, electrolyser and hinterland, in the given order. A desired one-sixth share of annual Dutch power production is upheld for the hinterland power demand, in correspondence with the current fossil contribution [33]. Using the projections of the *II3050*, a power consumption increase of between 50% and 100% is expected towards 2050 in the majority of scenarios [22]. As a result, the values for the hinterland load scaling factor are set using the following logic. An increase with a factor 1.5, or 50%, while aiming for one-sixth supply yields a scaling factor of $1.5/6 = 0.25$ for the low demand scenario. This is continued for 75% and 100% power increase, leading to scaling factors of 0.29 and 0.33 for the middle and high demand scenarios, respectively.

The design of the cases and the system configurations under consideration are presented in the corresponding sections of the results.

5.2. Low Demand

As an initial investigation of the relations between configuration design and *KPIs*, the low demand scenario is used. This is due to the configurations not exerting excessive strain on the system by reaching its design limits for component sizes, which are defined later in this section. Firstly, the different *KPI* outcomes of local, import and combined configurations are examined through the use of distinctive system designs that represent each type of characteristic. The sensitivity of *KPIs* to specific, single parameters is tested for these three system configurations in subsection 5.2.3. Subsequently, it is observed how specific *KPIs* change depending on a variety of system configurations with multiple altered parameters, representing a multitude of combinations between electrolysis and cracking-intensive designs.

5.2.1. Distinctive Pathways

Three types of distinct configurations are defined in Table 5.2. The lowest demand scenario serves as a foundational analysis, emphasizing a base case that is manageable for both local and import pathways within system constraints. For this demand scenario, three pathways are investigated to see how systems with 100% local hydrogen production, 100% import and a combined configuration behave and which values for *KPIs* they produce.

Low Demand Scenario	
Pathway	**Description**
Local	Only domestic hydrogen production
Combined	Balanced hydrogen origins
Import	Only imported hydrogen

Table 5.2: Explored pathways in the low demand scenario.

By evaluating these three types of configurations, the study aims to reveal the differences and similarities of local and import pathways in terms of *KPI* performance, highlighting the trade-offs. The configuration designs are chosen to represent systems with a specific hydrogen origin, based entirely on local electrolysis or ammonia import.

A list of values for the case-specific input parameters is shown in Table 5.3. The full local production case is designed to achieve 0% loss of load with minimal overdesign, similar to the import case. The combined pathway balances local production and imports, with system sizing logically falling between the boundaries of the first two cases. Overdesign of hydrogen production is again avoided to maintain sensibility in *KPI* analysis. For the same reason, the wind farm capacity is set at 18 GW for all configurations, as the local configuration requires at least this capacity to achieve 0% loss of load for hydrogen. The operational strategy has a distinct hierarchy. First, *HIC* power is satisfied, after which the electrolyser is prioritised up to its rated capacity. The remainder is delivered to the hinterland or labeled as a potential power surplus. For hydrogen, *HIC* has first place in the distribution as well, which means hinterland takes the first loss of load. The ammonia cracker constantly operates at full capacity, so no adjusted load factor is considered, as mentioned in section 4.5.

Low Demand Scenario

Component	**Local Pathway**	**Combined Pathway**	**Import Pathway**
Wind Farm	18 GW	18 GW	18 GW
Electrolysis	14 GW	4 GW	0 GW
Ammonia Cracker	0 $MtH_2.y^{-1}$	0.46 $MtH_2.y^{-1}$	1.03 $MtH_2.y^{-1}$
Hydrogen Storage	8 $caverns$	2 $caverns$	0 $caverns$
	= 48 $ktonH_2$	= 12 $ktonH_2$	= 0 $ktonH_2$

Power Hierarchy	**Hydrogen Hierarchy**
1. *HIC*	1. *HIC*
2. Electrolyser	2. Hinterland
3. Hinterland	

Table 5.3: System configuration parameters and operational strategy for the comparison between a local, combined and import case in the lowest demand scenario.

Each of these configurations has a distinct hydrogen production profile, which are shown side-by-side in Figure 5.1.

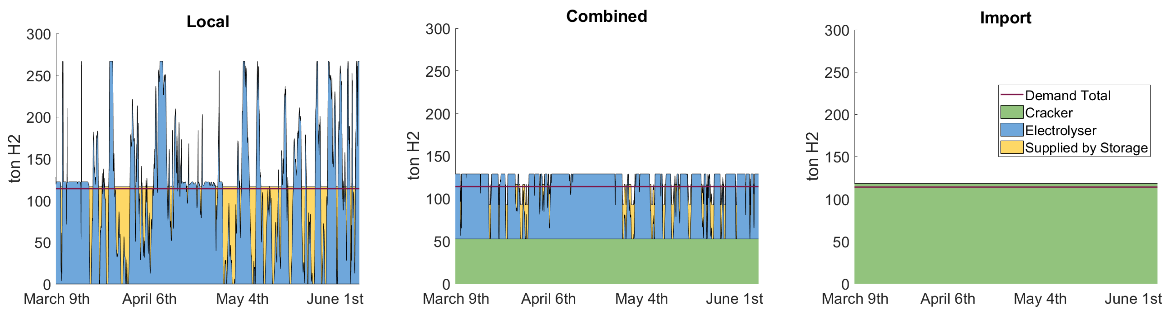

Figure 5.1: Hydrogen production for an indicative time period for a local, combined and import configured case.

It can be observed that the local configuration has a considerable overcapacity in electrolysis power compared to the demand at any instant. This power is necessary to provide enough additional hydrogen for storage, such that the storage holds enough hydrogen to support periods of lower wind power. Additionally, a significant amount of caverns is necessary for the storage to be able to deliver the complete hydrogen output in absence of electrolysis production. It is worth noting that the sharp peaks around March 9^{th} are caused by the reduced hydrogen production of the electrolyser, as a result of a full storage. This behaviour is also observed in the model demonstration case of section 4.6, where the production is ramped down to slightly over the momentary demand level to account for system losses.

An elevated baseload support from import leads to a reduction of the required storage output for the combined configuration. As a result, a lower extraction rate is allowed, which decreases the amount of caverns in this situation. The combined case has a reduced hydrogen overcapacity requirement as well, following from the fact that the instantaneous production surplus that needs to be stored is inherently decreased. Consequently, a reduced electrolysis capacity is required. As the wind power capacity does not change, nor the hierarchy in power distribution or *HIC* power demand, the electrolyser has more full load hours compared to the local production case. This phenomenon contributes to the reduced storage requirement, as reflected in the less pronounced yellow surface area of hydrogen supplied by storage.

The import configuration demands no storage of hydrogen at all, of course in consideration of this research's general assumption of uninterrupted ammonia influx.

5.2.2. Impact of Supply

This section discusses the *KPI* values associated with each of the three configurations from subsection 5.2.1. They are shown in Table 5.4 below.

Low Demand Scenario			
KPI	**Local**	**Combined**	**Import**
Affordability			
Capital Expenditure	96.0 $Billion$ €	69.6 $Billion$ €	59.7 $Billion$ €
Operational Expenditure	2.82 $Billion$ €$/y$	5.3 $Billion$ €$/y$	9.33 $Billion$ €$/y$
Security of Supply			
Loss of Load			
HIC Hydrogen	0%	0%	0%
HIC Power	4.4%	4.4%	4.4%
Hinterland Hydrogen	0%	4.9%	0%
Hinterland Power Supply			
Volume	22.5 $\%_{total}$	62.5 $\%_{total}$	84.3 $\%_{total}$
Variability	0.0947 $[-]$	0.1156 $[-]$	0.0881 $[-]$
Domestic Hydrogen Production	100%	54.3%	0%
Sustainability			
Annual-equivalent CO_2 Footprint	1.38 $MtCO_2/y$	2.47 $MtCO_2/y$	3.85 $MtCO_2/y$
Spatial Footprint			
North Sea	83,880 km^2	83,880 km^2	83,880 km^2
Land	162 ha	62.3 ha	22.3 ha
Annual Ammonia Shipments	0	71	158

Table 5.4: Key performance indicator values for the local, combined and import configurations in the low demand scenario.

Different *KPIs* vary considerably between the local and import pathways. The local system has a lower *OPEX*, at the cost of a higher *CAPEX*-intensity. The loss of load for *HIC* power is identical, as the power hierarchy prescribes it receives the same power in all three configurations. The local case has a higher spatial footprint on land, although it has fewer carbon emissions. It has been established that the power supply volume to the hinterland increases considerably for configurations which rely more on ammonia import for their hydrogen. This is due to the fact that their decreased power consumption in electrolysis frees up power to be delivered to the hinterland. For additional insight into the varying periodic dynamics of the hinterland power supply, figures on the residual demand profile and variability for each configuration have been added in Appendix A.

The relation between hinterland power supply volume and the variability of the residual profile is further discussed in subsection 5.2.4.

5.2.3. Parameter Sensitivity

A sensitivity analysis examines how specific model parameters influence *KPI* outcomes. This analysis identifies whether fixed parameters significantly affect results and whether their influence differs between local and import pathways. The parameters considered are the cost of ammonia, length of the offshore power cable and electrolysis conversion energy. Based on the demonstration case in section 4.6, these parameters were observed to be significant contributors of *KPI* values.

Ammonia Cost

In the model demonstration in section 4.6, it was observed that ammonia cost is a large factor of influence on the *OPEX* of the entire system. Figure 5.2 shows the sensitivity of the *OPEX* to the cost of ammonia based on the 900 USD/ton baseline value. The range of variation for the cost of ammonia is between approximately 500 and 1300 USD/ton, which is considered within expectation boundaries by the Port of Rotterdam. It can be seen that the local configuration is of course not affected, as it does not involve any ammonia. For both the combined and import configurations ammonia cost fluctuations have a strong influence on the cost, as was expected from its large share in the *OPEX* seen in section 4.6. Either has a symmetric effect across the downwards and upwards sensitivities, as the relation between ammonia cost and *OPEX* is linear. It should be noted that the total *OPEX* of the import configuration is almost double that of the combined configuration, as seen in subsection 5.2.2. Therefore, the absolute difference in *OPEX* is considerably higher as well.

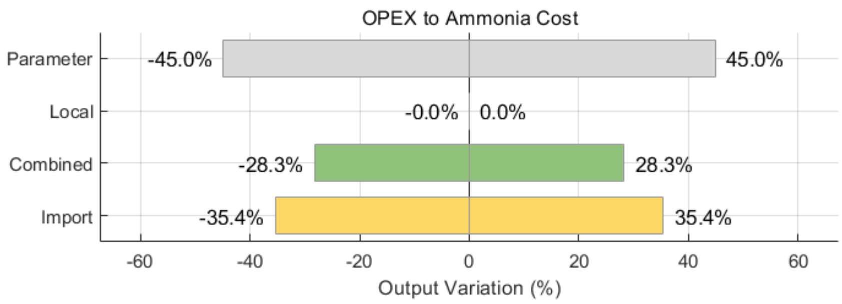

Figure 5.2: Parameter sensitivity of *OPEX* to the cost of ammonia for the local, combined and import configurations.

Length of Offshore Power Cable

The influence of this parameter on system investment cost is relevant, as wind farms need to be situated at increasing distances from the coast, consequently requiring more substantial cable lengths. Besides, it was noticed in section 4.6 that it can constitute a considerable share of the *CAPEX* of the system. The baseline length of 110 km is varied 45% either direction, corresponding to adjusted lengths of around 60 and 160 km, respectively.

From Figure 5.3, it can be observed that the magnitude of sensitivity of the configurations with a heavier reliance on ammonia is higher. This can be attributed to the lower total *CAPEX* associated with these system designs. As a result, a *CAPEX* variation of the same component has more relative impact. Another remarkable observation is the symmetry for each type of configuration. The symmetry between sensitivity to positive and negative cable length variation suggests that the relation is linear. This is reasonable, as the *CAPEX* increases linearly with cable length variations, which is an assumption in this research that is clearly reflected in this sensitivity analysis.

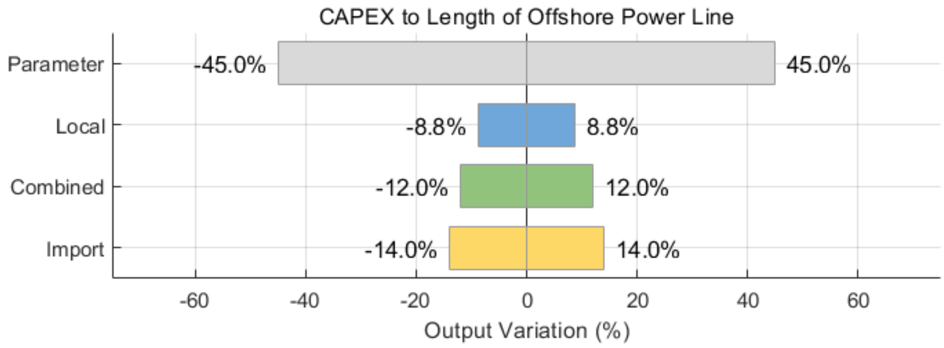

Figure 5.3: Parameter sensitivity of *CAPEX* to the length of the offshore power transmission for the local, combined and import configurations.

Electrolysis Conversion Energy

The conversion energy of electrolysis is the variable that relates its power consumption and hydrogen production volume. This parameter exerts influence on several variables. However, in the context of the standard power distribution hierarchy of this research, the *KPI* that is influenced most is the hinterland power supply volume. The rationale for this is that the electrolyser conversion energy impacts the power required to produce the hydrogen that is in demand. Hence, lower conversion energy translates into greater power availability for the next-in-line consumer, which is the hinterland in this configuration. The electrolyser conversion energy is varied 12.5% in positive and negative directions, corresponding to approximately 45 and 58 kWh/kgH_2.

The sensitivity of hinterland power supply to the electrolyser conversion energy is shown in Figure 5.4. It is demonstrated that a lower conversion energy results in considerable increase of power supply to the hinterland, while a higher conversion energy allows a decreased proportion of the demand. However, it is important to note that the local configuration generates a relatively low power supply for the hinterland as a whole. This is the reason why the absolute increase in supply is limited.

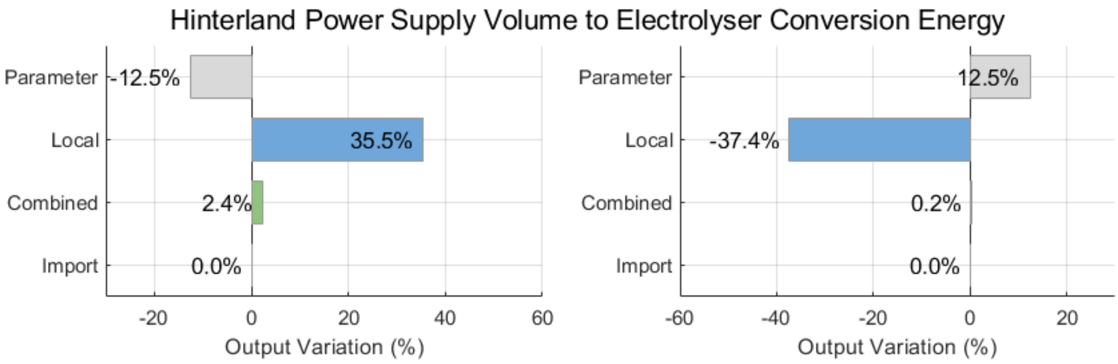

Figure 5.4: Parameter sensitivity of hinterland power supply volume to the electrolyser conversion energy for the local, combined and import configurations.

5.2.4. Key Performance Indicator Trade-Offs

This section will create ranges for the design variables of wind farm, electrolyser, cracker and hydrogen storage capacities. As a result, each possible combination has distinct values for *KPIs*, which means the trade-offs between specific *KPIs* can be investigated for a wide range of slightly deviating system configurations. Favourable or otherwise potentially useful combinations of *KPI* values can be investigated to determine which system configurations underpin them.

The ranges of design variables that are run through the model are specified for the low demand scenario in Table 5.5. These ranges all start at zero except for the wind farm capacity, the lower boundary of which is set at 10 GW. This is around the total confirmed capacity destined for the *HIC* at the time of writing. The upper limits of these ranges are chosen by the practical capacity boundaries. Due to the practical limits of creating a considerable amount of landfalls for offshore wind in a heavily industrialised port area, a 20 GW limit is considered for the wind capacity in this research. Electrolysis is constrained by a 14 GW boundary condition, as this has proven sufficient to reach 0% loss of load for hydrogen in subsection 5.2.1. The same logic for the upper limit has been upheld for the ammonia cracker and hydrogen storage.

Component Capacity	**Low Demand Scenario**
Wind Farm	10 - 20 GW 2 GW increments
Electrolyser	0 - 14 GW_e 2 GW_e increments
Ammonia Cracker	0 - 1.03 $MtH_2.y^{-1}$ 0.17 $MtH_2.y^{-1}$ increments
Hydrogen Storage	0 - 8 $caverns$ 2 $caverns$ increments
Total Configurations	1680

Table 5.5: Ranges for design variables per demand scenario, including increment sizes.

In all cases, the same distribution hierarchies are respected, which are shown in Table 5.6.

Power Hierarchy	**Hydrogen Hierarchy**
1. *HIC*	1. *HIC*
2. Electrolyser	2. Hinterland
3. Hinterland	

Table 5.6: Distribution hierarchies in the *KPI* comparison.

Two separate *KPI* trade-offs are investigated. First, the *CAPEX*, *OPEX* and the total hydrogen loss of load are considered, after which the hinterland power supply volume and the variability of its demand residual are discussed.

CAPEX, OPEX & Hydrogen Loss of Load

The relation between *CAPEX* and *OPEX* of all configurations is shown in Figure 5.5. The colour scale illustrates the total hydrogen loss of load, with lighter coloured markers denoting unfavourable, high values for this *KPI* and dark blue markers indicating system designs that perform well on this metric. The left subfigure shows all configurations, regardless of loss of load, while the right side only shows designs with at maximum 10% loss of load. It should be noted that for clarity, the colour scale was adjusted for the right figure with the filtered values.

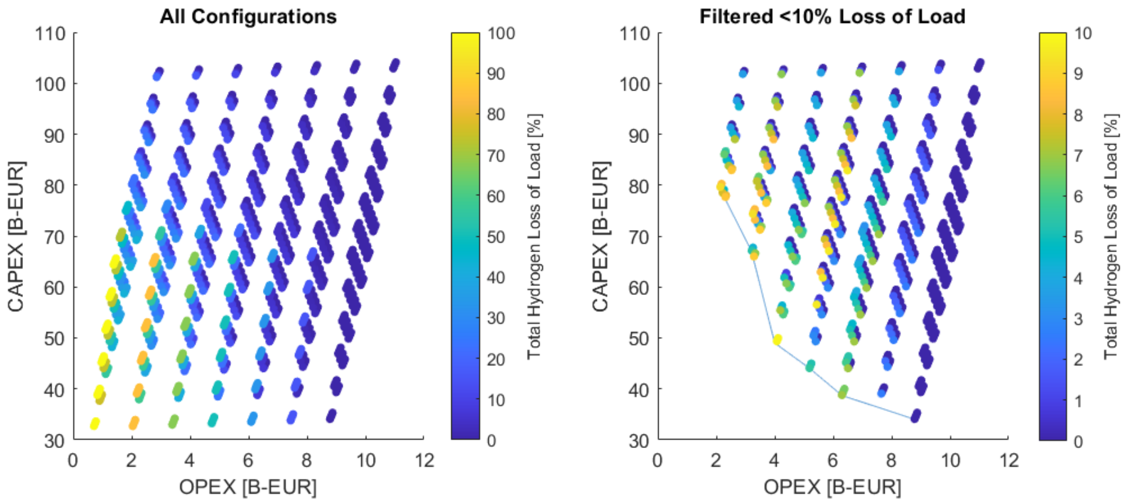

Figure 5.5: Relation between *CAPEX*, *OPEX* and hydrogen loss of load for the low demand scenario.
Left: all configurations, regardless of loss of load.
Right: filtered set of configurations with at maximum 10% hydrogen loss of load, including a Pareto front

The pattern of the configurations in the scatter plot is remarkable, and originates from the strategy in which the variables are swept across the different system designs. The horizontal spacing is composed of seven steps, which can be attributed to the step size of the ammonia cracker capacity. The modest gradient of these variations reflects the limited *CAPEX* increase for the ammonia cracker compared to its *OPEX* increase resulting from higher ammonia consumption. The vertical pattern is due to the ratio of wind and electrolysis capacity. The marginal *CAPEX* for combined wind and corresponding offshore power transmission capacity is of similar magnitude as the marginal investment cost for electrolysis. As the variation in these parameters has the same step size, the vertical progression is less distinctly attributable to a single parameter. Instead, it is caused by the combination of wind and electrolysis capacity variations. The minor variation that is responsible for the off-diagonal dashes of the seesaw figure is the hydrogen storage capacity. It has both a low *CAPEX* and *OPEX* for its predetermined step size compared to the other three configuration parameters, which is why configurations with higher storage capacities have positions that are only slightly to the top-right compared to the previous design.

Configurations with specific characteristics have different locations within the figure. Left bottom values in the left subfigure are systems with little to no electrolysis, cracking or storage capacity at all. The right subfigure provides a more detailed insight in configurations that perform relatively well. The front that encloses the bottom left of the area populated with system designs is of specific interest, as it provides insight in the trade-off between *CAPEX* and *OPEX*. Starting from the left, following this front to the bottom right resembles the shift in reliance from a local to an import-heavy system design with similar loss of load characteristics. The configurations in the left, local-focused part of this front have at least 16 GW of wind capacity and 8 GW_e electrolysis capacity, in combination with a minimum of 4 caverns. The indicated front is steep on the left side due to the high capital intensity of additional wind and electrolysis to achieve similar loss of load compared to systems that have a stronger hydrogen baseload support from ammonia cracking. An additional observation is that configurations in the top left area have the most active storage supplies, up to 25% of total hydrogen demand. The system designs that correspond to this have similar configurations to the local case in the low-demand scenario of subsection 5.2.1: high wind, electrolysis and storage capacities and little to no ammonia cracking.

Hinterland Power Supply: Volume & Residual Variability

The relation between the supplied volume and the variability of the residual demand profile of the hinterland is subjected to more elaboration. This proposition is founded upon the ambiguity that has been observed in the variability of both the local, combination and import configurations discussed in subsection 5.2.1. Figure 5.6 shows the relation in more detail, across the range of configurations specified in Table 5.5.

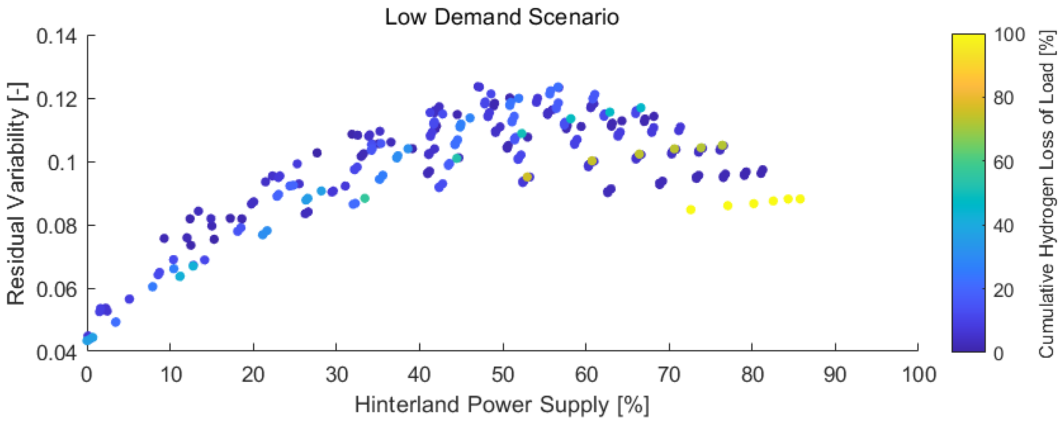

Figure 5.6: Relation between hinterland power supply and the variability of residual demand.

The lower left corner of the figure indicates that the original grid demand exhibits its own degree of variability. In the absence of supply, the residual demand is equivalent to the complete hinterland demand, with a variability of 0.0434. Conversely, the right-hand side of the figure illustrates the variability in the absence of electrolysis. This is equivalent to the maximum hinterland supply that the system is capable of delivering, with the exception of the HIC power supply. The maximum variability values are found in configurations with maximum wind capacity, medium electrolysis and smaller crackers. When comparing the power distributions and residual profile shapes of these configurations, it was observed that the high variability in these systems originates from a sizeable overcapacity for wind power. All of these designs had nearly 30% potential power surplus (curtailment), and the height of the wind power profile compared to the grid load results in a delivered power profile that resembles a square wave shape. Consequently, this results in strong spikes in the residual profile, which in turn impacts the variability.

The curvature of the figure is pronounced and corresponds to the observations made in subsection 5.2.1. In this section, it was suggested that the increasing prevalence of zero-residual instances in the higher supply volumes has a dampening effect on the variability. In order to verify this, the same range of system configurations was analysed for variability, but with the zeros filtered out. It was found that the suggested dampening effect of zeros in the set occurs. In case the zeros are filtered, the variability of the residual continues to increase in proportion with the supplied volume. This finding suggests that as the power supply increases, the residual profile becomes more disordered, despite a concurrent decrease in its volume. The corresponding figure can be found in Appendix A.

5.3. Alternative Cases

In addition to the primary case study, which comprises thorough identification of the relations within the system, alternative cases are run. These have been designed as experiments to learn about alternative system components and operation strategies. Initially, a case involving an electric ammonia cracker is investigated, followed by a modification to the power distribution hierarchy in the subsequent case.

5.3.1. E-cracker

An electric cracker (e-cracker) is an ammonia cracking reactor in which the reaction heat is generated through electricity input. In this research, the process energy is obtained by default through parasitic ammonia fueling, in correspondence with the Fluor research and the configuration described in chapter 3. As a result of co-firing ammonia in the reactor, the ammonia-to-hydrogen conversion ratio of the cracking process increases, indicating higher ammonia consumption for the same hydrogen output. This section compares the e-cracker and original ammonia co-fired configurations.

This comparison involves two adjusted parameters: *HIC* power demand and ammonia cracking conversion ratio from ammonia to hydrogen. The e-cracker is assumed to result in an increased power demand for *HIC*, which also means it receives first place in the power distribution hierarchy, along with the original *HIC* power demand. In the e-cracker situation, there is a decrease in ammonia cracker conversion ratio due to the elimination of parasitic ammonia use. As the hydrogen yield of the cracker remains constant to maintain the same distribution, the necessity for ammonia import is reduced.

The energy balance is examined in order to ascertain the impact of the introduction of a new competitor for power consumption. A novel case configuration is selected for analysis, which is shown in Table 5.7. The system design is oriented towards a realistic power distribution, permitting only limited overdesign in power production. This configuration was deliberately designed to create a more pronounced influence of the change in power distribution in comparison to the previous configurations in subsection 5.2.1. This configuration bears a strong resemblance to the 'combined' low demand configuration from subsection 5.2.1. However, the configuration from the previous sections was designed to minimise hydrogen production overdesign instead. The primary distinction between the two cases lies in the configuration of wind capacity and the scaling factor of hinterland power.

Mutual Parameters			
Component	**Value**	**Component**	**Value**
Demand		**Configuration**	
HIC Hydrogen	0.5 $Mt.y^{-1}$	Wind Farm	14 GW
Hinterland Hydrogen	0.5 $Mt.y^{-1}$	Electrolysis	4 GW
Hinterland Power Scaling Factor	0.33	Ammonia Cracker	0.46 $MtH_2.y^{-1}$
		Hydrogen Storage	2 $caverns$

Power Hierarchy	**Hydrogen Hierarchy**
1. *HIC*	1. *HIC*
2. Electrolyser	2. Hinterland
3. Hinterland	

Table 5.7: System input parameters that are identical for both the ammonia-fueled cracker and e-cracker cases.

The two parameters that are adjusted between the e-cracker and the base case are shown in Table 5.8, which are *HIC* power demand and ammonia cracker conversion ratio. According to cracker operator Haldor Topsøe, 8 $MWh_e/tonH_2$ is needed to power an electric cracker [97]. At the production level specified in Table 5.7, this amounts to 3.7 $TWh.y^{-1}$. Resulting from the e-cracker consumption, annual *HIC* power demand increases to 13.7 TWh in this case. The ammonia conversion ratio of an e-cracker is 6 $tonNH_3/tonH_2$ [97]. This is considerably lower than the base case with ammonia fuel and tail gas co-firing. In this test case, the cracker energy requirement is essentially transitioned from the consumption of ammonia to the utilisation of electrons. For the base situation, the ammonia conversion ratio is employed consistently with the rest of the research.

Configuration-Specific Parameters		
Component	**Base**	**E-Cracker**
HIC Power Demand	10 $TWh.y^{-1}$	13.7 $TWh.y^{-1}$
Cracker Conversion Ratio	*confidential*	6 $tonNH_3/tonH_2$

Table 5.8: Configuration parameters for the base ammonia-fueled and e-cracker cases.

The wind power distributions of both cases are given in Figure 5.7. The *HIC* retains its primary priority, consequently resulting in a substantial annual increase from 15% to 20% of the potential wind power production. This increase is partially offset by a reduction in the power supplied to the electrolyser and hinterland. Additionally, the system also has a marginally decreased potential power surplus (curtailment), indicating a higher consumption rate.

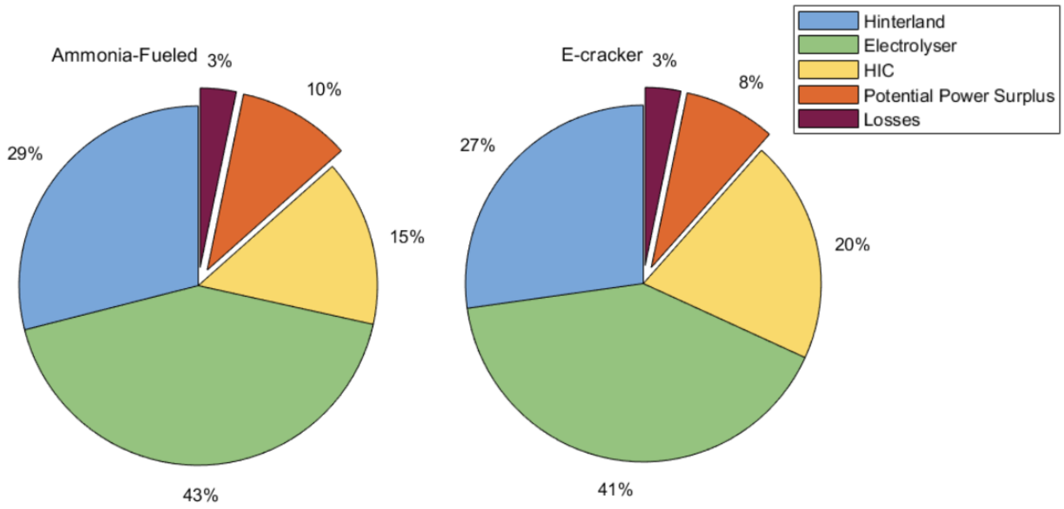

Figure 5.7: Power distribution of the ammonia-fueled cracker and e-cracker.

Table 5.9 confirms that the hinterland not only receives a lower share of power, but a slightly lower share of its demand is fulfilled. In line with Figure 5.7, the lower power share allocated to the electrolyser results in lower full load hours and thus decreased production. This leads to a higher total loss of load for hydrogen and a minor decrease in the share of domestic hydrogen production. This dynamic is expected to increase with a larger installed capacity for the ammonia cracker, as 8 $TWh.y^{-1}$ is added for each $MtH_2.y^{-1}$ that is achieved through cracking. This amounts to a doubling of the current *HIC* power demand [33].

Component	Base	E-Cracker
Power		
Hinterland Power Supply Volume	48.7%	45.7%
Hydrogen		
Electrolyser *FLH*	6,720	6,465
Total Hydrogen Loss of Load	10.1%	13.5%
Domestic Hydrogen Production	52.9%	51.9%
Ammonia		
Ammonia Ships	71	56

Table 5.9: Key performance indicator comparison for the base ammonia-fueled and e-cracker cases.

5.3.2. Power Allocation Hierarchy

To evaluate the impact of different power distribution strategies, alternative power allocation hierarchies are tested. The same system configuration are used as outlined in subsection 5.3.1 and detailed in Table 5.7, with the original ammonia-fueled cracker. These variations allow for a parallel comparison of power distribution effects and key *KPI* outcomes. Three different configurations are considered, which are shown in Table 5.10. The baseline priority has the same power distribution hierarchy as is used in the rest of the cases to serve as a reference for comparison. The 'Electrolysis priority' hierarchy favours local hydrogen production by degrading *HIC* power, while the final operational strategy promotes the hinterland power demand.

Baseline Priority	Electrolysis Priority	Hinterland Priority
1. *HIC*	1. Electrolysis	1. Hinterland
2. Electrolysis	2. *HIC*	2. *HIC*
3. Hinterland	3. Hinterland	3. Electrolysis

Table 5.10: Alternative power allocation hierarchies.

The power distributions resulting from different allocation hierarchies are shown side by side in Figure 5.8. Since this system configuration features minimal overdesign in terms of power capacity, changes in power allocation hierarchy reveal clearer dynamics in system behaviour. When comparing hierarchies, the baseline and electrolysis-prioritised strategies exhibit similar power distributions. This could be attributed to the relatively small power demand of *HIC* compared to the installed wind capacity, making its impact on overall distribution less pronounced. However, when hinterland consumption is prioritised, it absorbs approximately half of the total potentially generated wind power. This shift primarily comes at the expense of electrolysis, as seen in the aggregated annual distribution.

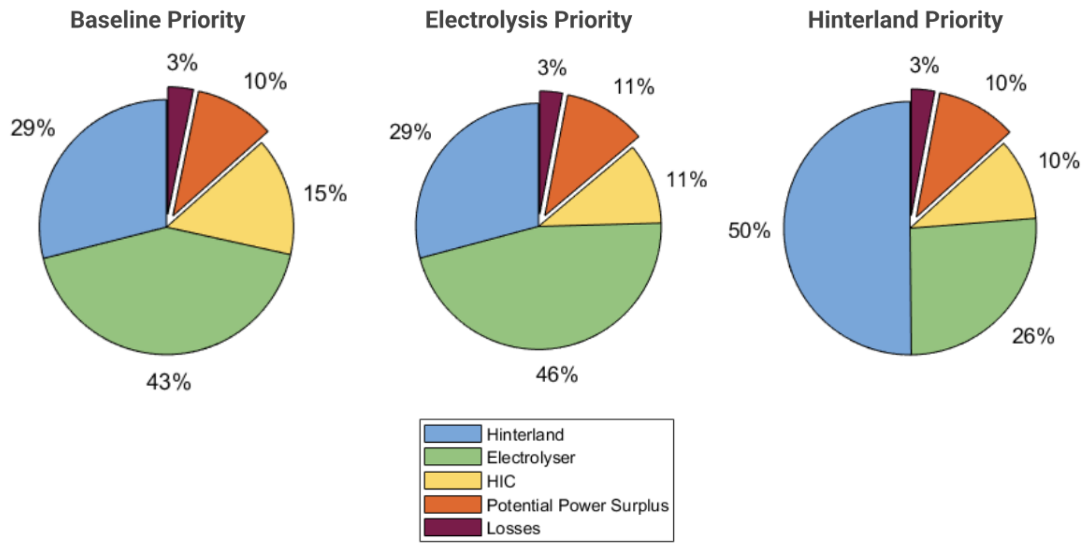

Figure 5.8: Power distribution of the alternative hierarchy cases, showing baseline, electrolysis and hinterland priorities from left to right.

The variations in *KPIs* resulting from the alternative power distribution hierarchies are listed in Table 5.11.

KPI	Baseline	Electrolysis	Hinterland
Total H_2 Loss of Load	10.1%	0%	48.3 %
HIC Power Loss of Load	5.2%	24.3%	33.9%
Hinterland Power Supply Volume	48.7%$_{demand}$	50.3%$_{demand}$	84.3%$_{demand}$
Hinterland Residual Variability	0.0973	0.0966	0.0701
Domestic H_2 Production	52.9%	55.5%	40.7%

Table 5.11: *KPIs* for the alternative power allocation hierarchies specified in Table 5.10.

A greater emphasis on electrolysis has been demonstrated to result in a decrease in hydrogen loss of load; conversely, placing it last-in-line has been shown to result in a significant loss of load. This finding serves to corroborate the hypothesis that hinterland power and local electrolysis compete for the same wind power, and that favouring either inevitably compromises the other. The same logic is applicable to the *HIC* power loss of load. It is even increased more if hinterland is given first priority compared to electrolysis. This could be due to the higher profile of the grid load compared to electrolysis at maximum capacity. As the electrolysis priority case has a 0% hydrogen loss of load, it is possible that the electrolyser is even ramped down at times in this situation, freeing up power for *HIC* to consume and thereby slightly dampening its loss of load compared to the hinterland priority case.

The implementation of a prioritised hinterland configuration results in a substantial elevation of the power supply volume from approximately 50% to 84.3%, representing the maximum capacity that this wind power profile can deliver to the designated grid load profile. Simultaneously, the variability of the residual grid profile decreases with the amount of power volume, which is behaviour that matches with the observations for larger supply volumes in subsection 5.2.4. The domestic hydrogen production closely resembles the amount of power allocated to the electrolyser, although it is somewhat deceptive in the hinterland priority case, as this has almost 50% loss of load as well.

5.4. Higher Demand Scenarios

To assess whether the relations identified for the low-demand scenario hold under increased system scaling, additional higher-demand scenarios were designed in section 5.1. Similar to the range of variation for the four design variables delineated for the low-demand scenario in subsection 5.2.4, Table 5.12 shows the ranges for the other demand scenarios as well.

Component Capacity	**Low Scenario** (repeated)	**Middle Scenario**	**High Scenario**
Wind Farm	10 - 20 GW 2 GW incr.	10 - 20 GW 2 GW incr.	10 - 20 GW 2 GW incr.
Electrolyser	0 - 14 GW_e 2 GW_e incr.	0 - 20 GW_e 4 GW_e incr.	0 - 20 GW_e 4 GW_e incr.
Ammonia Cracker	0 - 1.03 $MtH_2.y^{-1}$ 0.17 $MtH_2.y^{-1}$ incr.	0 - 2.59 $MtH_2.y^{-1}$ 0.43 $MtH_2.y^{-1}$ incr.	1.50 - 5.18 $MtH_2.y^{-1}$ 0.92 $MtH_2.y^{-1}$ incr.
Hydrogen Storage	0 - 8 $caverns$ 2 $caverns$ incr.	0 - 8 $caverns$ 2 $caverns$ incr.	0 - 8 $caverns$ 2 $caverns$ incr.
Total Configurations	1680	1260	900

Power Hierarchy	**Hydrogen Hierarchy**
1. *HIC*	1. *HIC*
2. Electrolyser	2. Hinterland
3. Hinterland	

Table 5.12: Top: Ranges for design variables per demand scenario, including increment sizes. **Bottom**: Distribution hierarchies.

This range is predicated on the minimum output required to facilitate all hydrogen production, as well as the practical upper limit of what could be realised. The 20 GW limit mentioned in subsection 5.2.4 remains for the wind capacity, with an upgraded 20 GW_e electrolysis boundary condition. This is equalised to the maximum wind capacity, as the 14 GW_e electrolysis capacity from the low-demand scenario is not sufficient to supply the increased demands. Besides, augmenting electrolysis capacity beyond that of wind capacity provides no benefit in this study, given the constraint of no power import from the hinterland.

In the high demand scenario, a cracker capacity of no less than 1.5 $MtH_2.y^{-1}$ is considered. In addition to the maximum achievable electrolysis capacity, this would at least be necessary to meet the momentary hydrogen demand. Therefore, this cracking capacity is regarded as the minimum boundary. The upper ranges of the cracker capacity are set at the level at which 0% loss of load was observed, while hydrogen production in this situation was only attributed to the cracker.

5.4.1. CAPEX & OPEX

This section examines the relationship between *CAPEX* and *OPEX* under increased demand conditions. By analysing the impact of scaling up system components, it is assessed how investment and operating costs evolve as hydrogen demand grows. Figure 5.9 presents the distributions for system configurations that maintain a maximum hydrogen loss of load of 10%. This figure simplifies the scatter plot in Figure 5.5 by focusing on the approximate area that all configurations cover in the distribution for each demand scenario. The highlighted areas in each case represent all configurations that meet the specified loss of load threshold.

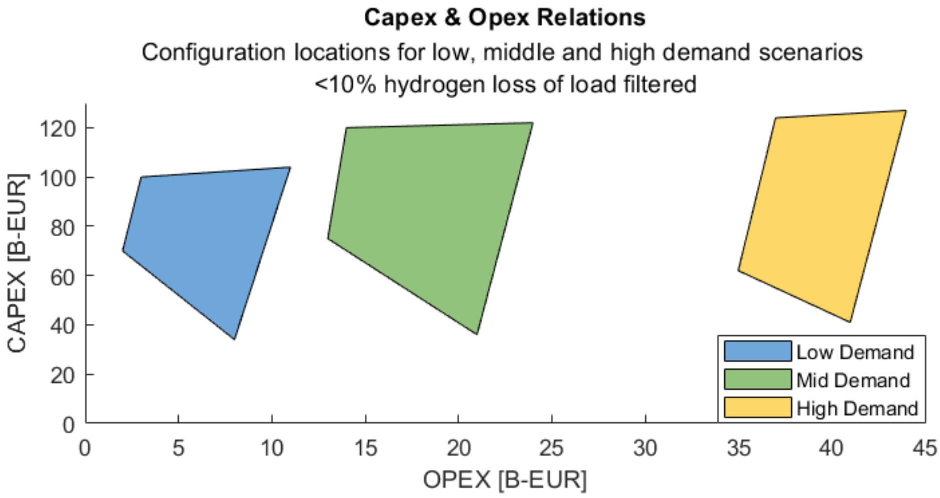

Figure 5.9: Areas covering the configurations with at maximum 10% hydrogen loss of load. Indicated for low, middle and high demand scenarios.

A clear trend emerges: while *CAPEX* approaches an upper limit, *OPEX* continues to rise. This is a direct consequence of the capacity constraints imposed on wind power and electrolysis. Configurations at the upper boundary of the plotted areas correspond to maximum capacity for both wind and electrolysis. Beyond the maximum achievable levels of hydrogen production within the specified range of wind and electrolysis capacity, only increasing ammonia import could cover higher hydrogen demand. The expansion of cracking capacity is associated with a low investment cost. However, the additional ammonia import necessitated for the increased cracking operation results in a high *OPEX*. As long as no constraint is imposed on the size of the ammonia cracker, there is no limit to the hydrogen demand that could be satisfied. Further details on the underlying trends in middle and high-demand scenarios can be found in Appendix A, where similar scatter plot figures as in Figure 5.5 are shown.

5.4.2. Domestic Hydrogen Production & Hinterland Power

The trade-off between domestic hydrogen production and power supply to the hinterland is further examined in Figure 5.10. It employs a colour scale to be able to identify extremes with high losses of load for hydrogen. Dark blue markers highlight superior performance on this metric.

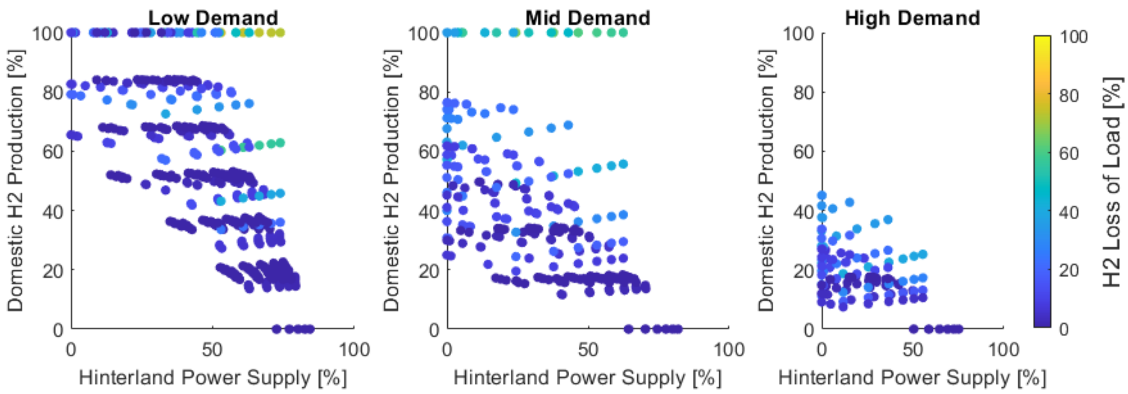

Figure 5.10: The relation of domestic hydrogen production and hinterland power supply volume for low, medium and high demand scenarios.

This figure confirms the negative correlation previously identified in subsection 5.2.2, demonstrating that higher domestic hydrogen production consistently leads to reduced power allocation for the hinterland across a broader range of system configurations. The lighter-coloured configurations near the top of each individual scatter plot are extremes, due to their high hydrogen loss of loads. When disregarding these values, the correlation is particularly evident. System designs that are oriented towards achieving considerable domestic hydrogen production and ensuring a high level of hinterland power supply in parallel are also associated with a greater incidence of hydrogen loss of loads. On the other hand, low loss of loads are often achieved at the expense of either hydrogen domesticity or hinterland power. This observation reinforces the inherent trade-off between hydrogen production and hinterland power allocation in terms of power distribution.

One notable observation is the variation in maximum achievable domestic production between demand scenarios. In the mid-demand scenario, domestic production shares are lower than in the low-demand scenario, or the loss of load is considerably higher. In the high-demand scenario, domestic production never exceeds 50%. This limitation is partly attributed to the lower boundary of 1.5 $MtH_2.y^{-1}$ cracker capacity range in the high-demand case, implemented to avoid configurations with extreme hydrogen loss of load. These cases would rely entirely on hydrogen production through electrolysis, which would be insufficient to supply the hydrogen demand. Consequently, the hydrogen supply is completely domestic, yet insufficient to meet demand.

5.4.3. Ammonia Shipments & Domestic Hydrogen Production

Figure 5.11 shows the relation between domestic hydrogen production and the amount of annual ammonia shipments required in the configurations. The shaded areas cover all configurations with a hydrogen loss of load of maximum 10%, for each respective demand scenario.

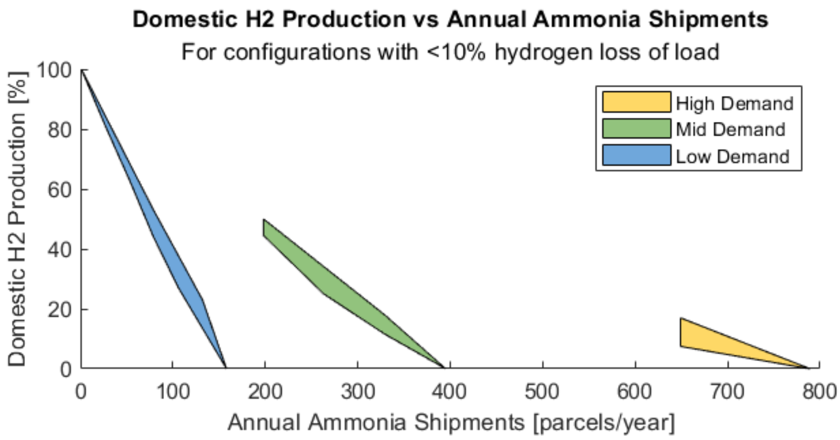

Figure 5.11: The relation of domestic hydrogen production and ammonia shipments for low, medium and high demand scenarios. Only configurations with under 10% hydrogen loss of load are considered.

The dispersion of the areas is particularly distinct, showing similarity to subsection 5.4.1. In scenarios where demand is high, there is a substantial reliance on ammonia imports in comparison to other scenarios. As the configurations are once again filtered to show only cases with limited hydrogen loss of load, it becomes evident that domestic hydrogen production is limited in the middle and high demand scenario. This is in accordance with the observed maximum domestic production values of the shaded areas, which are approximately 50% and 20% for the middle and high demand scenarios, respectively. It is shown that not a single configuration with higher domestic production achieves the specified loss of load maximum. The figure of the original scatter plot for the low demand scenario is shown in Appendix A.

Figure 5.11 also indicates the minimum ammonia shipments required for all configurations with a limited hydrogen loss of load. In the low demand scenario, the option of full local hydrogen production is a possibility, thus resulting in configurations with zero ammonia import. In the moderate demand scenario, the specified loss of load can be achieved with a minimum of approximately 200 ammonia shipments per year, up to nearly 400 for systems that are entirely ammonia-driven. Conversely, high demand with limited loss of load commences at 650 annual shipments, which equates to approximately two per day.

6 Discussion

The objective of this research is to provide an understanding of the techno-economic impact of renewable hydrogen supply—through ammonia imports and local electrolysis—on the interests of various stakeholders in the Port of Rotterdam. The preceding chapters have explored the system objectives and key performance indicators associated with different supply pathways. A numerical model was developed to systematically compare the hydrogen supply pathways on these key performance indicators. Subsequently, this model was populated with case information specific to the Port of Rotterdam.

This chapter reflects on the results, aiming to distill key insights and connect the study's findings to its original objective. The central question of this discussion is: how do these findings translate into the real world? To answer this, the chapter first provides a summary of the key findings on system design and their relation to key performance indicators. These results are then interpreted in a broader context, exploring how they translate into real-world implications. Finally, the chapter reflects on the methodology and limitations of the study, evaluating the assumptions, simplifications, and methodological constraints that shape the conclusions and identifying potential avenues for further research. By addressing these aspects, this chapter provides a critical perspective on the research outcomes, highlighting both their relevance and their limitations in shaping future hydrogen supply strategies.

6.1. Results Interpretation

The results of this study highlight the fundamentally different impacts of hydrogen supply through ammonia cracking versus local electrolysis based on offshore wind. These differences are clearly reflected in the key performance indicators in terms of affordability, security of supply, and sustainability.

Affordability

In terms of affordability, local hydrogen production is capital expenditure-intensive due to the high upfront investment required for offshore wind and electrolysis capacity. Hydrogen storage cost is similarly dominated by upfront investment, despite its comparatively modest scale relative to the required wind and electrolysis capacities. As a result, operational expenditure for local system configurations remains relatively low. In contrast, the import pathway is highly *OPEX*-driven, as the recurring cost of ammonia imports constitutes the dominant share of annual system expenses, while the ammonia cracker itself has a comparatively low *CAPEX* compared to the required components for the local pathway.

Security of Supply

The security of supply also differs considerably between the two pathways. Assuming a constant influx of ammonia, the hydrogen supply derived from imports offers a stable baseload production, thereby ensuring a higher degree of reliability on the short term. In contrast, local hydrogen production is subject to fluctuations due to its reliance on offshore wind conditions. This renders hydrogen storage a necessary component in order to mitigate the impact of these fluctuations. Moreover, the significant reliance on electrolysis gives rise to a competitive dynamic with other electricity consumers, such as the Rotterdam harbour-industrial cluster and the hinterland. The findings demonstrate that cases characterised by lower electrolyser consumption — signifying reduced local hydrogen production — exhibit increased power volumes delivered to the hinterland. This observation underscores a trade-off between prioritising hydrogen production and ensuring the electricity supply to other sectors.

Sustainability

From a sustainability perspective, local electrolysis-based hydrogen production has a significantly lower CO_2 footprint due to its reliance on solely offshore wind power. In contrast, ammonia import carries a higher carbon footprint, as the abroad production of hydrogen and the subsequent synthesis of ammonia frequently relies on multiple electricity sources with a higher combined emissions intensity. Furthermore, the spatial impact of the two pathways differs. Ammonia cracking facilities are relatively compact, while the land area required for electrolysis with similar hydrogen supply security is significantly higher. Additionally, the requirement for offshore space to accommodate wind power generation is substantial, particularly in scenarios where a considerable electrolysis capacity must be incorporated alongside existing power demand of the Rotterdam harbour-industrial complex and hinterland.

The findings emphasise that no single pathway is inherently superior, but rather that each has distinct characteristics that must be weighed based on stakeholder priorities, infrastructure constraints, and long-term strategic goals. The subsequent sections will delve deeper into the implications of these results within the broader context of energy system development and policy considerations.

6.2. Reflection on Results

The findings of this study offer insights into the trade-offs involved in renewable hydrogen development pathways and the relations between various system parameters. Nevertheless, it is important to consider the implications of this study within the broader context of hydrogen development and the energy transition, which is the focal point of this section.

Power

A fundamental finding is that the distribution of wind power is a crucial system design choice. The extent to which consumers have access to power, and the circumstances in which they do not, exerts a significant influence on a number of key performance indicators. These include domestic hydrogen production and loss of loads–instances in which a portion of demand remains unsatisfied. The introduction of substantial electrolysis capacity, driven by local hydrogen production objectives, inevitably results in compromises regarding the power consumption of other users. In view of the anticipated limitations on the maximum wind capacity that can be installed, this represents a crucial trade-off between stakeholder values.

The study also reveals a trade-off in hinterland power supply. Whilst the provision of electricity to the hinterland results in a reduction of the absolute demand volume, it also leads to a considerable increase in the variability of the residual demand profile. This finding suggests that, in most system configurations, the provision of wind power to the hinterland renders the remaining load more volatile. This increased variability of the residual demand was observed across the entire range of electrolysis capacities, which always have priority over the hinterland in the power distribution hierarchy. Therefore, it is not merely attributable to the low hierarchy position of hinterland power demand but also to the profile shape of the wind power. This variability in residual demand can give rise to operational challenges in its supply, underscoring the necessity for balancing strategies, including storage, flexible generation, and import mechanisms.

Hydrogen

The maximum feasible production level for hydrogen from local electrolysis is constrained by the maximum wind capacity. While electrolysis can contribute to the availability of hydrogen, the results of the study indicate that in scenarios with higher hydrogen demand, increased ammonia imports are necessary. If a situation would arise where ammonia import volumes were to be constrained, whether by physical limitations or strategic policy decisions, an upper boundary for hydrogen availability would be established. This emphasises a crucial aspect in the formulation of demand objectives, as system limitations begin to impact key performance indicators.

The role of hydrogen storage is also an important factor in system design. In a configuration focused on local production, storage is able to provide supply continuity. The results of this study indicate that, in order to maintain a functioning hydrogen storage system, there is a necessity for an overcapacity of wind power and electrolysis. However, this approach has been shown to result in a substantial increase in *CAPEX* and to intensify competition with other electricity consumers. Despite the challenges associated with the storage infrastructure, the cost implications of the storage itself do not appear to be a dominant factor when compared to the wind and electrolysis assets that would be needed to support the storage system. This finding lends further support to the notion that a fundamental trade-off in the system design is the allocation of capacity contingency for enhanced security of supply, which in turn impacts the other key performance indicators.

It is important to note that the extraction and injection rates of the hydrogen storage cavern can act as limiting factors in the supply. In scenarios of low demand, a single cavern is capable of delivering only one-sixth of the hourly hydrogen demand. This underscores the necessity for a substantial number of caverns in configurations reliant on local hydrogen production to achieve the required hydrogen output.

Ammonia

For ammonia imports, spatial considerations are a major factor of interest for decision-making. While ammonia cracking and storage require relatively modest space in the importing region, its production abroad involves significantly larger land areas due to the additional losses incurred by a more elaborate supply chain that incorporates additional conversion and transportation steps. The economic rationale for favouring imports is partially influenced by the scarcity of available land area in the vicinity of the Rotterdam harbour-industrial cluster, as opposed to the more expansive, potentially lower-cost locations for ammonia production overseas. However, this spatial trade-off must be weighed against exposure to international supply chain risks and ammonia cost fluctuations.

The potential role of e-crackers introduces an additional layer of complexity. Electrified ammonia cracking introduces an additional electricity demand, thereby increasing the strain on power distribution. Parallel to this, more ammonia-inefficient cracking methods – including those reliant on ammonia co-firing – are in effect parasitic consumers of costly ammonia. This poses a challenging trade-off: utilising renewable electricity for cracking exerts pressure on the power system, while cracking with parasitic ammonia-fueling leads to significantly higher operational costs. A more detailed assessment is therefore necessary to evaluate the feasibility of different ammonia cracking methods.

Moreover, the study draws attention to several considerable scale implications. The high hydrogen-demand scenario requires approximately twice the current global annual volume of ammonia shipped, solely for Rotterdam and its hinterland. The present volume of transported ammonia is almost exclusively composed of fossil ammonia, thereby providing further insight into the extent to which the global capacity for renewable ammonia production must be scaled up. Furthermore, the consistent and frequent shipment of ammonia, as is necessary for the majority of middle and higher hydrogen demand scenarios, poses a potential risk to public support of this pathway due to the toxic nature of the chemical.

The discussion of the research insights presented in this section demonstrates that the effective design of a hydrogen supply system is a balancing act of a wide range of interests and limitations. The distribution of system resilience through capacity contingency and operational flexibility of components is an additional layer of complexity that is influenced by the key performance indicators.

6.3. Methodology Reflection & Study Limitations

This section reflects on the methodological choices made in this study, their implications, and the limitations that arise from them. While the chosen approach provided valuable insights into hydrogen supply system design, certain simplifications were necessary, and some influential factors were beyond the study's scope. Recognising these limitations is essential for interpreting the results in context and identifying areas for future research.

6.3.1. System Objectives Framework

The system objectives – affordability, security of supply and sustainability – functioned as useful guiding principles for the structuring of the analysis. They provided a clear framework for assessing trade-offs and allowed measurable factors of interest to be categorised effectively. However, these objectives inherently do not capture the full complexity of real-world decision-making. While these objectives do highlight key dimensions of system performance, aspects such as political feasibility, regulatory constraints, and economic competitiveness relative to fossil-based alternatives were not explicitly included.

A further key limitation of the system objectives approach lies in its application from a whole-system perspective, as opposed to an individual stakeholder perspective. The study considered aggregate costs and benefits, yet it did not address the question of how these would be distributed among governments, industry, and consumers. This methodological choice carries significant implications, as it can result in the optimal configuration of a system, as perceived at the macro level, being financially unfeasible or unattractive for specific actors at the micro level. To illustrate this point, consider the example of an oversized ammonia storage and cracking facility. Such a facility could significantly improve system-wide security of supply at a relatively low capital expenditure. Nevertheless, unless the economic benefits for the system as a whole are reflected in financial returns for the investor, such infrastructure may not be constructed. This underscores the discrepancy between system-wide optimisation and real-world implementation, wherein investment decisions are influenced by stakeholder incentives rather than purely systematic efficiency. It is important to acknowledge this inherent limitation in the generated results, as this was explicitly not the objective of this research.

Moreover, the study did not evaluate the attractiveness of hydrogen supply compared to fossil-based alternatives. The analysis was predicated on the assumption of a fully renewable system, with no consideration given to the economic and policy mechanisms that would be required to effect the transition away from fossil fuels. In reality, the affordability of hydrogen is often assessed in relative terms: hydrogen supply pathways must compete not only with each other but also with existing fossil-based options. These remain more cost-effective without additional regulatory measures to penalise their use. Future research could incorporate direct comparisons with fossil-based hydrogen to provide a more comprehensive view of the economic landscape in which hydrogen supply chains will develop.

6.3.2. Key Performance Indicators

The use of key performance indicators in this study provided a structured way to quantify system performance across different hydrogen supply configurations. However, while *KPIs* offer clear, measurable insights, they also impose limitations on the scope of analysis. Not all relevant factors, such as policy feasibility, social acceptance, or long-term strategic value can be easily expressed in a metric suitable for direct comparison. As a result, while expanding the set of *KPIs* could enhance the comprehensiveness of the study, some aspects of hydrogen supply system development remain inherently difficult to capture through this approach.

The selection of *KPIs* has been demonstrated to have a substantial influence on the conclusions that can be drawn. For instance, this study suggests that hydrogen storage is a potential way to improve security of supply in systems leaning on local electrolysis. However, the analysis does not account for the practical feasibility of building the required hydrogen infrastructure, such as pipelines spanning large parts of the Netherlands. The absence of a *KPI* that specifically addresses the developmental complexity or investment risks associated with such infrastructure contributes to an incomplete representation of the real-world trade-offs involved.

Therefore, while *KPIs* are essential for quantitative analysis, they should always be interpreted in the broader context of decision-making. Real-world hydrogen supply development is shaped not only by cost, security, and sustainability metrics but also by factors such as political will, industrial strategy, and regional development priorities, which are less easily quantified. Recognising these limitations is crucial when applying the study's findings to policymaking and investment strategies.

6.3.3. System Configuration & Modeling

The study's system configuration and modeling choices were designed to isolate the impact of different hydrogen supply pathways for stakeholders near the Port of Rotterdam. However, these assumptions introduce certain limitations that should be considered when interpreting the results.

A fundamental presumption is the management of ammonia imports. The present study focuses on the end-use impacts of ammonia cracking in Rotterdam. Although the total lifetime CO_2 footprint of imported ammonia is accounted for, this research does not account for other regional impact of ammonia production overseas, such as the environmental or economic effects in exporting regions. Renewable hydrogen and subsequently ammonia can be produced using a variety of electricity sources, and as a result, their carbon footprint and sustainability impact can vary significantly depending on location. Another important assumption is that ammonia imports provide a stable baseload hydrogen supply. While this simplifies the system dynamics, real-world ammonia imports may be subject to variability due to global market conditions, logistical constraints, or supply chain interruptions.

The system model excludes several components of the energy system that have the potential to influence real-world feasibility. The model does not consider power storage or imports from hinterland regions, thereby limiting the flexibility of the local energy system. Moreover, the power distribution model does not include other renewable energy sources, such as solar power. However, in reality, solar generation has the potential to complement offshore wind production, particularly during the summer months, thereby potentially altering the competition for power between electrolysis and industrial demand. Furthermore, the method used to scale hinterland power demand is relatively simplistic. The model employs a static scaling factor that is applied to the aggregate annual demand profile, presuming that the potential power consumption in the hinterland remains constant throughout the year. However, in reality, wind power availability is significantly higher in winter months, while solar power could play a larger role in summer. This discrepancy suggests that curtailment (also termed 'potential power surplus' in this study) in winter may be overestimated, and that wind power may contribute a greater share of hinterland power demand than the study indicates. A more detailed demand modeling approach, incorporating seasonal and geographical variations, could refine these insights further.

Certain technical simplifications also influence the results. The study does not account for additional hydrogen compression energy requirements, which could add a substantial power demand component. Besides, the development of the power grid was not explicitly considered. Many cost factors, efficiencies, and boundary conditions were also simplified for modeling purposes, meaning that the absolute cost and yield estimates should be interpreted with caution, while relative trends and trade-offs remain more robust.

6.3.4. Case Selection

The approach adopted in this study involves a substantial and intricate parameter space, with numerous demand types, supply components, and system configurations. Given the sheer number of possible combinations, only a limited subset of cases could be explored in detail. The selected cases were chosen to highlight key trade-offs in hydrogen supply, energy distribution, and system design in the context of the Port of Rotterdam, but they represent only a fraction of the potentially relevant configurations.

In addition to the cases examined in this study, there are numerous other scenarios that could be analysed. These include alternative hydrogen supply strategies, such as integrating different energy storage solutions, or exploring alternative renewable energy sources beyond offshore wind. Furthermore, location-specific characteristics, such as grid constraints, or demand variations and consumer hierarchy could significantly affect the feasibility and performance of different supply pathways.

7 Conclusion

The objective of this research is to provide an understanding of the techno-economic impacts of renewable hydrogen supply pathways —through ammonia imports and local electrolysis— on the interests of various stakeholders in the Port of Rotterdam. This study is motivated by the increasing need to develop a sustainable, reliable and cost-effective hydrogen supply system that can support industrial decarbonisation while balancing key trade-offs. It functions as an exploratory investigation into the relations between various system designs and the differences in their characteristics.

The identification of trade-offs is a key aspect of the study. In order to achieve this objective, the research firstly identifies the main system objectives for hydrogen supply and translates these into concrete key performance indicators. A numerical model is developed to evaluate different supply configurations, assessing their impact on indicators of affordability, security of supply, and sustainability. The model is then applied in a case study for the Port of Rotterdam, where various hydrogen and power demand scenarios are explored to understand the system dynamics in different circumstances.

Key Findings

This research emphasises the complexity of the energy transition and highlights the necessity of a system-wide perspective in designing a robust hydrogen supply chain. The findings indicate that no single supply pathway is universally optimal, with each pathway entailing distinct trade-offs that must be carefully balanced. Achieving an effective hydrogen strategy requires consideration of the interplay between affordability, security of supply, and sustainability, while also accounting for the diverse priorities of different stakeholders.

The findings highlight fundamental trade-offs between local hydrogen production and ammonia imports. Firstly, systems relying on offshore wind-powered local electrolysis offers a factor of three lower operational cost and a reduced CO_2 footprint. However, it comes at around 50% higher capital expenditure, an eight-fold spatial requirement increase in the port area and significant variability in hydrogen production due to fluctuating wind conditions. This variability gives rise to a considerable hydrogen storage requirement to ensure continuous supply, especially in light of the limitations in extraction and injection rates of the individual hydrogen storage caverns. These limitations determine how large the storage must be to be able to deliver a sufficiently large flow of hydrogen to meet the momentary demand. In contrast, ammonia import provides a stable baseload supply but is highly operationally expensive and introduces over double the CO_2 emissions depending on how the ammonia is produced overseas. These system designs exhibit a permanent, high sensitivity to the cost of ammonia as well. Local production enhances autonomy in terms of energy supply, reducing reliance on external sources. The alternative is to transfer the developmental challenges to other regions, where their significance may be reduced due to the distinct characteristics of the area. However, this is done at the cost of increased import dependence.

An intricate key system dynamic observed is the competition for wind power between electrolysis and other electricity consumers, such as the hinterland and Rotterdam harbour-industrial complex. Configurations with low electrolysis capacities are capable of providing considerably more power to other consumers such as the hinterland. However, an increase in power volume delivery has also been demonstrated to result in a greater variability of the unmet demand. The study also shows that higher hydrogen demand can only be met by increasing ammonia imports, as local hydrogen production faces supply limits at scale. Additionally, the quantity of ammonia shipments in these scenarios is substantial, amounting to hundreds of 50 $kton$ shipments per year in higher hydrogen demand scenarios.

The management of such trade-offs invariably yields no single optimal solution, but rather is contingent on the values of the relevant stakeholders. In addition, it is evident that the decisive factors in determining the retention and attraction of specific industries do not exclusively involve the availability of renewable hydrogen. Other pivotal considerations include the accessibility of adequate and affordable power connections within the Dutch grid, the inclination of consumers towards the purchase of renewable products, and the level of competitiveness faced by domestically producing companies in the global market.

Limitations

It is important to recognise that key performance indicators measure different types of impact for different stakeholders. Whilst this study evaluates the system in its entirety, real-world decision-making involves costs and benefits distributed across industries, governments and consumers, each of whom have their own priorities. Design choices that enhance overall system resilience may not represent an attractive investment for individual stakeholders unless the system-wide benefits translate into sufficient incentives. Furthermore, the affordability of different hydrogen supply pathways is ultimately contingent on who bears the cost.

The study's findings should also be viewed in light of certain methodological simplifications and assumptions. The analysis does not account for all possible system constraints, such as developmental feasibility or the potential political and market dynamics. These factors have the potential to influence the results by introducing an additional dimension to the trade-off between the two hydrogen supply pathways. While the assumption that the ammonia cracker operates at constant capacity and is supplied by a regular import of ammonia facilitated clear comparisons, future studies could explore more dynamic import strategies to reflect real-world flexibility. The model also simplifies certain physical and economic processes, such as the representation of the hinterland power demand.

8 Recommendations

This study provides valuable insights into the techno-economic trade-offs of renewable hydrogen supply in the Port of Rotterdam. However, there are several opportunities for future research to expand on these findings and enhance the decision-making framework for hydrogen infrastructure development.

A noteworthy area for future research is the application of the model's versatility to explore diverse areas within the parameter space. It is well-suited to predict system behaviour under changing conditions, such as future years with updated cost structures and efficiencies. The trade-offs identified in this study are contingent on these evolving parameters. Consequently, the model could be used to assess how the impact of system configurations evolves over time. Besides, the adjustment of parameters to reflect the case for alternative industrial hubs could offer insight into the trade-offs specific to these areas. Beyond the specific focus on ammonia imports and local electrolysis, the model could be adapted to evaluate alternative hydrogen supply pathways. By substituting ammonia with liquid organic hydrogen carriers or alternative transport methods, insights could be offered into different hydrogen supply strategies. Furthermore, the incorporation of new key performance indicators tailored to different system designs would facilitate more extensive comparative assessments of hydrogen logistics.

Another key area for improvement is the enhancement of the resolution of specific model components. A more detailed representation of hinterland power demand and its interaction with alternative renewable power sources could improve the accuracy of power distribution insights. Furthermore, the testing of more advanced operational strategies and power allocation hierarchies would allow for a deeper understanding of how delicate adjustments in power distribution affect overall system performance, and how they could contribute to a better-performing system. The expansion of the range of key performance indicators is another significant direction for future research. Whilst the present study encompasses affordability, security of supply and sustainability, the addition of further KPIs related to development feasibility, policy acceptability and infrastructure constraints has the potential to provide a more comprehensive understanding of the system.

An additional research question relates to the optimal placement of contingency and flexibility within the system. Future studies could investigate strategic storage options. For example, whether the system should rely on ammonia storage and an oversized cracker with a lower capacity factor, akin to the role of gas turbines in the current power system, or whether hydrogen storage in salt caverns would provide a more resilient alternative.

Lastly, incorporating a stakeholder value assessment would enhance the practical relevance of the study's conclusions. By identifying how different stakeholders prioritise specific KPIs, future research could narrow down the range of viable configurations and provide a more refined decision-making framework. This would be a crucial step towards translating system-level insights into actionable development.

Bibliography

[1] UNFCCC. Paris agreement. *https://unfccc.int/process-and-meetings/the-paris-agreement visited 2024-08-19*, 2016.

[2] Rijksoverheid. Klimaatakkoord 2019. *https://open.overheid.nl/documenten/ronl-7f383713-bf88-451d-a652-fbd0b1254c06/pdf visited 2024-08-19*, 2019.

[3] European Commission. Green deal: Fit for 55. *https://www.consilium.europa.eu/en/policies/green-deal/fit-for-55/ visited 2024-08-19*, 2021.

[4] International Energy Agency (IEA). Co2 emissions from energy combustion and industrial processes, 1900-2021. *https://www.iea.org/data-and-statistics/charts/co2-emissions-from-energy-combustion-and-industrial-processes-1900-2021 visited 2024-08-19*, 2022.

[5] Energie in Nederland. Broeikasgassen 2022. *https://energieinnederland.nl/cijfers/2022/broeikasgassen visited 2024-08-19*, 2023.

[6] CBS Open Data. Elektriciteitsverbruik 2022. *Energie Nederland*, 2023.

[7] International Energy Agency (IEA). Country insights: The netherlands. *IEA: Data and Statistics*, 2024.

[8] Centraal Bureau voor de Statistiek. Energiebalans: aanbod en verbruik, sector. *CBS Statline Dataportaal*, 2024.

[9] Centraal Bureau voor de Statistiek. Dossier broeikasgassen. *https://www.cbs.nl/nl-nl/dossier/dossier-broeikasgassen/welke-sectoren-stoten-broeikasgassen-uit- visited on 2024-08-19*, 2023.

[10] Nederlandse Emissieautoriteit. Co2 uitstoot. *https://www.emissieautoriteit.nl/actueel/nieuws/2024/04/15/recordda co2-uitstoot-door-lagere-industriele-productie-en-schonere-stroom visited on 2024-08-19*, 2024.

[11] European Network of Transmission System Operators for Electricity. Transparancy platform. *https://transparency.entsoe.eu/*, 2024.

[12] Centraal Bureau voor de Statistiek. Windenergie. *CBS Statline Dataportaal*, 2024.

[13] International Energy Agency (IEA). Offshore wind energy outlook 2019. *https://iea.blob.core.windows.net/assets/495ab264-4ddf-4b68-b9c0-514295ff40a7/Offshore*$_{W}ind_{O}utlook_{2}019.pdf, 2019.$

[14] Mahdi Fasihi Tuomas Koiranen Christian Breyer Gabriel Lopez, Dominik Keiner. From fossil to green chemicals: sustainable pathways and new carbon feedstocks for the global chemical industry. *Royal Society of Chemistry: Energy Environmental Science*, 2023.

[15] International Energy Agency (IEA). Global hydrogen review 2022. *IEA*, 2022.

[16] International Energy Agency (IEA). Ammonia technology. *IEA: Ammonia Technology Roadmap*, 2021.

[17] Kosala Gunawardane. Evolution of hydrogen energy and its potential opportunities around the globe. *Hydrogen Energy Conversion and Management*, 2024.

[18] Hannah Hyunah Cho, Vladimir Strezov, and Tim J. Evans. Environmental impact assessment of hydrogen production via steam methane reforming based on emissions data. *Energy Reports*, 2022.

[19] R.C. Segers M. Weeda. The dutch hydrogen balance, and the current and future representation of hydrogen in the energy statistics. *TNO CBS*, 2020.

[20] International Energy Agency (IEA). Tracking clean energy progress 2023. *IEA: Tracking Clean Energy Progress 2023*, 2023.

[21] Yuliya Pleshivtseva, Maksim Derevyanov, Andrey Pimenov, and Alexey Rapoport. Comparative analysis of global trends in low carbon hydrogen production towards the decarbonization pathway. *International Journal of Hydrogen Energy*, 2023.

[22] Netbeheer Nederland. Integrale energiesysteemverkenning 2030-2050. *https://open.overheid.nl/documenten/ronl-7219ac2558977a6050ac4db764d2ddebb156df32/pdf*, 2023.

[23] Guido Collodi. Hydrogen production via steam reforming with co2 capture. *Chemical engineering transactions*, 19:37–42, 2010.

[24] Catherine Louise Jones Sarah Karen Kimpton Ida Synnove Bukkolm, Erik Andreas Hektor. Blue hydrogen in a low-carbon energy future. *DNV*, 2021.

[25] Andi Mehmeti, Athanasios Angelis-Dimakis, George Arampatzis, Stephen McPhail, and Sergio Ulgiati. Life cycle assessment and water footprint of hydrogen production methods: From conventional to emerging technologies. *Environments*, 5, 02 2018.

[26] International Renewable Energy Agency (IRENA). Global hydrogen trade 2022. *IRENA*, 2022.

[27] International Energy Agency (IEA). Global hydrogen review 2023. *IEA*, 2023.

[28] Wisam Alsaba, Saad Ali Al-Sobhi, and Muhammad Abdul Qyyum. Recent advancements in the hydrogen value chain: Opportunities, challenges, and the way forward–middle east perspectives. *International Journal of Hydrogen Energy*, 2023.

[29] European Commission. supplementing directive (eu) 2018/2001 of the european parliament and of the council by establishing a union methodology setting out detailed rules for the production of renewable liquid and gaseous transport fuels of non-biological origin. *Official Journal of the European Union https://eur-lex.europa.eu/legal-content/EN/TXT/PDF/?uri=CELEX:32023R1184*, 2023.

[30] European Parliament and Council of the European Union. Directive (eu) 2023/2413 of the european parliament and of the council. *Official Journal of the European Union*, 2023.

[31] Rotterdam Port Authority. Facts and figures about the port. *https://www.portofrotterdam.com/en/experience-online/facts-and-figures*, 2024.

[32] Port of Rotterdam. About. *https://www.portofrotterdam.com/en/news-and-press-releases/port-of-rotterdam-in-full-transition-in-2023*, 2023.

[33] Port of Rotterdam. Energiebalans haven- en industriecomplex 2021. *Energiebalans*, 2021.

[34] CES Werkgroep Port of Rotterdam/Moerdijk. Cluster energie strategie 2022. -, 2022.

[35] Port of Rotterdam. Hydrogen vision 2030. -, 2020.

[36] Hans Elzenga en Bart Strengers. Productie, import, transport en opslag van waterstof in nederland. *Achtergrondstudie binnen het project Planbureau voor de Leefomgeving: Trajectverkenning Klimaatneutraal 2050*, 2024.

[37] Energiebeheer Nederland. Energie in nederland: Uitstoot van broeikasgassen. *https://energieinnederland.nl/cijfers/2021/broeikasgassen*.

[38] CES Werkgroep Port of Rotterdam/Moerdijk. Cluster energie strategie 2024. -, 2024.

[39] Roel Breure. Interviews by author. *N. Schumacher, Business Developer Hydrogen*, June 26th 2024.

[40] Roel Breure. Interviews by author. *T. Besseling, Commercial Project Manager Hydrogen*, June 24th 2024.

[41] Roel Breure. Interviews by author. *Site Manager Electrolysis*, July 2nd 2024.

[42] Zhiyuan Fan and S. Julio Friedmann. Low-carbon production of iron and steel: Technology options, economic assessment, and policy. *Joule*, 2021.

[43] International Energy Agency (IEA). Global hydrogen review 2024. *IEA*, 2024.

[44] Rotterdam Wind Power Hub. Internal meetings project team. *Port of Rotterdam*, 2024.

[45] Rijksoverheid. Ijmuiden ver tenders. *Noordzeker en Zeevonk II winnen tenders windparken op zee IJmuiden Ver Alpha en Beta*, 2024.

[46] AirLiquide. Curthyl. *https://nl.airliquide.com/energietransitie-de-benelux/waterstof-voor-industrie-en-transport/curthyl*, 2024.

[47] Shell Nederland. Holland hydrogen i. -, 2022.

[48] Port of Rotterdam. Rotterdam: Europe's hydrogen hub. -, 2024.

[49] International Energy Agency (IEA). North-west european hydrogen monitor 2024. *IEA*, 2024.

[50] Alfa Laval, Hafnia, Haldor Topsoe, Vestas, and Siemens Gamesa. Ammonfuel. *https://hafnia.com/wp-content/uploads/2020/08/Ammonfuel-Report-an-industrial-view-of-ammonia-as-a-marine-fuel.pdf*, 2020.

[51] Camel Makhloufi and Nouaamane Kezibri. Large-scale decomposition of green ammonia for pure hydrogen production. *International Journal of Hydrogen Energy*, 2021.

[52] Power2X Advario. E-saf hub port of rotterdam. *https://advario.com/power2x-and-advario-to-develop-world-scale-e-saf-hub-in-the-port-of-rotterdam/*, 2024.

[53] Planbureau voor de Leefomgeving and DNV. Eindadvies basisbedragen sde++ 2023. *SDE*, 2023.

[54] RVO. Programma energie hoofdstructuur. *Rijksdienst voor Ondernemend Nederland*, 2020.

[55] RVO. Programma verbindingen aanlanding wind op zee (vawoz) 2031-2040. *Rijksdienst voor Ondernemend Nederland*, 2023.

[56] Fluor. Executive summary of pre-feasibility for ammonia cracking in the port of rotterdam. -, 2023.

[57] Wouter Jacobs. Commodification of green ammonia. *Presentation Discussion - Erasmus Commodity Trade Center*, 2024.

[58] Hans van 't Noordende and Peter Ripson. A one-gigawatt green-hydrogen plant. *https://ispt.eu/media/Public-report-gigawatt-advanced-green-electrolyser-design.pdf*, 2022.

[59] Port of Rotterdam. Hydrogen imports prioritisation. *Port of Rotterdam*, 2024.

[60] Roel Breure. Interviews by author. *J. van de Kamp, Bid Lead System Integration*, July 25th 2024.

[61] Roel Breure. Interviews by author. *Project Lead Electrolysis*, June 20th 2024.

[62] RVO. Conceptregeling-vergunningverlening-ijmuiden-ver-gamma-a. *https://www.rvo.nl/sites/default/files/2024-11/Conceptregeling-vergunningverlening-IJmuiden-Ver-Gamma-A.pdf*, 2024.

[63] RVO. Conceptregeling-vergunningverlening-ijmuiden-ver-kavel-beta. *https://www.rvo.nl/sites/default/files/2024-01/Bijlage-IJmuiden-Ver-kavel-Beta.pdf*, 2024.

[64] Remco de Boer. Droomland: Het nederlandse energie- en klimaatbeleid en wat ervan terecht kwam. 2024.

[65] Remco de Boer Jesse Frederik. Hoe nederland al zijn klimaatdoelen haalde (en toch niemand tevreden was). *De Jesse Frederik Show - Podcast*, 2024.

[66] Mario Draghi. The future of european competitiveness. *European Commission*, 2024.

[67] CEO of Port of Rotterdam Boudewijn Siemons. Panel for students. *at World Energy Congress Rotterdam 2024*, 2024.

[68] B. Hofman D. Ekimova, I. Dijkstra. Grid fee outlook for the netherlands 2045. *Aurora Energy Research*, 2024.

[69] Remco de Boer. In search of europe's energy future: Guido janssen, co-ceo at nyrstar budel. *Studio Energie Podcast*, 2024.

[70] International Energy Agency (IEA). Global hydrogen production co2 emissions and average emissions intensity in the net zero scenario, 2019-2030. *IEA*, 2022.

[71] Michael Barnard. The future is electric. *Cleantechnica*, 2024.

[72] Remco de Boer. In search of europe's energy future: Spencer dale, chief economist at bp. *Studio Energie Podcast*, 2024.

[73] Roel Breure. Interviews by author. *A. van Wijk, Em.Prof.Dr. Future Energy Systems, TU Delft*, July 24th 2024.

[74] Roel Breure. Interviews by author. *D. Gondim Uribe, Business Manager Clean Ammonia*, July 2nd 2024.

[75] Port of Rotterdam Authority. Highlights annual report 2023. *Port of Rotterdam*, 2023.

[76] Energy Transition Model. Working with lole in etm. *Documentation on ETM*, visited Dec 2nd 2024.

[77] Stanislas Gillet. Qualifying the intermittency of different sources of electricity. *https://www.linkedin.com/pulse/qualifying-intermittency-different-sources-production-gillet*, 2023.

[78] Hans Schneider. Subjectieve energiesysteem voor nederland. *https://www.linkedin.com/pulse/mijn-subjectieve-energiesysteem-hans-schneider?utm*$_{source} = shareutm_{m}edium = member_{a}ndroidutm_{c}ampaign = share_{v}ia, 2023.$

[79] Expertteam Energiesysteem 2050. Energie door perspectief: rechtvaardig, robuust en duurzaam naar 2050. *Min. EZK, RVO, TNO, URL: https://open.overheid.nl/documenten/ronl-79f8093ac883c0413d412e2b9b1d092c1cdc7338/pdf*, 2023.

[80] Roel Breure. Interviews by author. *M. Stoelinga, Business Manager Energy Infra*, November 7th 2024.

[81] Ali Azadeh, Mansoureh Hasannia Kolaee, and Vahid Salehi. The impact of redundancy on resilience engineering in a petrochemical plant by data envelopment analysis. *Proceedings of the Institution of Mechanical Engineers, Part O: Journal of Risk and Reliability*, 230(3):285–296, 2016.

[82] US Government Department of Energy. Challenges in h2 infrastructure. *https://www.energy.gov/sites/default/files/2024-09/hfto-mypp-hydrogen-infrastructure.pdf*, 2024.

[83] European Commission. European critical raw materials act. 2023.

[84] Yuen Ip, Shit Chew, and David Randall. Ammonia toxicity, tolerance, and excretion. *Fish Physiology*, 20:109–148, 12 2001.

[85] Mohammad-Reza Tahan. Recent advances in hydrogen compressors for use in large-scale renewable energy integration. *International Journal of Hydrogen Energy*, 2022.

[86] The Global Home of Chemical Engineers. Hydrogen flammability. *The Elemental*, 2024.

[87] A. Viré M. Zaaijer. Introduction to wind turbines. *TU Delft Master's Course*, 2023.

[88] N. Buckman. Wind turbine aerodynamics: Theory of drag and power. *Massachusetts Institute of Technology, https://nbuckman.scripts.mit.edu:444/homepage/wp-content/uploads/2016/03/WindTurbine*$_{Paper}2 - 1.pdf, 2015.$

[89] TenneT. 2 gw program. *TenneT, https://www.tennet.eu/about-tennet/innovations/2gw-program*.

[90] TenneT TSO. Ons werk op zee. *https://www.tennet.eu/nl/projecten/provincies/offshore*, visited Nov 28th 2024.

[91] Hasan Özcan Rami S. El-Emam. Comprehensive review on the techno-economics of sustainable large-scale clean hydrogen production. *Journal of Cleaner Production*, 2019.

[92] S. Shiva Kumar and Hankwon Lim. An overview of water electrolysis technologies for green hydrogen production. *Energy Reports*, 8:13793–13813, 2022.

[93] Roel Breure. Interviews by author. *Thyssenkrupp Nucera at World Hydrogen Summit*, May 14th 2024.

[94] M. Weeda L. Eblé. Evaluation of the levelised cost of hydrogen based on proposed electrolyser projects in the netherlands. *TNO Energy Minerals Transition*, 2024.

[95] IRENA. Green hydrogen cost reduction: Scaling up electrolysers to meet the 1.5□c climate goal. *International Renewable Energy Agency, Abu Dhabi*, 2020.

[96] Haldor Topsoe. Ammonia cracking basics. *crack the code: getting to know the basics of ammonia cracking*, 2024.

[97] Rasmus Nielsen. Topsoes ammonia cracking technology - delivering green hydrogen. *Ammonia Energy*.

[98] GasUnie. Hydrogen through gas pipelines. *Gasunie, https://www.gasunie.nl/en/expertise/hydrogen/hydrogen-through-gas-pipelines-safe-and-sustainable*.

[99] European Hydrogen Backbone (EHB). Analysing the future demand, supply and transport of hydrogen. *https://www.ehb.eu/files/downloads/EHB-Analysing-the-future-demand-supply-and-transport-of-hydrogen-June-2021-v3.pdf*, 2021.

[100] Strategy. Hyway27: Hydrogen transmission. *Strategy for Ministry of EZK*, 2021.

[101] National Waterstof Programma. Productie waterstof. *https://www.nationaalwaterstofprogramma.nl /themas/thema+productie/default.aspx visited 2024-08-19*, 2023.

[102] Gasunie. Waterstofnetwerk nederland. *https://www.gasunie.nl/projecten/waterstofnetwerk-nederland*, 2022.

[103] R. Groenenberg et al. Large-scale energy storage in salt caverns and depleted gasfields. *TNO*, 2020.

[104] Chico Sambo, Anireju Dudun, Silas Adeoluwa Samuel, Pascal Esenenjor, Nasiru Salahu Muhammed, and Bashirul Haq. A review on worldwide underground hydrogen storage operating and potential fields. *International Journal of Hydrogen Energy*, 2022.

[105] HyStock. 2024 hystock introduction. *HyStock*, 2024.

[106] Greenly. Life cycle analysis tools. *greenly.earth*, 2024.

[107] Gisela Mello, Marta Ferreira Dias, and Margarita Robaina. Wind farms life cycle assessment review: Co2 emissions and climate change. *Energy Reports*, 2020.

[108] S. Lensink and I. Pisca. Cost of offshore wind energy 2018. *Planbureau voor de Leefomgeving*, 2019.

[109] TNO. Pathways to potential cost reductions for offshore wind energy. *https://publications.tno.nl/publication/34637553/S0BkPF/TNO-2020-R11926.pdf*, 2020.

[110] BVG Associates. Wind farm costs. *Guide to an Offshore Wind Farm*, 2019.

[111] G. Bedon B.H. Bulder, E.T.G. Bot. Optimal wind farm power density analysis for future offshore wind farms. *TNO*, 2018.

[112] DNV TenneT. Power-to-hydrogen ijmuiden ver verkenning. *NetzTransparanz TenneT*, 2018.

[113] Renewables Ninja. Wind power. 2024.

[114] Rijksoverheid. Kosten net op zee. *https://windopzee.nl/onderwerpen/wind-zee/kosten/kosten-net-zee/*, 2023.

[115] K. Alvestad. Combined hydrogen and offshore wind production: Design and market value. *Department of Technology Systems, The Faculty of Mathematics and Natural Sciences, UNIVERSITY OF OSLO*, 2022.

[116] Vincent Knop. Life cycle analysis for alkaline electrolysis. *A World Of Energy*, 2022.

[117] T. Hennequin I.V. Concha J.F.Gomez T. Hajonides, B. SChoemaker. Costs and greenhouse gas emissions of international hydrogen supply chains. *TNO*, 2024.

[118] Roel Breure. Interviews by author. *W. van Betuw, Commercial Business Developer Hydrogen*, November 29th 2024.

A

Additional Model Runs

Residual Power Profile Comparison

The behaviour of the variability of the residual grid profile has a more ambiguous pattern compared to the volume. The residual profile closely resembles the original grid demand in the local configuration, as it delivers only minor power volumes to the hinterland. The combined configuration delivers greater volume; however, it also leaves a more variable hinterland residual demand profile. In case the residual profile is not near zero, its variability does not appear to differ much for each configuration. However, the import configuration leaves fewer instances of residual, as it introduces considerably more zero-residual time steps. This effect appears to dampen the variability value, leading to a relatively lower value compared to the combined configuration.

Local Configuration

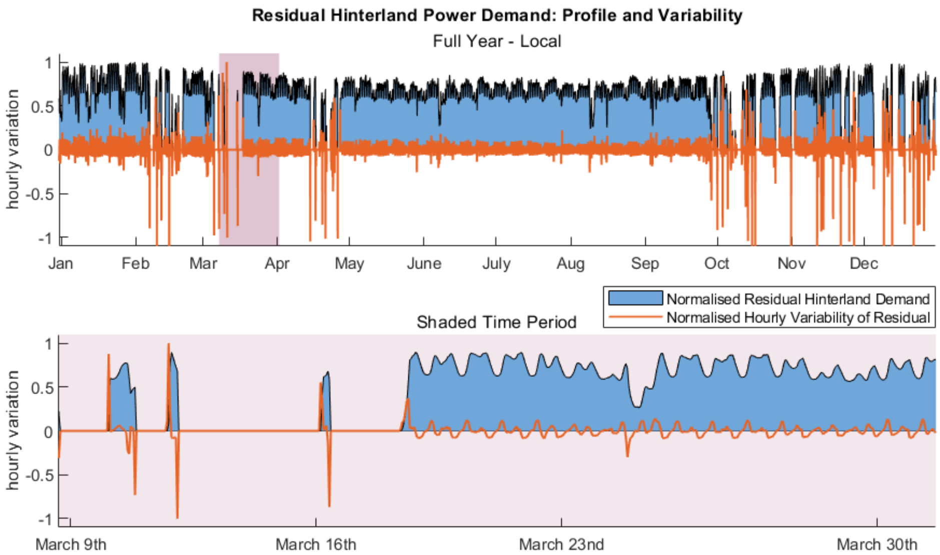

Figure A.1: The residual power demand profile for hinterland in the local configuration, which is the original hinterland power demand with the supplied power subtracted. The figure includes the hourly variability of the residual profile.

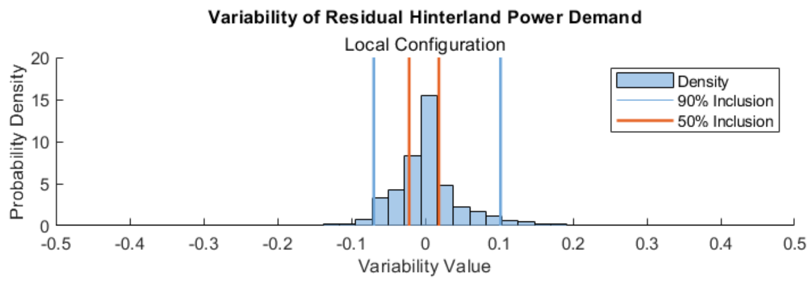

Figure A.2: Probability density figure of the hourly variability of the residual power profile, including 50% and 90% inclusion boundaries for the local configuration.

Combined Configuration

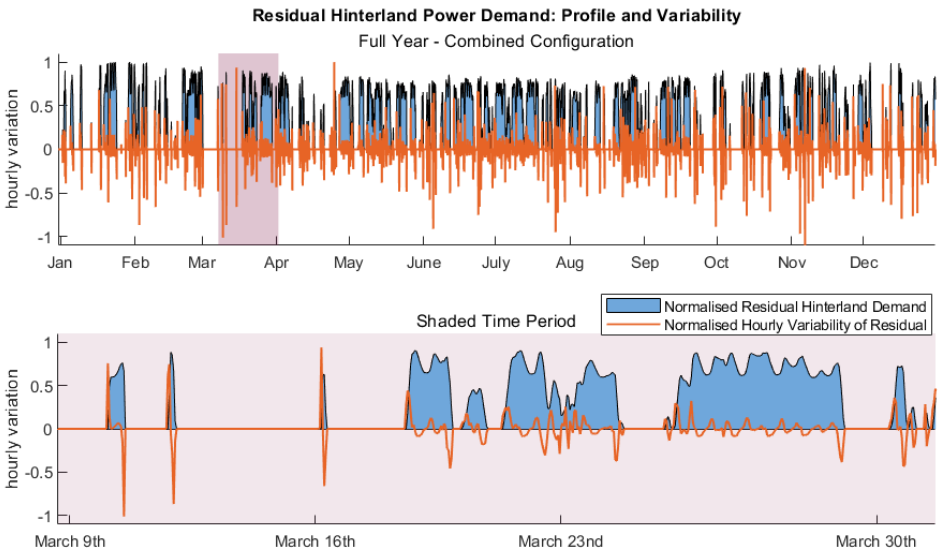

Figure A.3: The residual power demand profile for hinterland in the combined local and import configuration, which is the original hinterland power demand with the supplied power subtracted. The figure includes the hourly variability of the residual profile.

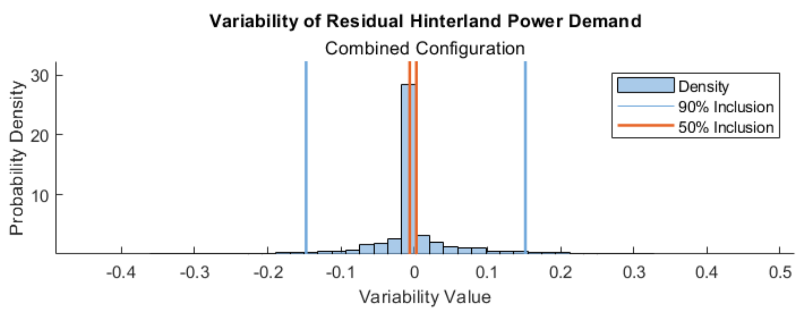

Figure A.4: Probability density figure of the hourly variability of the residual power profile, including 50% and 90% inclusion boundaries for the combined configuration.

Import Configuration

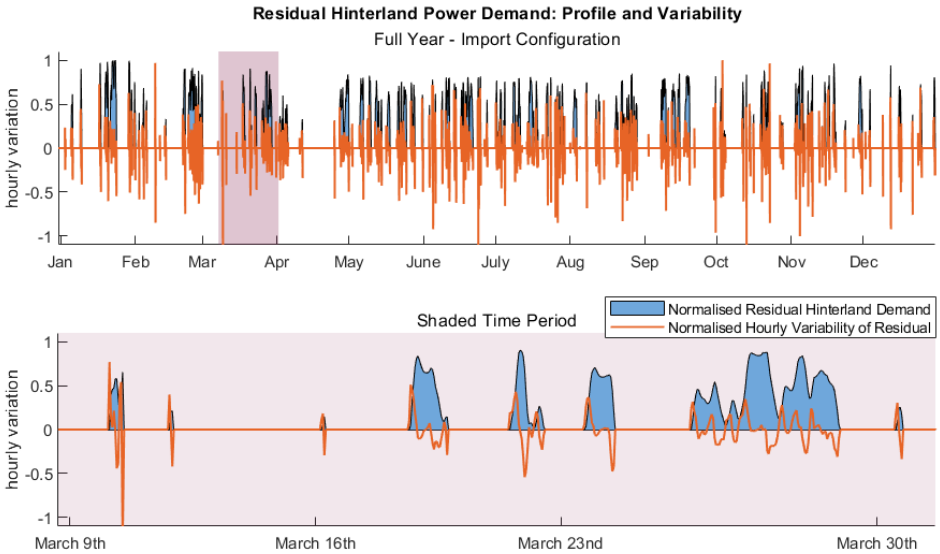

Figure A.5: The residual power demand profile for hinterland in the import configuration, which is the original hinterland power demand with the supplied power subtracted. The figure includes the hourly variability of the residual profile.

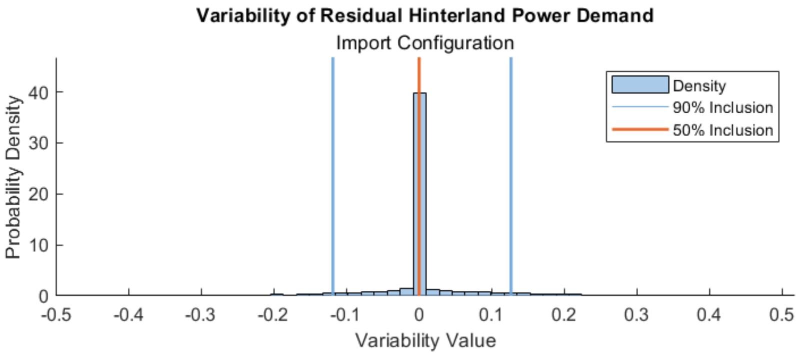

Figure A.6: Probability density figure of the hourly variability of the residual power profile, including 50% and 90% inclusion boundaries for the import configuration.

CAPEX & OPEX Relation

Middle & High Demand Scenarios

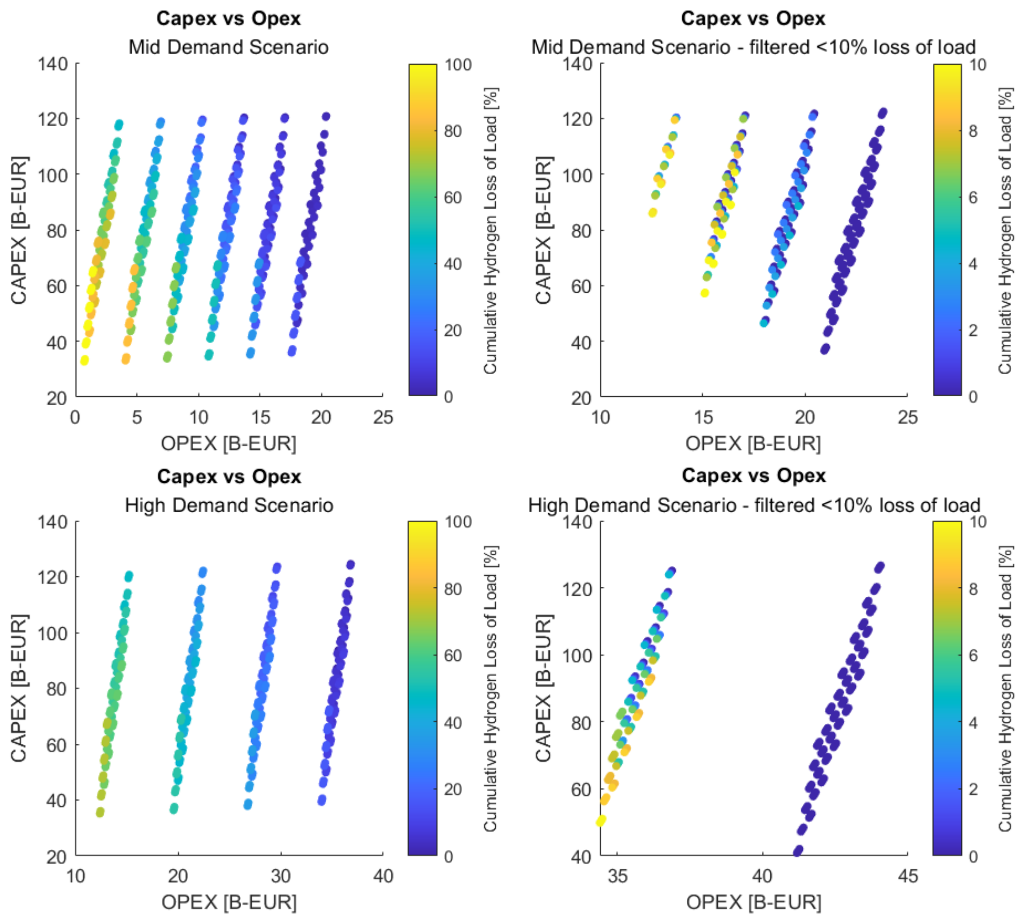

Figure A.7: Figure of the relation between Capex and Opex for the middle and high demand scenarios.

Hinterland Power: Residual Variability & Supply Volume

Middle & High Demand Scenarios

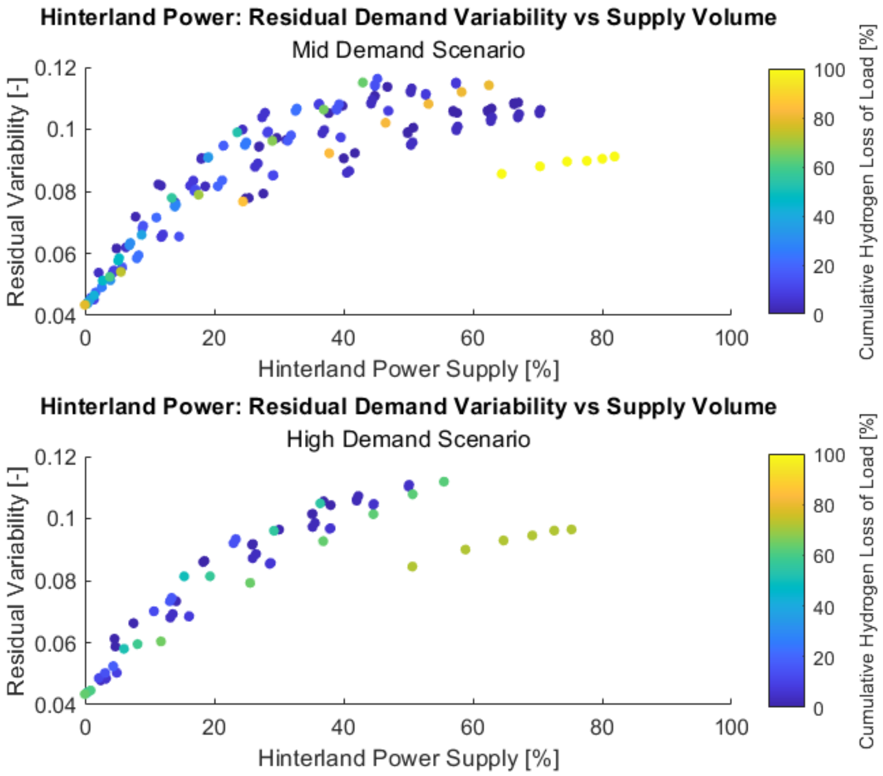

Figure A.8: Figure of the relation between residual hinterland demand variability and the supply volume for the middle and high demand scenarios.

Zeros Filtered Out

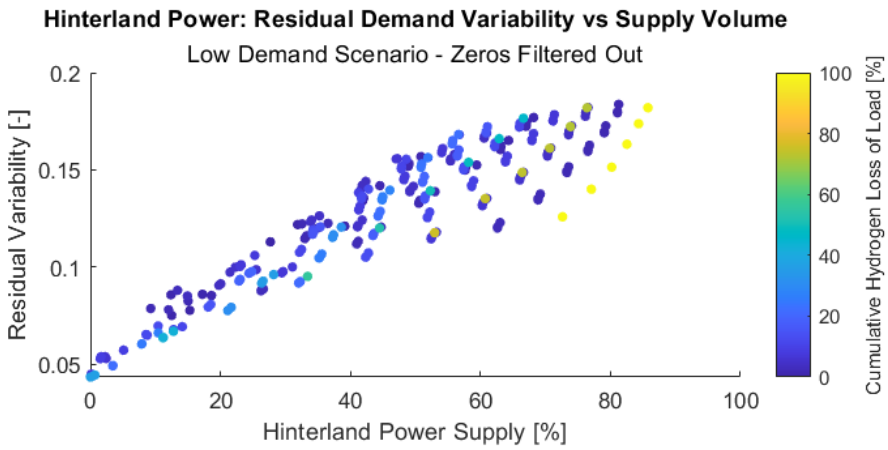

Figure A.9: Figure of the relation between residual hinterland demand variability and the supply volume for the low demand scenarios, but with zeros filtered out.

Ammonia Shipments & Domestic Hydrogen Production

Low Demand Scenarios

The filtered values represent the values at the top of the figure. Below these values are configurations that have similar ammonia cracker capacities, yet exhibit lower domestic hydrogen production. In essence, these cases can be attributed to inadequate electrolysis capacities in comparison to the selected values represented by the shaded area in this figure. Hence, their loss of load is insufficient to pass the filter of 10% loss of load given in Figure 5.10.

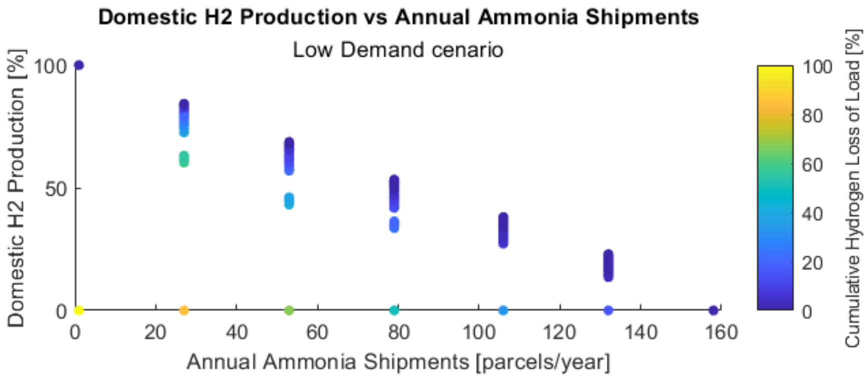

Figure A.10: Original scatter plot of the domestic hydrogen production and annual ammonia shipments for the low demand scenario.